國立臺灣大學生物資源暨農學院森林環境暨資源學系

碩士論文

School of Forestry and Resource Conservation

College of Bio-Resources and Agriculture

NATIONAL TAIWAN UNIVERSITY

Master Thesis

台灣山地與平地之降雨時空變異研究

Spatial and Temporal Variability in Rainfall at Mountainous and Lowland Areas of Taiwan

高世俊

Shih-Chun Kao

指導教授：久米朋宣 博士

Advisor: Tomonori Kume, Ph.D.

中華民國 100 年 6 月

June 2011

獻給我的家人、師長、好朋友們

This work is dedicated to my family, mentor, and friends.

國立臺灣大學碩士學位論文

口試委員會審定書

台灣山地與平地之降雨時空變異研究

Spatial and Temporal Variability in Rainfall at Mountainous and Lowland Areas of Taiwan

本論文係 高世俊 君（R98625057）在國立臺灣大學森林環境暨資源學系、所完成之碩士學位論文，於民國一００年六月二十二日承下列考試委員審查通過及口試及格，特此證明

口試委員：

________________ (指導教授)

________________ ________________

________________ ________________

系主任、所長 ________________

誌謝

拙作付梓，首先要感謝指導教授久米朋宣老師亦師亦友、燃燒青春的悉心指導，感謝日本九州大學小松光老師在理惠師母身懷六甲之刻仍撥冗指教，以及本系梁偉立老師不吝給我非常多的建議；感謝我敬愛的師長，亦是我求學生涯中重要標竿的口試委員們：本系榮譽教授陳信雄老師諄諄告誡勿忘森林水保之重要、亞熱帶學會金恆鑣老師退而不休地為我校正、本校地理系賴進貴主任照顧並指點空間研究之定位，以及不遠千里列席的本校海洋系三木健老師。感謝資源來源經濟部水利署與工程司李仲卿先生，以及本系技士林建村博士在公文流程上與大學以來各項大小事務上的幫忙。謝謝從大學以來的師長們：統計嚴師並惠予我 SCA 統計利器的中央研究院刁錦寰院士、教我觀察變遷資料的黃鍔院士，有用功的汪淮老師、大學導師應紹舜老師、笑嗨嗨的林文亮老師、出國種香菇的胡弘道老師、永遠的系主任郭幸榮老師、有問必答的羅漢強老師、愛家的鄭祈全老師、有情有義的趙榮台老師、迷惘時總是能點到要處的陳明杰老師、熱血的王亞男老師、wellokanyway 的系主任關秉宗老師、中研院的 William Wright 老師、帶我在合歡山做大專生研究的王立志老師、常出旅行團的邱祈榮老師、時常去宜蘭的盧道杰老師、超溫馨的鹿兒陽老師與師丈、五子登科的丁宗蘇老師、帥氣的林法勤老師、敏捷的葉汀峰老師，經濟系陳錦稷研究員伉儷，辦公室吳文統學長、董倫政先生、江育芳小姐、梁秀蓮小姐、張信謙學長、曾俊偉學長、陳盈達學長、洪志遠學長、周文進學長、張文慧學姐、蔡彥邦學長、鄭亦淳學姐、吳舜文學姐。

感謝 B93 可愛的唱歌火鍋團詹為巽同學與游舒婷同學、鄭博陽同學、林伯峰同學、張偉平同學，雖然大家會婊來婊去但是感情好的江宜穎同學、陶子婕同學、黃韻潔同學、劉璟瀚同學、蔡永信同學、許立昇同學、羅啟元同學、李雅筠同學跟陳泓碩同學、林大利同學、徐瀅茜同學、游旨价同學、陳泳升同學、李欣芸同學、吳慧雯同學、葉信甫同學、陳建仲同學、徐悅恆同學、孫葱同學、陳歆寧同學、余浩瀚同學、…等歪俊朋友 (詳見 Facebook)、實驗室的曾涵同學；可愛的學弟妹們許祐昇同學、張文馨同學、羅明慧同學、謝宜芳同學、陳美里同學、洪鳳栩同學、詹孟浚同學、陳天岳同學、邱子芸同學、蘇子堯同學。在 405 讀書室時期常打擾聊天的陳彥良學長、詹月德同學、王心慈同學、張懋如同學、黃于庭同學、張菀蓉同學、卓慧中同學、馬莉婷同學、文起祥同學、黃冠鳳同學；還有轉移給我們桌子與小物的長腿助理李思瑩小姐及陳亦瑱小姐，協助資料整理的王翎同學、何昀同學、吳美儀同學、黃皓瑜同學以及細心幫我繪圖的劉立元同學。

因為有你，才有這本雖薄情重的論文，感謝每一位你，成全了七年來大學的句點，祝福大家平安、健康、快樂。

辛卯年 季夏 吉旦

謹誌於

森林館四樓環境微氣候實驗室、台大藝術季搖滾區

摘要

在全球氣候變遷的情境下，降雨的變異受到許多學者關注，然而山地區域缺乏相關研究；本文旨在研究臺灣地區山地與平地之降雨量、日降雨強度、降雨日數等特性分佈的空間與時間變異，再應用本研究所得結果之季節趨勢，揉合時間序列分析與 ARIMA 模型進行各站台季節與逐月資料之一般模型建構與預測，並探討未來降雨情境對水文循環之影響。為此，本研究透過 1978 年至 2008 年間台灣 120 個水利署雨量站之年度與季節時序資料進行降雨量(Pr)、平均日降雨強度(η)、降雨日數比例(λ)之相關分析，並對於各項降雨特性的長期趨勢進行研究。本研究依參考文獻以海拔 1000 m 區分山地與平地區域，總體而言，山地區域的雨量與降雨日數均高於平地，而山地雨量之空間分佈主要由日降雨強度決定，平地區域雨量之空間分佈則由降雨日數與日降雨強度共同決定。年間降雨量的變異分析結果顯示，大多數站台不論在年度或季節方面，降雨量年間變化與日降雨強度年間變化具有較降雨日數為大的相關性，因此，降雨量在山地與平地的空間分佈所仰賴之降雨特性是不同的，在山地仰賴日降雨強度，而平地仰賴日降雨強度以及降雨日數。年度與季節等二種時間尺度下的長期趨勢分析顯示，趨勢顯著之站台佔全體站數之比例不高，其空間上之分佈亦不均一，因此，本研究推論降雨量之變化趨勢並非總體的現象，年雨量的長期趨勢與日降雨強度變化的長期趨勢呈顯著相關，具有顯著長期趨勢之站台主要分佈於中央山脈以西，而山地與平地的顯著站台比例相近；季節雨量的長期趨勢與日降雨強度變化的長期趨勢呈顯著相關，季節降雨量趨勢顯著之站台多位於平地部份，趨勢顯著之站台分佈亦不均一，因此，季節尺度下的長期降雨趨勢亦非總體的現象。

關鍵字: 氣候變遷、山區、平地、日降雨強度、降雨日數、時間序列分析。

Abstract

Variations in rainfall characteristics have been received a lot of attention in lowland areas while they were not clear in mountainous areas. This research first was to explore spatial and temporal variation of rainfall characteristics in the mountainous and lowland areas in Taiwan. As well, this research forecasted time series using ARIMA models, and then discussed possible impacts on hydrological cycles. To these aims, rainfall amount (Pr), daily rainfall intensity (η), and ratio of rain days (λ) between 1978 and 2008 from 120 stations in Taiwan were presented including annual spatial variation, temporal variations, and marginal long-term trend. In both of annual and seasonal time-scale analysis, spatial variation in Pr was highly explained by η at mountainous stations and by both η and λ at lowland stations, regardless of annual or seasonal datasets. The temporal variation of Pr was determined from η than λ at each station, this was consistent with mountainous and lowland areas. Long-term analysis showed that significantly increases in Pr were not distributed evenly in Taiwan and the changes were not a general phenomenon for the low ratio of total stations. Stations with changing rainfall characteristics located in the west of the central mountain range rather than the east. Further, in annual analysis, the ratio of these changing stations in the mountainous areas was almost same as those in the lowland areas. While I had found different spatial pattern of the long-term trend of Pr, η and λ in each season. Even so, long-term changes of rainfall were still uncommon phenomenon in Taiwan.

Keywords: Climate change, Mountainous, Lowland, Daily rainfall intensity, Rain days, Time series analysis.

Contents

Table List

Figure List

1

Introduction

1.1 Motivation of this research

Water plays the essential role in life, hydrology, water resource management, and relative study fields. As a Chinese poet, Li Bai, wrote in his famous poem, "*can't you see the Yellow River comes from the sky, running toward the ocean and never comes back*"? In hydrology, rainfall is regarded as the total input of the terrestrial hydrological cycles, and governs the spatial and temporal availability of water. As well as rainfall amount, rainfall characteristics such as rainfall intensity and rainfall duration contribute considerable effects on hydrological processes such as rainfall interception (e.g., Gash et al., 1995) and runoff regime (Beven, 2001; Wilby and Harris, 2006). More importantly, rainfall characteristics may determine available water resources and its planning and management. Hydrological models such as stochastic models require the rainfall characteristics as input for calculating the terrestrial water dynamics (e.g., D'Odorico et al., 2000; Porporato et al., 2004; Shinohara et al., 2010).

In recent decades, climate change greatly affects global hydrological cycle, water resources, even agriculture (Haskett et al., 2000; Oki and Kanae, 2006; Piao et al., 2009). The changing patterns of climate change, such as temperature and rainfall, have received much attention (Yu et al., 2002; Wada et al., 2004; IPCC, 2007; Liu et al., 2009). Furthermore, changes in rainfall characteristics have been reported in various regions around the world (IPCC, 2007). Therefore, besides examinations of spatial and temporal variations in these characteristics assuming the steady state, examinations on temporal trends in these parameters are important as well (Yu et al., 2002; Wada et al., 2004; IPCC, 2007; Liu et al., 2009). Clarifying the spatial and temporal variations in rainfall characteristics, and their long-term trends are indispensable for understanding of possible changes in terrestrial hydrological cycle responding to changes in rainfall regime (Yu et al., 2002; Wada et al., 2004; IPCC, 2007; Liu et al., 2009).

Rainfall characteristics in mountainous areas are regarded to be different from those in lowland areas. The orographic effect makes rainfall amounts in mountainous areas to be higher than lowland areas generally (Kerns et al., 2010; Teng et al., 2000). In mountainous areas, spatial and temporal variation in rainfall receives great concern in previous studies with a complicated topography (Shinohara et al., 2010; Qin et al., 2010).

Indeed, Taiwan is a highly mountainous island country. Either mountainous areas > 1000 m or 100-1000 m accounts for about one of third of Taiwan, respectively (Teng et al., 2000; Lin et al., 2010). Especially, the highest peak reaches nearly 4000 m in the central mountain range (CMR) of Taiwan. The CMR stretches across the island from north-northeast to south-southwest; the mean height of the CMR is 2000 m, and there are over 200 peaks with heights above 3000 m (Guan et al., 2009). As Taiwan is characterized by the CMR and unusually heavy rainfall, such as typhoons, considerable spatial and temporal variations can be expected. However, few studies have reported the rainfall characteristics and their long-term trends all over Taiwan.

Yeh and Chen (1998), Chen and Chen (2003) examined the spatial variation in rainfall amount using data recorded at 808 meteorological stations all over Taiwan, their analysis was based on only two months for a specific year (10 May to 27 June in 1987), and rainfall intensity and duration was not investigated. On the other hand, Hsu and Chen (2002) examined spatial and temporal variations in the rainfall characteristics (i.e., the numbers of rain days and heavy rain days) using data recorded at eight major meteorological stations in major cities over the past 100 years. They reported changes in the rainfall characteristics for some of the eight stations; in which, the annual rainfall increased in three stations, the number of rain days decreased in five stations, and the number of heavy rain days increased in three stations. Note that increases in rainfall and rainfall intensity were implied to have a correlation in their result. However, due to the limited number of the stations, it is still unclear whether changes in the rainfall amount and the rainfall characteristics are common in Taiwan or not. In addition, the rainfall characteristics in mountainous areas are generally different from those in lowland areas (Shinohara et al., 2010; Qin et al., 2010). Consequently, the results reported in Hsu and Chen (2002) based on lowland-station data might not be applicable to mountainous areas in Taiwan.

This thesis aimed at researching the nature of variations in rainfall characteristics in Taiwan using data recorded at 120 meteorological stations including both lowland and mountainous areas for the period between 1978 and 2008. Here I first examined spatial variations and then year-to-year variations in the mean annual rainfall, rainfall intensity, and the mean number of rain days for the 31-year study period. Then I would examine trends in these parameters during the period. As well, I would discuss about our results with other researches. Throughout the analysis, I focused on the following two points: (i) whether the variation in annual rainfall was caused by the variation in rainfall intensity or the number of rain days; and (ii) whether the results differed between lowland and mountainous areas.

Aimed at providing the basis of knowledge in this thesis, this chapter introduced a brief review on hydrological processes, brief review on relative literatures, and then presented the structure of this thesis.

1.2 Hydrological processes

Water properties

The hydrosphere contains about 1.4×10^{18} metric tons of water, which would be plenty enough to cover the Earth to a depth of 2.7 km in liquid water (Lee, 1980). Water, also known as H_2O in chemical formula, is a pure chemical substance combined of one oxygen atom linked to two hydrogen atoms (Lee, 1980; Zumdahl, 2005; Holliday et al. 2008). Water changes its state among gas, liquid, or solid at various places, which may take few seconds to millions of years to circulate in the hydrological cycle (Fig. 1) (Lee, 1980; Hewlett, 1981; Chen, 1990; Tsukamoto, 1992; Chang, 2006; USGS, 2010).

Polar water molecules attract other polar molecules and themselves. By this characteristic, not only water provides cohesion and adhesion on physical mechanism, e.g. capillary action, but also supports solutions' forming and lots of biochemical processes as the most common solvent. In addition, water has a large standard vaporization heat (i.e., the standard vaporization enthalpy, or latent heat) equivalent to 40.7 (kJ/mole) (597.3 Cal/g). (Johnson, 2003; Zumdahl, 2005; Holliday et al. 2008). During cold days, water on land surface or in soils would freeze. Ice, snow, and liquid water have some differences in their properties.

When water vapor cools down and compresses in volume, the vapor molecules re-form a liquid; this process is called ‘condensation’. Condensation is the reverse of vaporization. When the gas molecules release the latent heat, the water molecules will cluster instead of flying away from one another (Lee, 1980; Zumdahl, 2005; Holliday et al. 2008). In the atmosphere, the convection process brings gas water climbing toward sky, and then the condensation occurs by the temperature cools down, starting a hydrological cycle. In addition, the condensation in the air is a series of chemical process with aerosols as well. These kinds of study are, in detail, discussed in atmospheric particles science (Harrison and van Grieken, 1998). In a planetary view, water covers a thin layer on the surface of the planet, about 2.7 km in depth. Water in the world contains about 1.4×10^{18} tons; the most of water (97.398% of total water) is kept in ocean as saline water, and the rest freshwater accounts for about 3.6×10^{16} tons (2.602% of total water). In which, 77.2% of fresh water exists as ice; 22.4% of freshwater remains in underground or soils; the rest 0.4% is in lakes, rivers, and the air (Lee, 1980; Tsukamoto, 1992).

In a living world, almost all organisms on Earth rely on water and solar energy to survive directly or indirectly. Consisting all of the organisms and the abiotic factors in a given environment, an ecosystem relies on water to burst with life (Johnson, 2003; Nabors, 2004; Chen, 2006; Oki and Kanae, 2006). On the other hand, water supports crops to grow. When rainfall changes significantly, the agriculture and related economic business probably would face impacts. Potential risks on water resources were discussed (e.g., Oki and Kanae, 2006; IPCC, 2007), such as heavy rainfall events increased more frequently on most land areas; water stress on hundreds of millions of people; decreased water availability; and more droughts in mid-latitudes and semi-arid low latitudes. Consequently, water resources might be a critical problem to people in the world (Oki and Kanae, 2006; Mays, 2011), thus it has been concerned widely in areas of study, such as hydrology, biological sciences, engineering, physical sciences, social sciences, and their related braches. These topics are widely discussed in economic and agricultural sciences as well (Adams et al., 2004; Mendelsohn and Neumann, 2004; Fisher et al., 2005; Piao et al., 2009).

Hydrological cycle

Hydrological cycle consist of continuous processes of the mass movements and phase changes of water, in which water is evaporated or condensed among atmosphere, land surface, and oceans (Fig. 1). The hydrological cycle begins with condensation, wherein water vapor is cooled and forming small droplets as it is cooled in the atmosphere, and thus clouds are formed (Burton, 2008).

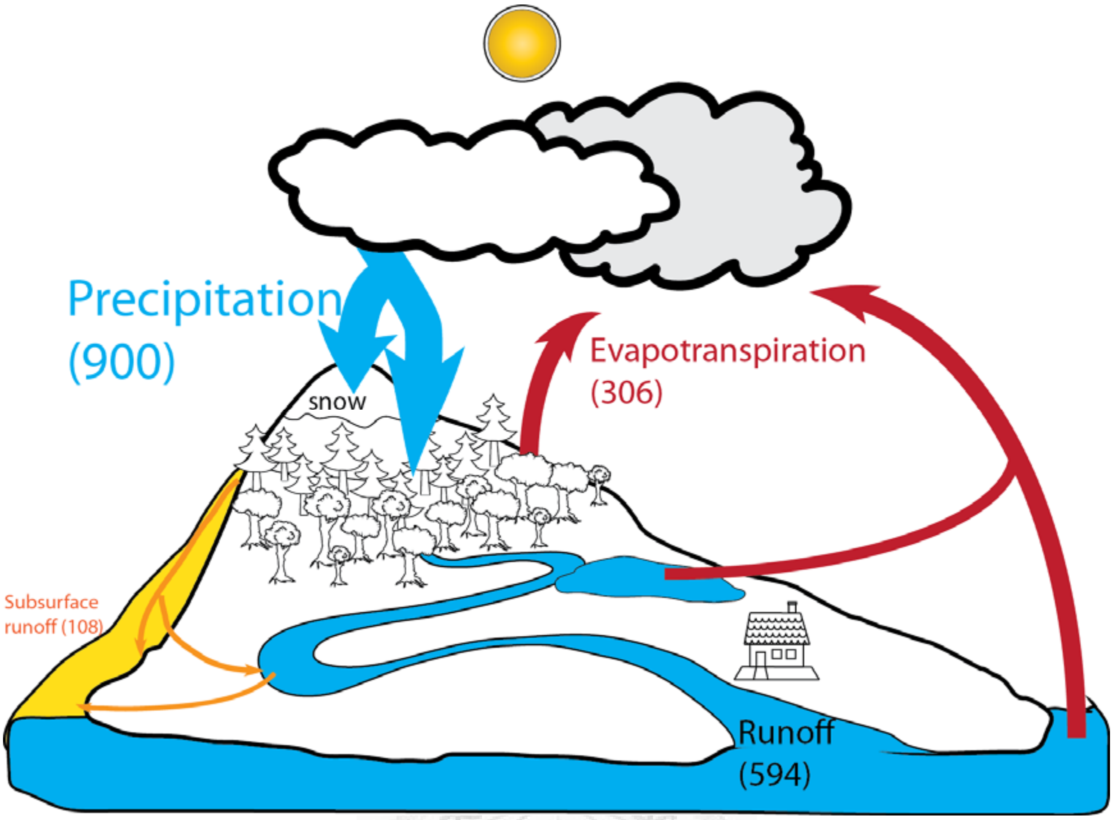

Figure 1. The terrestrial hydrological cycle with estimations in Taiwan.

Adapted from Chen (2006) and USGS (2010)

The unit of the numbers in Fig. 1 is $10^8 m^3$

Illustrated by Li-yuan Liu

The budget in the terrestrial hydrological cycle can be represented as:

$$\mathrm{Pr} = E + T + R + \Delta S + \Delta G + \Delta L$$

...Equation 1

in which, Pr is the precipitation, E is the evaporation, T is the transpiration, R is the runoff, ΔS and ΔG are the changes in soil moisture and ground water storage over the period of measurement, respectively, and ΔL is the leakage into or out of the catchment (Chang, 2006; Chen, 2006; Fleischbein et al., 2006).

Water evaporated from water surface on lands or oceans, then moves as moist air masses inland to the interior of the continent by wind. Then the air masses form convection and hence produce precipitation (Pr) falling on lands as they pass over coastal and interior mountain ranges (Lee, 1980; Chen, 1990; Bedient et al. 2008).

On the land surface, a proportion of precipitation returns to atmosphere via evaporation (E), E is indeed the process of water changes of state from liquid state to water vapor, and E is also occurring on water surface, such as river, pond, and other water bodies (Bedient et al. 2008).

The other portion of precipitation returns to atmosphere via transpiration (*T*). Plants can uptake vital water in soil and then transport water through their bodies. Finally, water loss from plants bodies via stoma on leaves or tissues to the surrounding area, resulting in increased humidity in the air. This loss of water from leaf surfaces is called transpiration. (Nabor, 2004; Bedient et al. 2008; Burton, 2008).

E and T can be combined and called evapotranspiration *(ET)*; ET is a maximum value of water loss as water vapor, while water supply in the soil is adequate at all times (Bedient et al. 2008). Some water enters the soil system as infiltration, and turns out as subsurface runoff, or ground water flow; the remaining portion of precipitation becomes surface flow, also known as runoff. Driven by the gravity, runoff runs downward to the river, or a reservoir, and then goes to the ocean, restarting a hydrological cycle once again (Chen, 1990; Bedient et al. 2008).

Note that forests spread broadly in mountainous Taiwan, which accounted for the 60% of the total land area (Su, 1984; Hsieh et al., 1994; Cheng et al., 2002) The hydrological processes in a forest is not as same as in other areas (Chen, 1996). Hence, the forest hydrology is an important study field in Taiwan. Consequently, I would introduce some basic ideas on forest hydrology in following sections.

Hydrological process in a forest

Forests cover about 3.95×10^{9} ha in the Earth. This is about one-third of total land area of the Earth surface, 1.3×10^{10} ha (Lee, 1980; Johnson, 2003; FAO, 2009). A forest is a dynamic ecosystem consisting of biological community and the non-living environment (Young, 1982; Burton, 2008). The Food and Agriculture Organization of the United Nations (FAO) makes a clear statement that a forest is an area > 0.5 ha with dominant species as trees, with the height > 5 m and the canopy cover >10% (FAO, 2009).

The precipitation derives from rainfall, snowfall, or fog drips. Here, the precipitation amount in a forest is regarded to be higher than open areas due to additional input by the fog, which is also called occult precipitation, horizontal precipitation, or cloud interception (Lee, 1980; Geiger et al., 2003; Chang, 2006; Chen, 2006). In a sub-tropical island like Taiwan, the snow would not be a main source of precipitation; thus, I assumed that the precipitation was mainly contributed by rainfall steadily while I also neglected the effect by fog.

Due to the structure of a forest, the hydrological processes would be different in a watershed view (Fig. 2). The partitioning of rainfall, such as throughfall, stemflow, and interception, is considered with rainfall characteristics, meteorological conditions, and vegetation structure (Gash et al., 1995; Staelens et al., 2008). The difference between Pr and the sum of throughfall (T_f) and stemflow (S_f) is called canopy interception (I_c).

$$I_c=Pr-(T_f+S_f)$$

…Equation 2

Ic is an important component of the hydrological budget of terrestrial ecosystems, and is significant in ET, owing to its later evaporation to the atmosphere (Crockford and Richardson, 2000; Staelens et al., 2008). While the litterfall would also intersect part of P, denoted as I_f.

In a forest, when rainfall amount exceeds the soil infiltration or percolation capacity, surface runoff would occur, while the subsurface flow runs. Infiltration (*F*) is the downward movement of water through the soil, F is also an important hydrological process because it marks the transition from fast-moving surface water to slow-moving soil and ground water. In a forest, F is affected by soil physical properties such as degree of compaction, moisture, permeability of subsurface layers, relative purity of infiltrating water, and soil microclimate (Lee, 1980). Therefore the quick runoff can be derived from:

$$Q_d=P-(I_c+I_f+F) \quad \text{…Equation 3}$$

F could be important input in mountainous area, however, our understanding on F have been still limited in Taiwan. Therefore, here I excluded fog precipitation elements from this study.

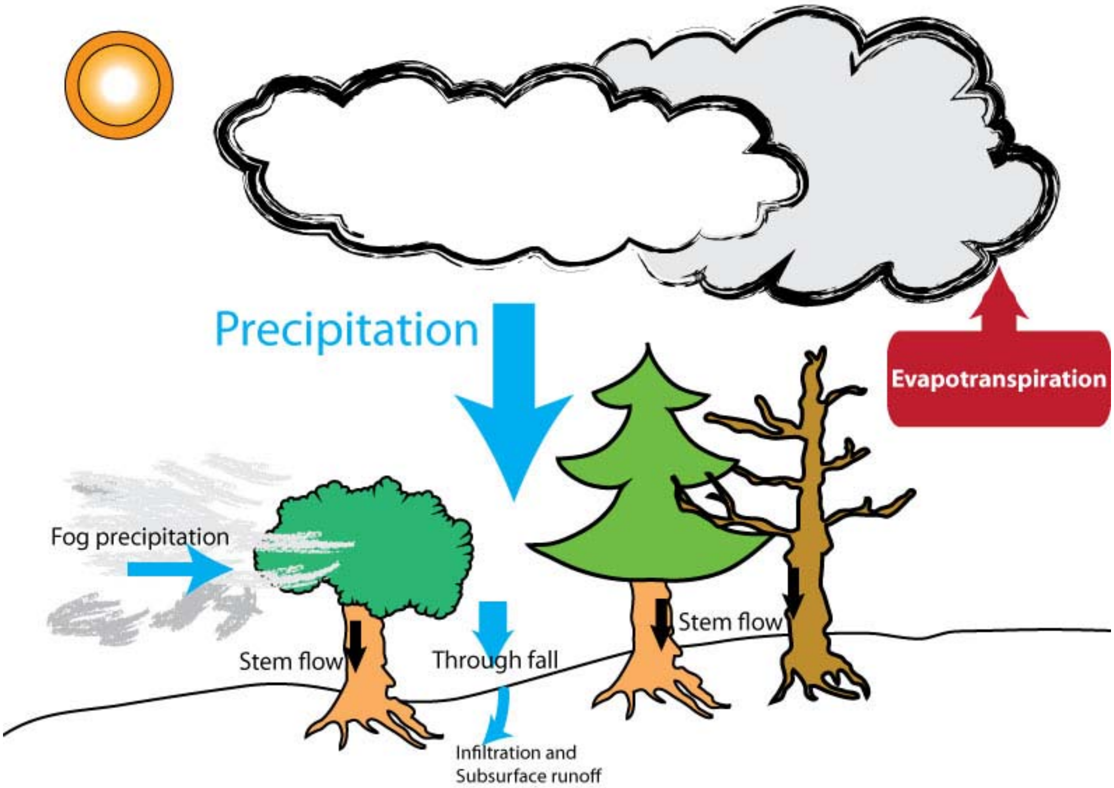

Figure 2. Rainfall partitioning in a forest

1.3 Relative studies about variations in rainfall

Global scale

IPCC (2007) showed that rainfall in lots of regions in the Earth increased in the past, while decreases showed in few regions. As well, anomalies in averaged rainfall occurred around recent decade frequently. Results from IPCC implied that rainfall amount became higher in most of regions during past decade; however, the intrinsic variation in finer spatial scales did not be considered. On the other hand, Zhang et al. (2007) simulated global rainfall trends using latitudinal zones per 10 degrees all over the world, it neglects the spatial variation among longitudes; the results showed that rainfall was increasing in high latitudes, but tropical-subtropical regions in north hemisphere showed neutral even declines.

Under-regional scale

Tesemma et al. (2010) investigated the Blue Nile basin during the period 1964–2003; they covered the average monthly basin-wide rainfall and monthly discharge data. At the Sudan–Ethiopia border, a rainfall–runoff model examined the causes for observed trends. There was no significant trend in seasonal and annual rainfall amount, significant increases in discharge during the long rainy season (June to September) were observed at all three stations.

In Japan, Xu et al. (2003) investigated step change and monotonic trend in 46 rain gauges during one century. Mann–Kendall and Mann–Whitney tests are applied to the averaged rainfall time series to detect trend. They indicated several step changes occurred in rainfall, but the time series did not exhibit significant evidence of monotonic trend during the past century. On the other hand, Shinohara et al. (2010) examined spatial and temporal variations in rainfall at mountainous areas in Japan. Their research examined spatial and temporal variations in rainfall data during summertime from 1976 to 2007, for 28 stations in mountain areas. They examined amount of annual rainfall, mean daily rainfall intensity, and ratio of rain days. 30-year period mean in rainfall amount and those in daily rainfall intensity had strong correlation for their 28 stations, indicating the spatial variations in rainfall amount are primarily related to daily rainfall intensity. In addition, year-to-year variations between time series indicate that rainfall amount series are primarily related to daily rainfall intensity series. Long-term trends are not common in mountain areas of Japan through their analysis.

In China, Qin et al. (2010) examined spatial and temporal trends by using the Mann–Kendall trend test in temperature and rainfall from 136 stations in southwest China for 50 years, including Tibet, Heng-duan mountains area, and west Sichuan Plateau. Annual rainfall showed insignificant trend, but statistically significant increasing trend has been detected in wintertime and autumn significant decreasing trend, indicating the trends were different under annual and seasonal time scale.

1.4 Structure of this thesis

In this chapter, I had emphasized the importance of understanding on rainfall characteristics in terms of hydrological cycles and showed our objectives of this study.

Chapter 2, *Methods and material,* introduces the dataset, statistical methods, and other techniques used in this thesis. I would present main analytical ways for time series and associated tools. As well, I have acquired the rainfall dataset from the Water Resource Agency (WRA), its attributes and period would be introduced in the chapter.

Chapter 3 presented the results and discussion with "*Annual variations in rainfall characteristics"*. It reported both the nature and related analysis of annual rainfall characteristics, such as spatial distributions, relationships between characteristics, year-to-year variations, and long-term trends.

Chapter 4 presented result and discussion with "*Seasonal variations in rainfall characteristics*". In this chapter, the data were collected during four seasons, i.e., spring (March, April, and May), summer (June, July, and August), autumn (September, October, and November), and winter (December, January, February).

Chapter 5, *Rainfall time series forecasting,* was based on the results in previous chapters and applied the time series analysis. This chapter aimed at finding a general model fitting and forecasting seasonal and monthly rainfall series. In this chapter, I would use two cases in seasonal and monthly rainfall amount in terms the applicability of this thesis. In Addition, I'd like to discuss possible impacts of long-term changes in rainfall characteristics on hydrological cycles.

Chapter 6, *Conclusion and prospects,* is a summary of this thesis, describing the main contribution of this thesis to our knowledge of hydrological processes. As well, a brief vision in future studies would be derived.

2

Methods and Material

This chapter would report on data set, collection statistical analysis, and tools used in this study. Statistical methods included the Mann-Kendall (MK) test with the Trend-free Pre-whitening (TFPW) process (Yue et al., 2002). The MK test and TFPW process were used to address the trends in the time series data. On the other hand, Pearson's *r* helped us to observe the relationships between time series.

2.1 Dataset and parameters

Definition of the mountainous and the lowland areas

To know the difference between the 120 stations including altitudes, this study used 1000 m as a threshold and separated all stations into two altitudinal groups, mountainous stations above 1000 m, and lowland stations below 1000 m. Nevertheless, according to Taiwan's legislative definition, the Soil and water Conservation Act, the mountainous areas should be areas with either altitudes larger than 100 m, or the slope larger than 5% (Executive Yuan, 2003). In addition, the Land Restoration Act of Taiwan and the National Spatial Development Plan (CEPD, 2010) restricted the mountainous areas as where the altitude is higher than 1500 m. Actually, the land between 100-1000m accounts for 33% of Taiwan, and areas above 1000 m another 33% of Taiwan (Lin et al., 2010), and the areas above 1000 m tends to have foggy forests and weather conditions, while it varies from the north to the south Taiwan (Su, 1984; Hsieh, 1994). Therefore, it was hard to follow above specific or legislative standard to distinguish the mountainous and the lowland areas in a scientific way, thus, this research used 1000 m as the border due to the standard from Shinohara et al. (2010).

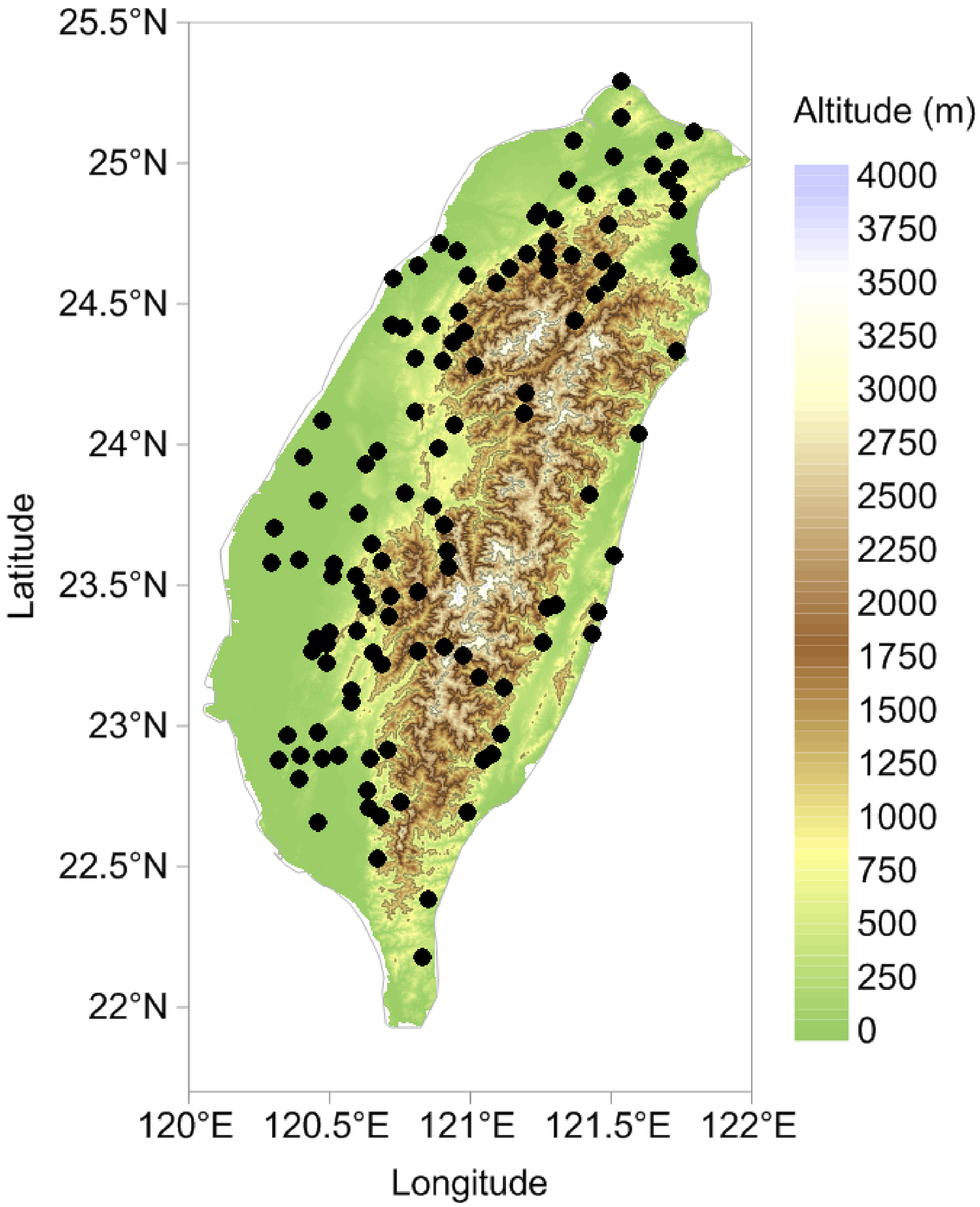

Figure 3. Spatial distribution of the 120 WRA stations

Rainfall data

Rainfall dataset were collected from the official records published by the Water Resource Agency (WRA) of Taiwan. The WRA installed 233 rain gauge stations around the island for water resource management (WRA, 2009). There are about 173 stations' data with hourly data and generally available for the period between 1978–2008. At these stations, rainfall is recorded with a resolution of 0.1 mm.

I excluded 113 stations due to incomplete records more than three years during the study period; in which, I assumed a missing month as the missing data was more than three days, and I regarded the data for the year as missing when the missing months exceeded three. Consequently, I remained 120 stations for the analysis (Fig. 3). The stations covered the whole Taiwan. There are 16 and 104 stations locating in the mountainous areas with the altitude of > 1000 m and the lowland areas with the altitude of < 1000 m, respectively. As well, among the 120 stations, 95 and 25 stations located in the west and the east of the Central Mountain Region (CMR), respectively.

Rainfall parameters

Here I use two parameters for examining rainfall characteristics, the daily rainfall intensity (η) and the ratio of rain days (λ). Theoretically, rainfall amount is a function of the two parameters (e.g., Katz and Parlange, 1998; Furrer and Katz, 2008), which are useful not only for studying rainfall variation, but also for hydrological applications, e.g. soil moisture dynamics (Kumagai et al., 2009; Shinohara et al., 2010).

The daily rainfall intensity (η) is derived from the amount of rainfall in a given period. The ratio of rain days (λ) is calculated from the ratio of rain days to a given period, λ is therefore proportional to rain days, representing the rainfall duration in a given period. The two parameters are given by:

$$\eta = \frac{\mathrm{Pr}}{D_{\mathrm{Pr}}} \quad \text{…Equation 4}$$

$$\lambda = \frac{D_{\mathrm{Pr}}}{D} \quad \text{…Equation 5}$$

According to the definition by the Central Weather Bureau (WRA, 2009), Pr is the amount of rainfall (mm) in a given period, D is the number of days in a given period, and D_{Pr} is the number of rain days in a given period. In this case, a rain day is defined as a day when the daily rainfall exceeds 0.1 mm/day.

Aimed to know spatial and temporal variations of rainfall, the parameters would be examined in following processes. First, this study calculated Pr, η, and λ at each station for each year from rainfall records; and then averaged to obtain 31-year mean Pr, η, and λ at each station from 1978 to 2008, i.e. $\overline{\mathrm{Pr}}$, $\bar{\eta}$, and $\bar{\lambda}$.

Then, this study examined the correlations not only between $\overline{\mathrm{Pr}}$ and $\bar{\eta}$, but also between $\overline{\mathrm{Pr}}$ and $\bar{\lambda}$. This helps this study to examine whether inter-annual rainfall variation is determined by spatial variation in rainfall intensity (η), or in ratio of rain days (λ), this is in accordance with Shinohara et al. (2010).

2.2 Relationship analysis

Here, I would first examine spatial variations in Pr, η, and λ. To this aim, I calculated Pr, η, and λ at each station for each year from raw rainfall data, and then averaged to obtain the period mean Pr, η, and λ at each station from 1978 to 2008, i.e., $\overline{\mathrm{Pr}}$, $\bar{\eta}$, and $\bar{\lambda}$, respectively. On the basis of these data, I had mapped the interpolated rainfall characteristics to represent spatial variations in $\overline{\mathrm{Pr}}$, $\bar{\eta}$, and $\bar{\lambda}$ for the whole Taiwan. I finally examined the correlation between $\overline{\mathrm{Pr}}$ and $\bar{\eta}$ and between $\overline{\mathrm{Pr}}$ and $\bar{\lambda}$ to determine whether the spatial variation in $\overline{\mathrm{Pr}}$ was explained by $\bar{\eta}$ or $\bar{\lambda}$ (Shinohara et al., 2010).

Second, I examined year-to-year variations in Pr, η, and λ for the study period. I verified the correlations between Pr and η and between Pr and λ for each station to determine whether the year-to-year variation in Pr was explained by η or λ (Shinohara et al., 2010).

Third, I examined temporal trends in Pr, η, and λ during the period (Shinohara et al., 2010). As well, I evaluated the trends using the Mann-Kendall test (Mann, 1945; Kendall, 1975; detailed in *Section 2.3*) and investigated whether significant trends were commonly observed or not. Then, I would examine the correlation in Mann-Kendall's statistical parameter between Pr and η, and between Pr and λ to determine whether the trends in Pr were explained by η or λ. Throughout the analysis, I investigated whether the results differed between lowland and mountainous areas.

2.3 Trend analysis

To analysis the trend in a time series, there are many statistical approaches available, such as Mann-Kendall (MK) test (Mann, 1945; Kendall, 1975), intervention analysis model (Peña et al., 2000; Box et al., 2008), and Hilbert–Huang transform (Wu et al., 2007; Huang and Wu, 2008; Rudi et al., 2010). This study applied the MK test, which is a rank-based non-parametric statistical method and very useful to detect trend in time series. As well, the MK test provided the statistic of a trend, based on statistical principle, and I might verify whether the trend was significant or not, further, the MK test is widely used in hydrological researches, while other trend analytical methods were not. In addition, Yue et al. (2002) and Rivard and Vingneault

(2009) report that serial correlation, which refers to a non-independent residual besides a trend, would disturb results of the MK test, leading to a disproportionate rejection of no trend. Therefore, to avoid the wrong recognition of a trend, the trend-free pre-whitening (TFPW) procedure is suggested to apply on uni-variate hydrological time series (see Yue et al., 2002). Here this study assumed a series, X_t, and the TFPW procedure is show below (Shinohara et al., 2010).

Trend-free prewhitening procedure

First, remove the trend in X_t using Sen's slope, *b*, and get the residual, X'_t,

$$X_t' = X_t - bt$$

…Equation 6

$$b = \text{Median}\frac{(X_J - X_L)}{(J - L)}, \forall L < J$$

…Equation 7

Second, prewhitening the residual (X'_t) using the lag-1 autocorrelation coefficient, Φ_1, thus we can get the prewhitened residual $Y't$,

$$Y'_t = X_t' - \phi_1 X'_{t-1}$$

...Equation 8

where

$$\phi_1 = \frac{\text{cov}(X_t, X_{t+1})}{\text{var}(X_t)} = \frac{\sum_{t=1}^{n-1}[X_t - E(X_t)][X_{t+1} - E(X_t)]}{\sum_{t=1}^{n}[X_t - E(X_t)]^2}$$

...Equation 9

Note that the Y'_t is actually a residual series with less AR(1), i.e., more like an independent series. I did not apply a complicated prewhitening procedure, such as the transfer function in Box and Jenkins (2008) or Tiao (Peña et al., 2000), which would be much rigor with rigorous mathematical and statistical procedures. While I followed the methodology of Yue et al. (2000), the effectiveness is to verify the trend and reduce influences by the residual with autocorrelation.

Third, put back b in the pre-whitened series,

$$Y_t = Y_t' + bt$$

…Equation 10

Mann-Kendall test

Finally, we may apply the MK test on the processed series, Y_t, to detect the significance of trend. The null hypothesis H_0 is that a series is independent and identically distributed; the alternative hypothesis H_1 is that a monotonic trend existing in a series. The statistics of standardized test Z is

$$Z = \begin{cases} \dfrac{S-1}{\sqrt{var(S)}} & \text{, if S} > 0 \\ 0 & \text{,if S=0} \\ \dfrac{S+1}{\sqrt{var(S)}} & \text{, if S<0} \end{cases}$$

…Equation 11

$$\mathrm{var}(S) = \frac{n(n-1)(2n+5) - \sum_{m=1}^{n} t_m m(m-1)(2m+5)}{18}$$

…Equation 12

in which the statistic of Kendall’s tau, S, is,

$$S = \sum_{i=1}^{n-1} \sum_{j=n+1}^{n} \mathrm{sgn}(Y_j - Y_i)$$

…Equation 13

$$\mathrm{sgn}(\theta) = \begin{cases} 1 \text{ , if } \theta > 0 \\ 0 \text{ , if } \theta = 0 \\ -1, \text{ if } \theta < 0 \end{cases}$$

…Equation 14

Note that n is the number of data points, m is the number of tied groups (a tied group is a set of sample data having the same value), and t_m is the number of data points in the m^{th} group. E.g. in a sequence {1, 9, 4, 9, 4, 4, 5}, this study have n=7, m=2, t_1=2 for the tied value 9, and t_2=3 for the tied value 4.

The probability value, p, is

$$p = \frac{1}{\sqrt{2\pi}} \int_{-\infty}^{Z} e^{\frac{-t^2}{2}} dt$$

…Equation 15

The standardized MK statistic Z follows the standard normal distribution with mean of zero and variance of 1. The null hypothesis H_0 is accepted if $-Z_{1-\frac{\alpha}{2}} \le Z \le Z_{1-\frac{\alpha}{2}}$, where $\pm Z_{1-\frac{\alpha}{2}}$ are the 1-α/2 quantiles of the standard normal distribution corresponding to the given significant level, α, for the test. E.g. for an α=0.05, $Z_{1-\frac{\alpha}{2}}$ equals to 1.96. Herein this study use α depending on the situations as 0.1, 0.05, and 0.001 in this study.

2.4 Time series analysis and forecasting

I had induced the TFPW procedure to obtain the tendency, which was upward or downward, in a time series of rainfall, but I would like to infer its future changes. Thus, the *time series analysis* was applied. Time series analysis is a classical method to build stochastic models, and it is suitable for uni-variate and multivariate statistics widespread in environmental studies, economic models, business estimation, and engineering, etc. (Tiao et al., 1975; Box et al., 2008; Mills et al., 2011). Box et al. (2008) illustrate five areas of application, including forecasting series, transfer function for input and output variable, intervention for uncommon events, interrelationships among related variables, and control schemes. Here I simply introduced the processes for analyzing and building a stochastic model through time series analysis.

Tentative specification on data

First of all, I observed the time-series plot to check the pattern leaning to stationary or non-stationary, which leads to whether the differencing is required or not, e.g. first-order differencing, $\nabla^d Z_t = Z_t - \theta_1 Z_{t-1} = (1-\phi_1 B)Z_t$, (d=1, ϕ_1=1). Note that the B is hence called *backward operator*, which refers a backward differencing and follows rule of linear calculation (see Box et al., 2008); further, a_t is a white noise and identically distributed (i.e., i.i.d.) with mean and variation of the series. Second, I examined the autocorrelation function at lag-*k* (ACF, ρ_k, Eq. 16) and partial autocorrelation function (PACF, ϕ, Eq. 17) of the series.

$$\rho_k = \mathrm{cov}[Z_t, Z_{t+k}]$$

…Equation 16

$$\begin{bmatrix} 1 & \rho_1 & \cdots & \rho_{k-1} \\ \rho_1 & 1 & \cdots & \rho_{k-2} \\ \vdots & \vdots & \vdots & \vdots \\ \rho_{k-1} & \rho_{k-2} & \cdots & 1 \end{bmatrix} \begin{bmatrix} \phi_{k1} \\ \phi_{k2} \\ \vdots \\ \phi_{kk} \end{bmatrix} = \begin{bmatrix} \rho_1 \\ \rho_2 \\ \vdots \\ \rho_k \end{bmatrix}$$

…Equation 17

If either of the two functions had cutouts within a specific time lag, e.g., *k* period, I might fit a lag *k* moving-average (MA) or an auto-regressive (AR) model according to the ACF or PACF cut-out, respectively. An AR(k) model forms as $\phi(B)\tilde{Z}_t = a_t$ toward Z_{t-k} and a MA(k) model forms like $\tilde{Z}_t = \theta(B)a_t$ toward $a_{t\text{-}k}$. Note that since a_t is identically distributed, the ACF and the PACF of a_t should be very insignificant or near zero for all time lag (for any lag period).

Fit model and estimate parameters

With the order of differencing, ACF, and PACF cut-off, I would fit a model combining AR and MA model. Thus a general form, autoregressive integrated moving average model (ARIMA) with AR (*P*), MA (*Q*), and a differencing order (*d*), is derived as $\phi(B)\nabla^d Z_t = \theta(B)a_t$. E.g. $(1\text{-}0.5B)(1\text{-}B^2)Z_t=(1\text{-}0.2B\text{-}0.23B^4)a_t$ is called a ARIMA (1,2,4) model for the AR order as one, differencing order is two, and the MA order as four. The parameters of an ARIMA model could be estimated from such as Bayesian, conditional likelihood, exact likelihood, or maximum likelihood, etc. Herein this study, I took the exact likelihood the most for parameter estimation in fitted ARIMA model. Note that the parameters in an ARIMA model should exceed the significant level (i.e., t value >1.96 at 0.05 level); on the other hand, the R^2 of the model would not be critical comparing to linear model owing to the model should revised according to the residual (Box et al., 2008).

Diagnosis check on residual

A fitted ARIMA model has same properties with other statistical model, which is the residual analysis. If the residual did not present as independent series, i.e., both ACF and PACF were insignificant, then, the model should be modified. The method of modifying a model is simply; first fit another model to the residual series, and then apply the residual to the original model. E.g. a model, $(1-B)Zt=(1+0.6B)c_t$, while the residual c_t is not independent and could be fitted as $(1-B)c_t=(1-0.8B)a_t$, where a_t is independent. Thus, we might obtain $(1-B)(1-B)Z_t=(1+0.6B)(1-0.8B)a_t$.

Intervention analysis

Uncommon events in a time series play as *outliers* easily, their influences can be categorized in three types, which are additive outlier (AO), innovational outlier (IO), and level shift (LS), these outliers can be added into a fitted ARIMA model. According to the study by Box and Tiao (1975), at given time, *T*, when outlier appears, AO is a pulse as $wP_t^{(T)}$, where w is the magnitude of the pulse, and $P_t^{(T)}$ would be 1 when $t=T$, and 0 otherwise; IO is a $w(1-\delta B)^{-1} P_t^{(T)}$, where the δ controls the IO to be a line or curve, and $P_t^{(T)}$ would be 1 when $t=T$, and 0 otherwise; LS is a step upward or downward with a time series, the component of LS appears as the IO one, while the $P_t^{(T)}$ would be 1 when t is larger than or equals to T. However, the outliers should be some abnormal incidents during the study period, and we could acquire outliers in time series according to fitted model. Note that here the T refers to time; do not confuse this with the transpiration one in former introduction part.

3

Annual variations in rainfall characteristics

This chapter analyzed spatial and temporal variations in annual rainfall characteristics in Taiwan. First, this chapter reported on spatial variation and year-to-year relationship between rainfall characteristics. Second, it was to find differences in rainfall characteristics relationships between lowland and mountainous areas. Third, it examined long-term trends of rainfall characteristics to look at whether a significant trend existed or not at each station. Finally, we could discuss about some potential impacts of changes in rainfall characteristics on hydrological cycle in Taiwan.

3.1 The patterns of long-term period means of rainfall characteristics

Figure 4 showed spatial distributions of $\overline{\mathrm{Pr}}$, $\overline{\eta}$ and mean D_{Pr}, which was proportional to $\overline{\lambda}$. $\overline{\mathrm{Pr}}$ ranged between 1214 mm for station #42 and 4749 mm for station #11, the former was in the central-west and the latter was in the north. $\overline{\eta}$ varied between 11.7 mm/day for station #102 and 34.5mm/day for station #82; the former was in the north, and latter was in the southwest. $\overline{\lambda}$ ranged between 0.19 (i.e., D_{Pr}=68 days) for station #57 at central-west and 0.58 (i.e., D_{Pr} = 213 days) for station #11. The larger values of $\overline{\mathrm{Pr}}$, $\overline{\eta}$ and mean D_{Pr} were mostly found around the mountainous areas along the central mountain region (CMR) (Fig. 4).

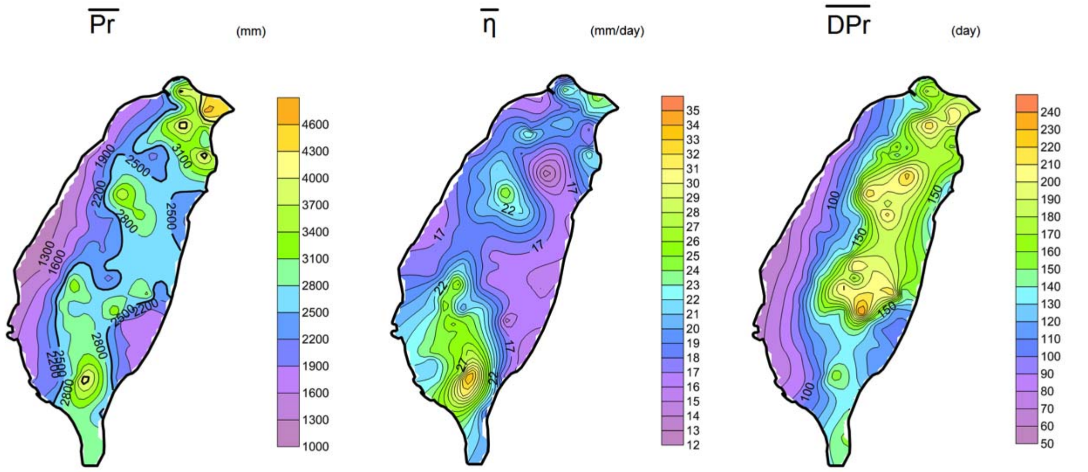

Figure 4. Contour map for annual rainfall characteristics of $\overline{\mathrm{Pr}}$ (mm), $\overline{\eta}$ (mm/day), and mean $\overline{D_{\mathrm{Pr}}}$ at 120 stations through 1978 to 2008.

In addition, I had obtained significant relationships in $\overline{\mathrm{Pr}}$-altitude (r=0.34, p<0.01) and $\overline{\lambda}$-altitude (r=0.68, p<0.01), while the relationship in $\overline{\eta}$-altitude (r=0.08, p>0.1) and $\overline{\eta}$-$\overline{\lambda}$ (r=0.08, p>0.1) were not significant (see Table 1). Large $\overline{\mathrm{Pr}}$ values were observed at stations on slopes in the west of the CMR, which would be partly explained by the prevalent wind (e.g., northeastern and southwestern monsoon) in the mei-yu season, typhoons, and orographic rain (Chen and Chen, 2003; Guan et al., 2009). In addition, we could see localized heavy rainfall events in mountainous areas owing to the orographic effects, such as orographic lifting, orographic blocking, and thermally driven circulations (Chen et al., 1991; Johnson and Bresch, 1991;

Akaeda et al., 1995; Li et al., 1997; Chen, 2000; Yeh and Chen, 2002).

On the other hand, large $\overline{\mathrm{Pr}}$ values observed in northeastern hilly areas would be partly explained by the advection, and the frontal systems (e.g., Mei-yu season) in these areas (Yeh and Chen, 1998; Chen and Huang, 1999; Yen and Chen, 2000; Chen and Chen, 2003; Yeh and Chen, 2004; Chen et al., 2005). These different meteorological systems occurring between mountain and lowland could be a reason for the differences of the determining factors of the spatial variations in Pr.

Table 1. Correlation matrix for 31-year period mean rainfall characteristics and spatial variables

	$\overline{\mathrm{Pr}}$	$\bar{\eta}$	$\bar{\lambda}$	Elevation (m)	Longitude (E)	Latitude (N)
$\overline{\mathrm{Pr}}$	1.00					
$\bar{\eta}$	0.54	1.00				
$\bar{\lambda}$	0.72	-0.08	1.00			
Elevation (m)	0.34	0.08	0.68	1.00		
Longitude (E)	0.49	-0.34	0.70	0.11	1.00	
Latitude (N)	0.18	-0.33	0.35	0.03	0.63	1.00

On the other hand, large $\overline{\mathrm{Pr}}$ values observed in northeastern hilly areas would be partly explained by the advection, and the frontal systems (e.g., Mei-yu season) in

these areas (Yeh and Chen, 1998; Chen and Huang, 1999; Yen and Chen, 2000; Chen and Chen, 2003; Yeh and Chen, 2004; Chen et al., 2005). These different meteorological systems between mountain and lowland could be a reason for the differences of the determining factors of the spatial variations in Pr.

Cue of the pattern of Pr in η or λ

To examine factors determining spatial variations in $\overline{\mathrm{Pr}}$, I calculated their Pearson correlation coefficients (*r*) between $\overline{\mathrm{Pr}}$, $\overline{\eta}$, $\overline{\lambda}$ and the altitude. In all 120 stations, significant and positive relationships were found in $\overline{\mathrm{Pr}}$-$\overline{\eta}$ (*r*=0.54, p<0.01), $\overline{\mathrm{Pr}}$-$\overline{\lambda}$ (*r*=0.72, p<0.01), $\overline{\mathrm{Pr}}$-altitude (r=0.34, p<0.01), and $\overline{\lambda}$-altitude (r=0.68, p<0.01). Note that the relationship between $\overline{\mathrm{Pr}}$-$\overline{\lambda}$ was stronger than $\overline{\mathrm{Pr}}$-$\overline{\eta}$, thus I would suggest that annual rainfall amounts were generally more dependent on number of rain days than daily rainfall intensity in annual and whole Taiwan scale. The correlation coefficients (r) of $\overline{\mathrm{Pr}}$-altitude and $\overline{\lambda}$-altitude suggested that rainfall amount and rain days normally increased with increases in elevation probably owing to the orographic effects.

3.2 Comparison between the mountainous and the lowland areas

To understand the differences in the spatial variations between the mountainous and the lowland areas, I examined the relationships in rainfall characteristics between the mountainous stations and the lowland stations (Fig 5). I observed a stronger correlation between $\overline{\mathrm{Pr}}$ and $\overline{\lambda}$ (r=0.72, p<0.01) than between $\overline{\mathrm{Pr}}$ and $\overline{\eta}$ (r=0.54, p<0.01) when using the whole dataset for the 120 stations. In lowland areas (Fig. 5c and 5d), I obtained different results from those of mountainous areas (Fig. 5a and 5b). The correlation was stronger for the relationship between $\overline{\mathrm{Pr}}$ and $\overline{\eta}$ (R^2=0.646, p<0.001) than between $\overline{\mathrm{Pr}}$ and $\overline{\lambda}$ (R^2=0.0615, p>0.05) These results suggest that $\overline{\eta}$ and $\overline{\lambda}$ both explained the spatial variation of $\overline{\mathrm{Pr}}$ in the lowland areas, but only $\overline{\eta}$ primarily explained the spatial variation of $\overline{\mathrm{Pr}}$ in the mountainous areas; this meet equivalently results from the previous study, e.g., Shinohara et al. (2010)

The orographic effects along the CMR could have strong impacts on spatial distribution of rainfall and been reported in Taiwan (Teng et al., 2000; Wu et al., 2002; Chen and Chen, 2003; Kerns et al., 2010). Owing to the orographic lifting, orographic blocking, and thermally driven circulations, I could see localized heavy rainfall events in mountainous regions (Chen et al., 1991; Johnson and Bresch, 1991; Akaeda et al., 1995; Li et al., 1997; Chen, 2000; Yeh and Chen, 2002). Further, tropical storms and typhoons affect spatial distribution of rainfall in Taiwan (Lee et al., 2006; Tsai and Lee, 2009). For example, Typhoon Herb (31^{th} July, 1996) brought considerably large amounts of rainfall in Taiwan with the maximum rainfall of 1094 mm/day in the western slopes of the CMR (Chen and Chen, 2003). On the other hand, lowland hills in the north tend to have higher rainfall because of the effects of the advection and the frontal systems with the relatively larger-spatial and longer-time scale (Yeh and Chen, 1998; Chen and Chen, 2003). There different meteorological system between mountain and lowland could be a reason for the differences of the determining factors of the spatial variations in Pr.

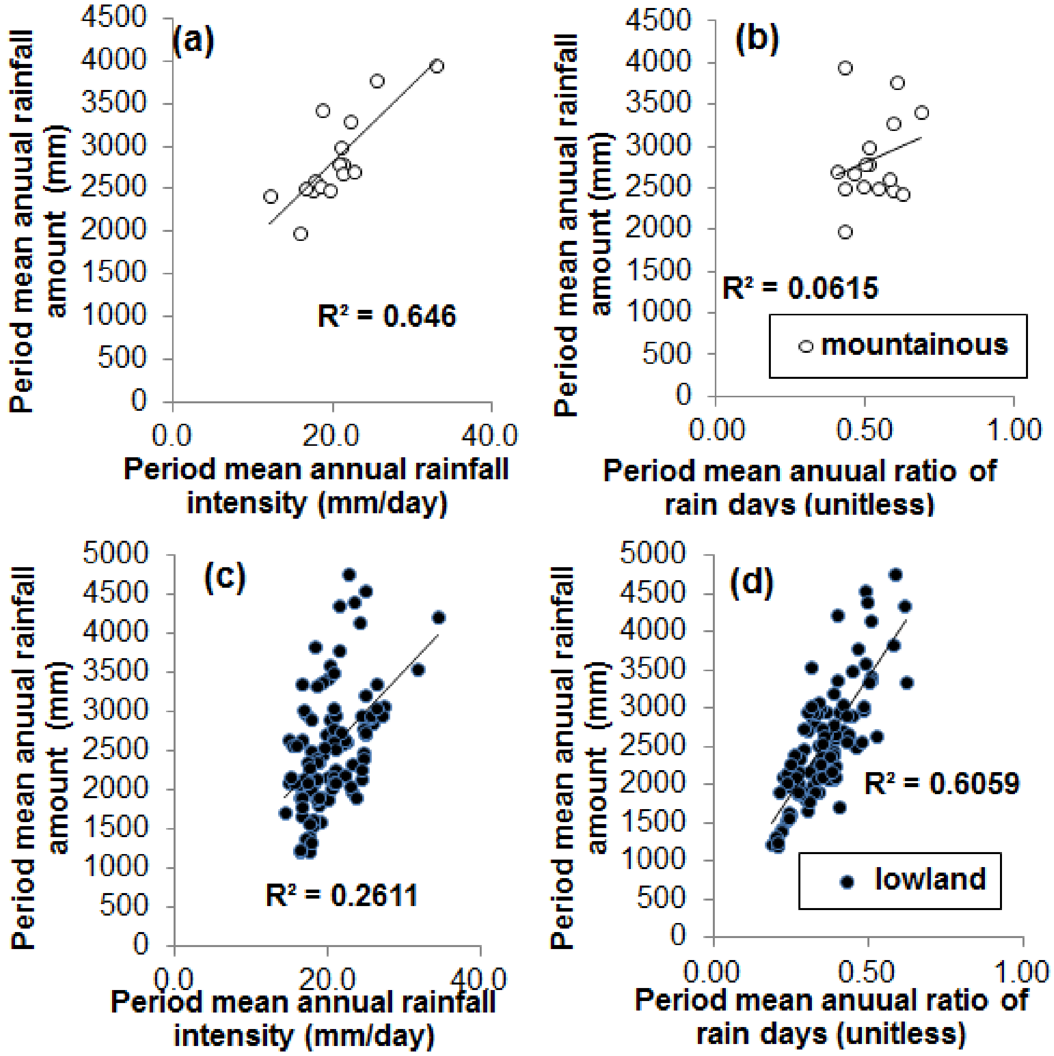

Figure 5. Relationships between period mean rainfall amount ($\overline{\mathrm{Pr}}$), period mean daily rainfall intensity ($\overline{\eta}$), and period mean ratio of rain days ($\overline{\lambda}$)

3.3 Year-to-year variation at each station

Aimed to see the changes at each station during the research period, I examined inter-annual correlations among annual Pr, η, and λ series at each station. Here I obtained significant ($p<0.01$) correlations between Pr and η for 91 stations (76%), and between Pr and λ for 58 stations (48%). The correlation was generally stronger in the relationship between Pr and η than in what between Pr and λ (Fig. 6). In Figure 6, the solid line represented the ratio of 1:1, and most stations located at the right-hand side of the line. Here, among the 120 stations, 110 stations (91.7%) had larger *r* value in Pr-η than those in Pr-λ, including 15 mountain stations and 95 lowland stations. Thus, the year-to-year variations in Pr were primarily explained by the year-to-year variations in η rather than by those in λ for both lowland and mountainous areas.

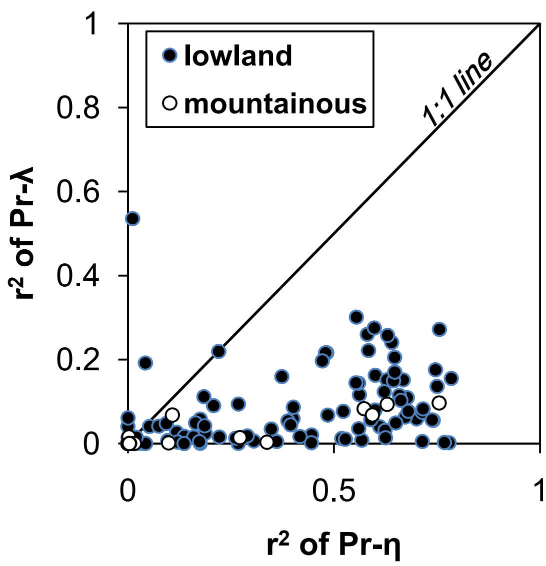

Figure 6. Comparison of correlation coefficient (r^2) between rainfall amount (Pr), ratio of rain days (λ) (r^2 of Pr-λ), and daily rainfall intensity (η) (r^2 of Pr-η) at 120 rain stations.

3.4 Trends in annual rainfall characteristics

Aimed to detect whether a rainfall series had a significant trend or not, this study applied the MK test on Pr, η, and λ series at 120 stations through TFPW (Fig. 7). Figure 7 also showed the spatial distribution of long-term trends and their statistics in Pr, η, and λ, respectively. Among the 120 stations, I observed significant ($p < 0.05$) trends in Pr for 13 stations; increased trends for 12 stations (10.0% of the total stations) and the decreased trend for one station (0.8% of the total stations). However, I did not observe significant trends in Pr for the other 107 stations. I observed significant trends in η for 37 stations (30.8% of the total stations) and in λ for seven stations (5.8% of the total stations). Thus, significant trends in Pr were not observed for most stations. These results were consistent for mountainous areas.

Among the 16 stations in the mountainous areas, I observed significant trends in Pr for only two stations. On the other hand, significant trends in η were observed for a number of stations. The stations with significant trends in Pr, η, or λ were generally located in west of the CMR. All the 13 stations with significant Pr trends were located in the west. Thirty-six among the 37 stations with significant η were located in the west. Two among the seven stations with significant λ trends were located in the west. Note that the long-term trends of Pr were not found at most of the stations (89.2 % of the total station), thus I would suggest that the change in Pr was not a general phenomenon in Taiwan.

Trends in Pr represented by Z statistics (Z_{Pr}) was more strongly correlated with trends in η represented by Z statistics (Z_{η}) than with trends in λ represented by Z statistics (Z_{λ}) (Fig. 8a, 8b). These results were consistent for the lowland and mountainous areas. Thus, trends in Pr were mainly corresponded to those in η rather than λ at most stations. Hsu and Chen (2002) examined trends in Pr for eight lowland stations in Taiwan. They observed significant increased trends in Pr for two stations with η. These trends were primarily caused by the trends in η, which agrees with our results.

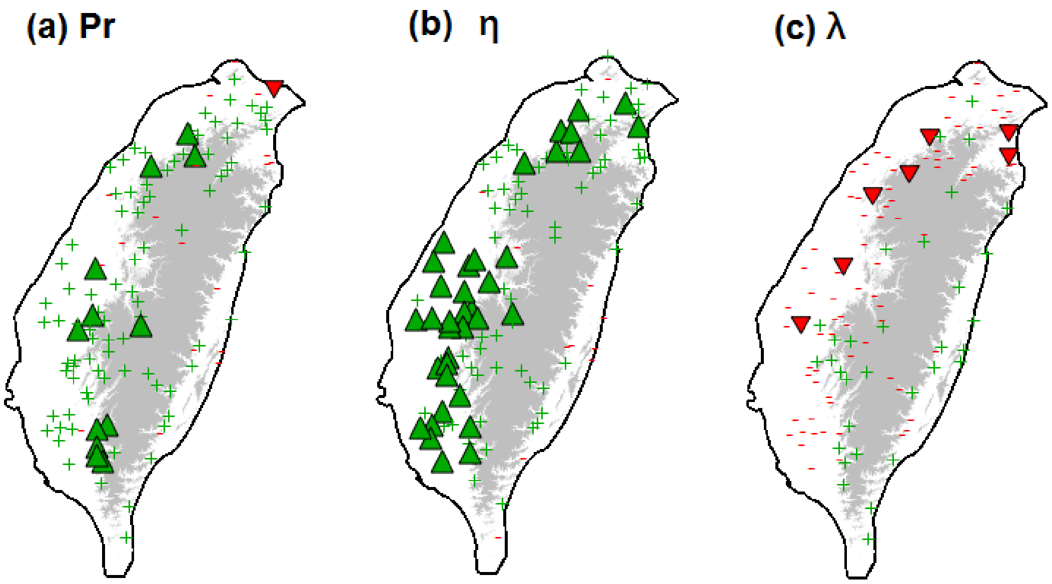

Figure 7. MK test of Pr, η, and λ trends' statistics of each station with TFPW process through 1978 to 2008. The plus (+) or minus (-) signs showed positive or negative trends without significant ($p>0.05$); at $p<0.05$ for solid triangles (▲, ▼); gray color indicated the mountainous areas.

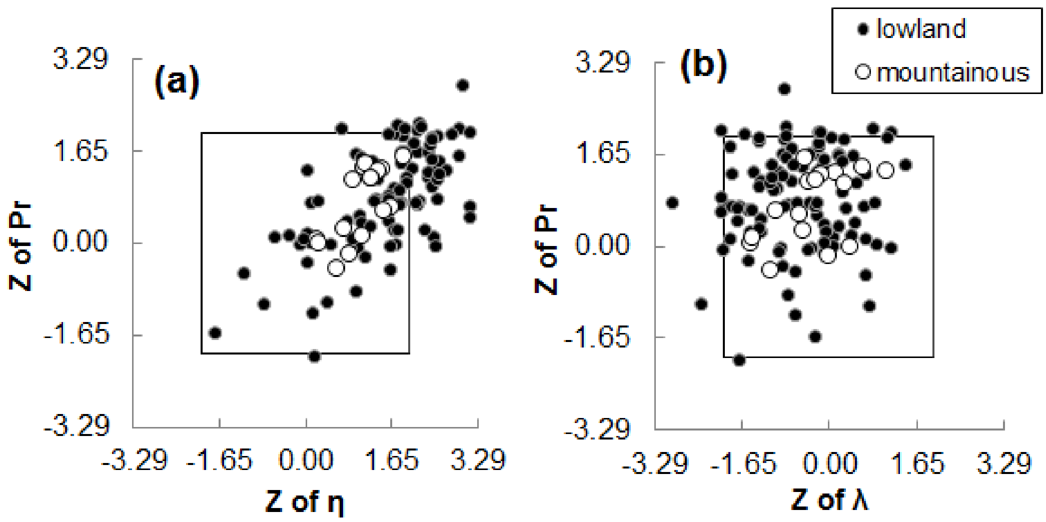

Figure 8. MK statistics comparison, (a) Z_{Pr} to Z_{η} and (b) Z_{Pr} to Z_{λ}; the solid line indicated the significant level ($p<0.05$) for each axis.

4

Seasonal variations in rainfall characteristics

In earlier chapter, I had examined annual rainfall characteristics during the past 31 years. In this chapter, I would like to analyze the variation in seasonal scale. According to previous study (e.g., Kumagai et al., 2010), I divided one year into four seasons; i.e., (i) the spring, March-April-May (ii) the summer, June-July-August, (iii) the autumn, September-October-November, and (iv) the winter, December-January-February. This chapter first presented the spatial variation in rainfall characteristics of each season. It analyzed the spatial tendency of Pr with its relationship to η or λ in each season. Then I would examine the temporal variation in rainfall characteristics to find out whether the Pr associated with η or λ in each season. As well, I used the TFPW process to test the trends in each seasons and its relationships with annual and seasonal variation, that is, aimed to clarify the question: which season's long-term rainfall changes could cause annual time-scale long-term rainfall changes?

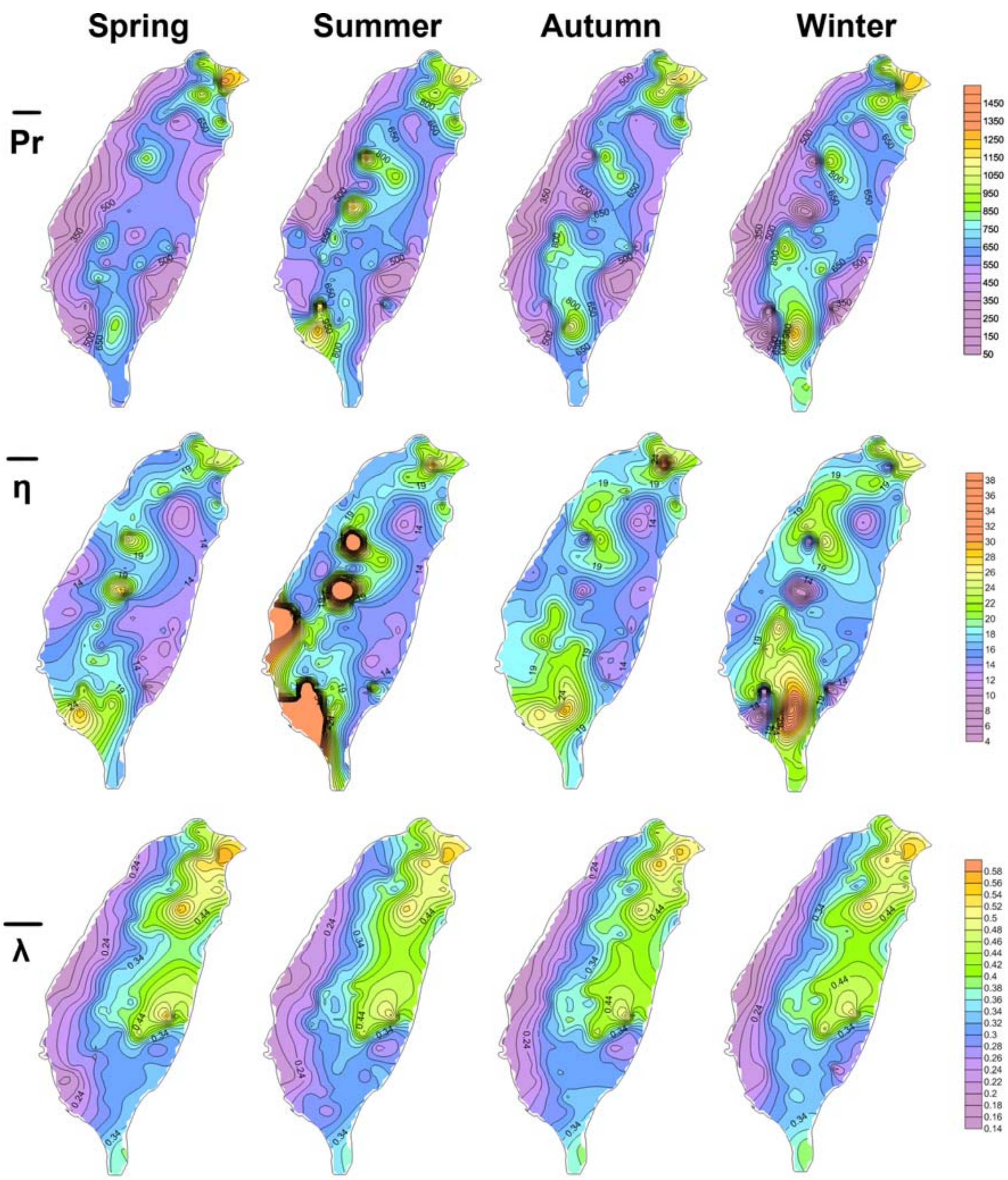

Figure 9. Seasonal period mean rainfall amount ($\overline{\mathrm{Pr}}$) (mm), period mean daily rainfall intensity ($\overline{\eta}$) (mm/day), and period mean ratio of rain days ($\overline{\lambda}$) at 120 stations through 1978 to 2008.

4.1 Spatial variation in seasonal rainfall characteristics

Spatial distributions of the 31-year period mean rainfall characteristics in each season were shown as Fig. 9. The large $\overline{\mathrm{Pr}}$, $\overline{\eta}$, and $\overline{\lambda}$ showed along the CMR, similar to the annual results in our previous chapter. To verify whether the spatial patterns in $\overline{\mathrm{Pr}}$ was corresponding to $\overline{\eta}$ or $\overline{\lambda}$, I examine the relationships between $\overline{\mathrm{Pr}}$, $\overline{\eta}$, and $\overline{\lambda}$ in the four seasons (Fig. 10, 11, 12, and 13). In the mountainous areas, $\overline{\mathrm{Pr}}$-$\overline{\eta}$ had a strong correlation (R^2=0.7509 in spring, R^2=0.717 in summer, R^2=0.5272 in autumn, and R^2=0.7784 in winter; $p<0.05$). By contrast, $\overline{\mathrm{Pr}}$ - $\overline{\lambda}$ (R^2=0.002 in spring, R^2=0.0025 in summer, R^2=0.4763 in autumn, and R^2=0.0266 in winter; $p>0.1$) did not show significance in their correlations (Fig. 10a, 11a, 12a, and 13a; and 10b, 11b, 12b, and 13b).

In the lowland areas, both $\overline{\mathrm{Pr}}$-$\overline{\eta}$ (R^2=0.3151 in spring, R^2=0.5118 in summer, R^2=0.5272 in autumn, and R^2=0.6493 in winter; $p<0.05$) and $\overline{\mathrm{Pr}}$-$\overline{\lambda}$ (R^2=0.4935 in spring, R^2=0.232 in summer, R^2=0.4763 in autumn, and R^2=0.3928 in winter; $p<0.05$) showed strong correlations (Fig. 10c, 11c, 12c, and 13c; 10d, 11d, 12f, and 13d). Consequently, during the four seasons, the spatial variation of Pr in the mountainous areas was explained by η, while η and λ determined the spatial variation in the lowland areas. Note that the $\overline{\eta}$ in summer time had larger values (about 120 mm/day at most) compared with other seasons (nearly 40 mm/day).

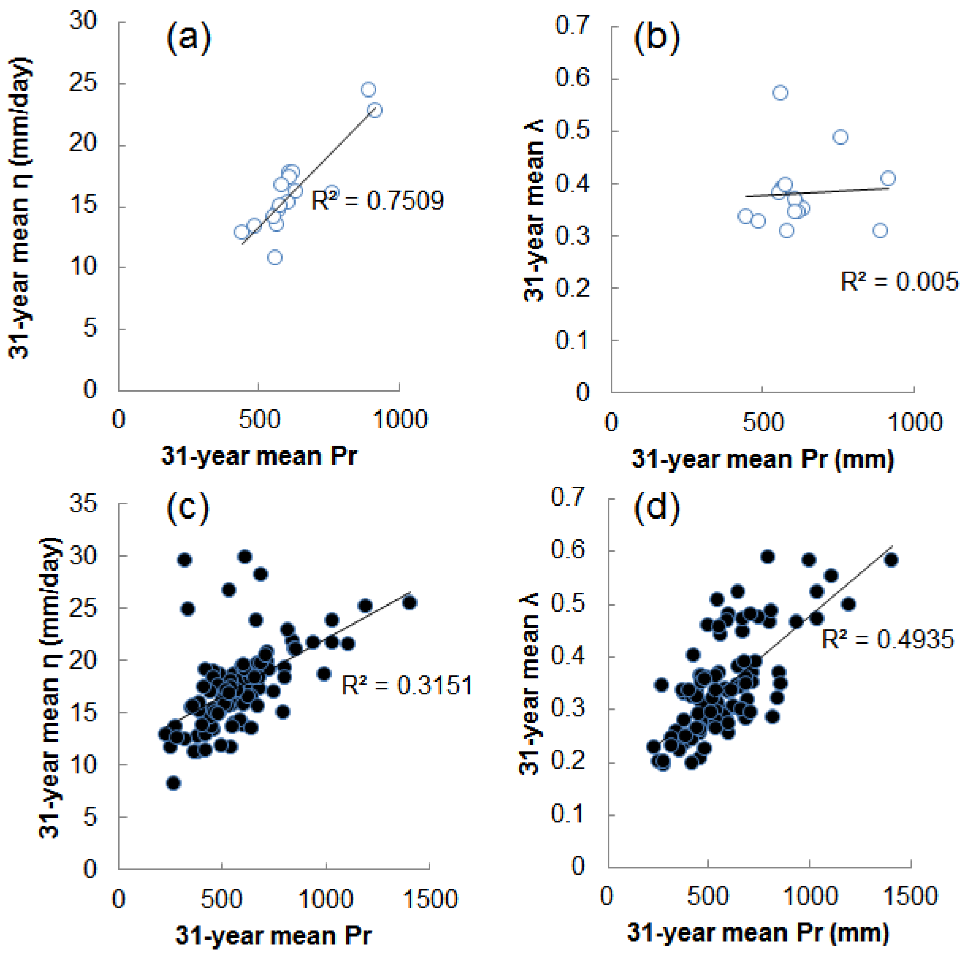

Figure 10. Relationships between the period mean rainfall amount ($\overline{Pr}$),the period mean daily rainfall intensity ($\bar{\eta}$), and the period mean ratio of rain days ($\bar{\lambda}$) in spring.

Note that the white and black dots represented the mountainous stations and the lowland stations, respectively.

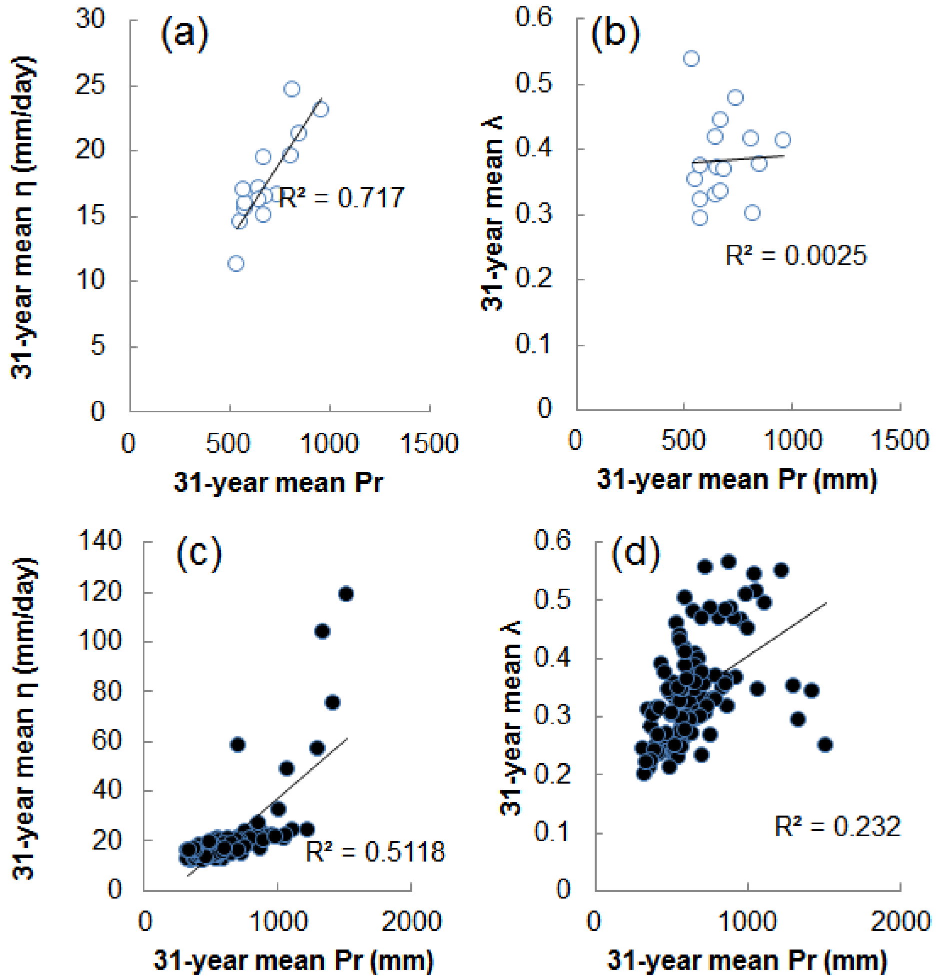

Figure 11. Relationships between the period mean rainfall amount ($\overline{Pr}$), the period mean daily rainfall intensity ($\overline{\eta}$), the period mean ratio of rain days ($\overline{\lambda}$) in summer.

Note that the white and black dots represented the mountainous stations and the lowland stations, respectively.

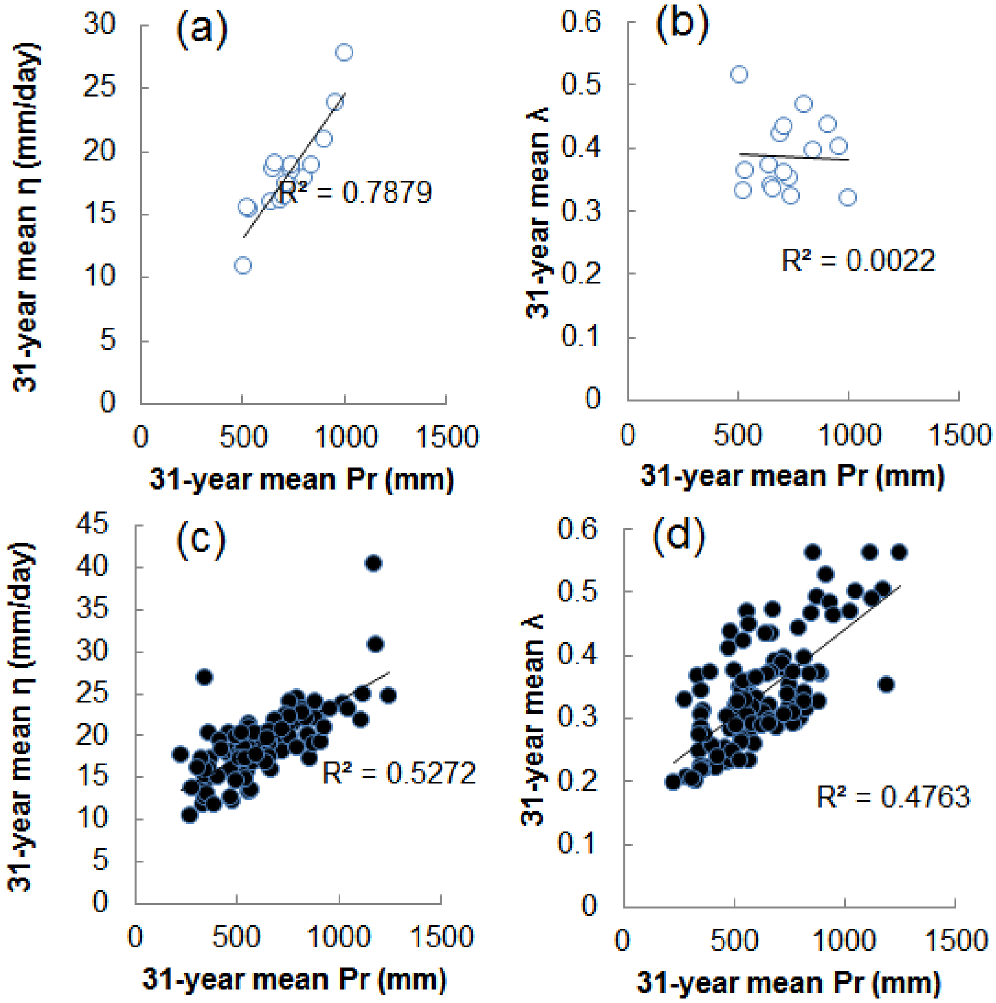

Figure 12. Relationships between the period mean rainfall amount ($\overline{Pr}$), the period mean daily rainfall intensity ($\overline{\eta}$), and the period mean ratio of rain days ($\overline{\lambda}$) in autumn.

Note that the white and black dots represented the mountainous stations and the lowland stations, respectively.

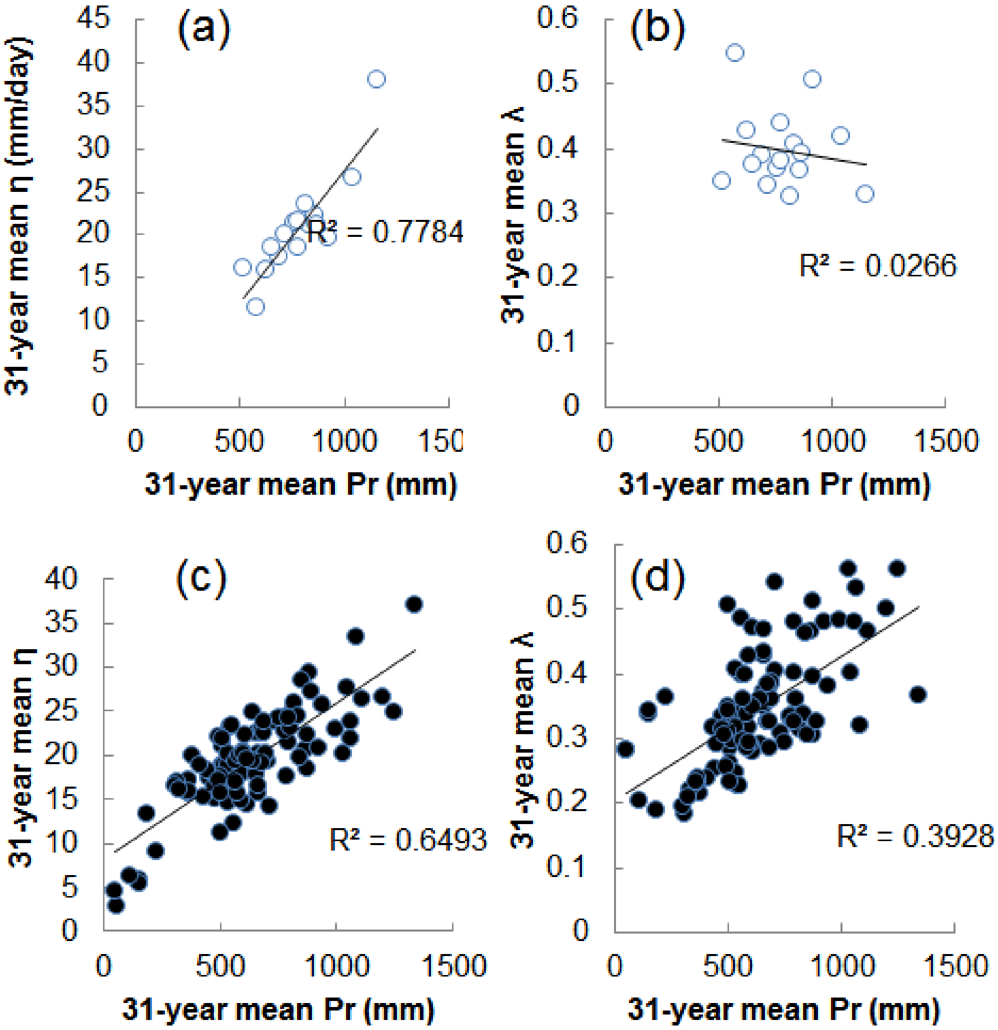

Figure 13. Relationships between the period mean rainfall amount ($\overline{Pr}$),the period mean daily rainfall intensity ($\overline{\eta}$), and the period mean ratio of rain days ($\overline{\lambda}$) in winter.

Note that the white and black dots represented the mountainous stations and the lowland stations, respectively.

4.2 Year-to-year seasonal variation

To verify whether the year-to-year variation of seasonal Pr was in accordance with η or λ, I examined correlation between Pr, η, and λ in each season at each station (Fig. 14). I calculated the correlation coefficients on Pr, η, and λ series in the 31 years, and every dot in Figure 14 represented one station. I obtained significant ($p<0.05$) correlations between Pr and η for 120 stations (100%) in spring, 116 stations (97%) in summer, 118 stations (98%) in autumn, and 120 stations (100%) in winter. Significant ($p<0.05$) correlations between Pr and λ were found in 108 stations (90%) in spring, 109 stations (91%) in summer, 110 stations (92%) in autumn, and 114 stations (95%) in winter, respectively. The correlation was generally stronger in the relationship between Pr and η than in what between Pr and λ (Fig. 14). The dots in Fig. 14 were mostly located in the right-hand side of the 1:1 line, leaning to the *r* of Pr-η side; these results were consistent for lowland and mountainous areas. Thus, the year-to-year variations in seasonal Pr were primarily explained by the year-to-year variations in seasonal η rather than by those in seasonal λ for both lowland and mountainous areas.

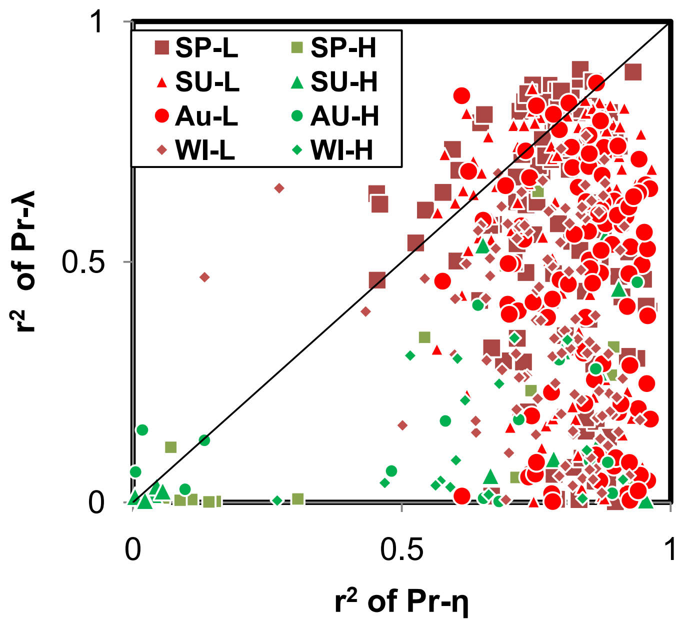

Figure 14. Comparison of correlation coefficient (*r*) between seasonal rainfall amount (Pr), seasonal ratio of rain days (λ) (r of Pr-λ), and seasonal daily rainfall intensity (η) (r of Pr-η) at 120 rain stations.

4.3 Trends in seasonal rainfall characteristics

To detect whether seasonal rainfall series had significant trends or not, I applied the MK test on Pr, η, and λ series at 120 stations through TFPW (Fig. 15). The results of trend analysis in the four seasons showed different patterns with those of annual time-scale (Fig. 7). Figure 15 showed the spatial distribution of long-term trends and their statistics in seasonal rainfall characteristics in spring, summer, fall, and winter, respectively.

Trends analysis

Among the 120 stations, I first observed significant ($p<0.05$) trends in year-to-year seasonal Pr; nine stations (7.5% of all stations) decreased in spring, five stations (4.2% of all stations) increased in summer, five stations (4.2% of all stations) increased and two stations (1.7% of all stations) decreased in winter.

Second, in examinations of long-term seasonal η, we may see one stations (0.8% of all stations) had increased trends and eight stations (6.7% of all stations) decreased in spring, nine stations (7.5% of all stations) increased in summer. Four stations (3.3% of all stations) increased in autumn. As well, 11 stations (9.2% of all stations) increased and one station (0.8% of all stations) decreased in winter.

Third, in λ examinations, we may find 15 stations (12.5% of all stations) decreased in spring while one stations (0.8% of all stations) increased. Four stations (3.3% of all stations) increased in summer while five stations (4.2% of all stations) decreased. Two stations (1.7% of all stations) increased in autumn while 11 (9.2% of all stations) stations decreased. As well, three stations (2.5% of all stations) increased while six stations (5% of all stations) decreased in winter.

I could not suggest significant trends in seasonal rainfall characteristics as a general phenomenon in the whole Taiwan. In Pr, the most changed stations showed in spring accounting for 7.5% of total stations, while the rest 92.5% of stations did not changed. On the other hand, the low ratios of changed stations in η and λ also met that the change was not widespread in the whole Taiwan. On the other hand, we could see different long-term trends in each season. Although long-term trend in Pr in spring showed mostly decreasing trends, the long-term trend in Pr in summer, winter showed mostly increasing trends. Overall, characteristics of long-term trend of rainfall and their spatial distribution could be different between annual and seasonal time-scale.

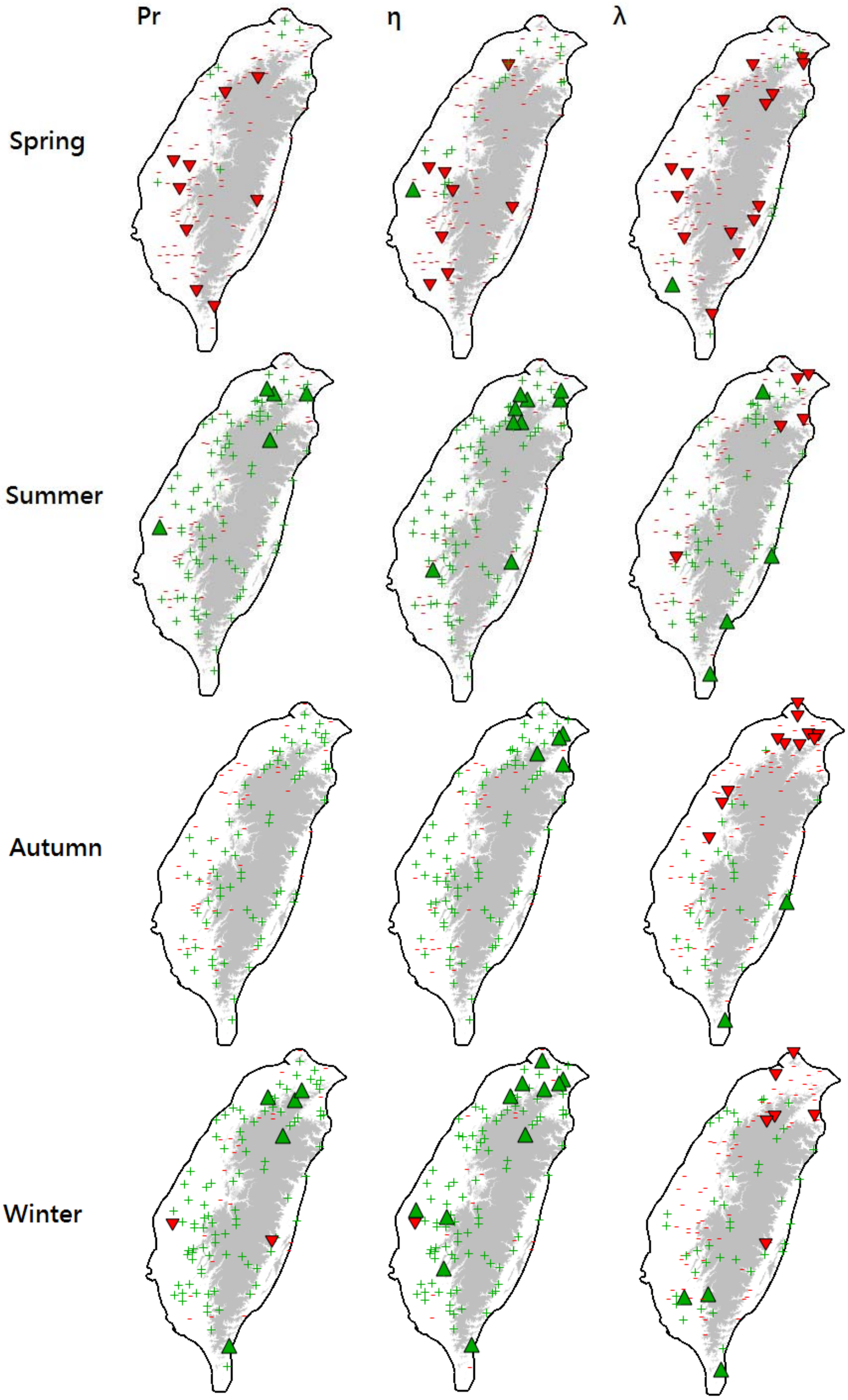

Figure 15. Seasonal trends in rainfall amount (Pr), daily rainfall intensity (η), and ratio of rain days (λ). "+", "-", "▲", and "▼"showed positive, negative, significant positive, and significant negative ($p<0.05$); gray indicated the mountainous areas.

Comparison between the mountainous and the lowland stations

In annual analysis, we did not obtain obvious discrepancy of significant trends between the mountainous and the lowland stations. Here I examined the seasonal trends and their spatial distribution between the mountainous and the lowland stations. In the 16 mountainous stations, we obtained only one station showed significance in summer Pr, winter Pr, summer η, winter η, and spring λ, respectively. The rest stations with significant trends were located in the 104 lowland stations. Therefore, the changes in seasonal rainfall characteristics were located in the lowland areas rather than the mountainous areas. Nevertheless, the number of stations in the mountainous areas was essentially less than the lowland one, thus, in order to understand the mountainous case, more rain stations would be necessary.

Cue of trends in seasonal Pr with those in seasonal ones

The trends in annual Pr had strong relationships with those in annual η, and hence we could consider the seasonal case as the annual one as well. To see the relationships among seasonal rainfall characteristics, here I made a tentative diagnosis using correlation coefficients between trends of Pr, η, and λ at each station (Fig. 16 and 17).

In the seasonal trends analysis, Pr in each season showed significant ($p<0.05$)

relationships with η and λ equivalently, in which seasonal Pr had stronger relationships with seasonal η than seasonal λ generally (Fig. 16, 17).

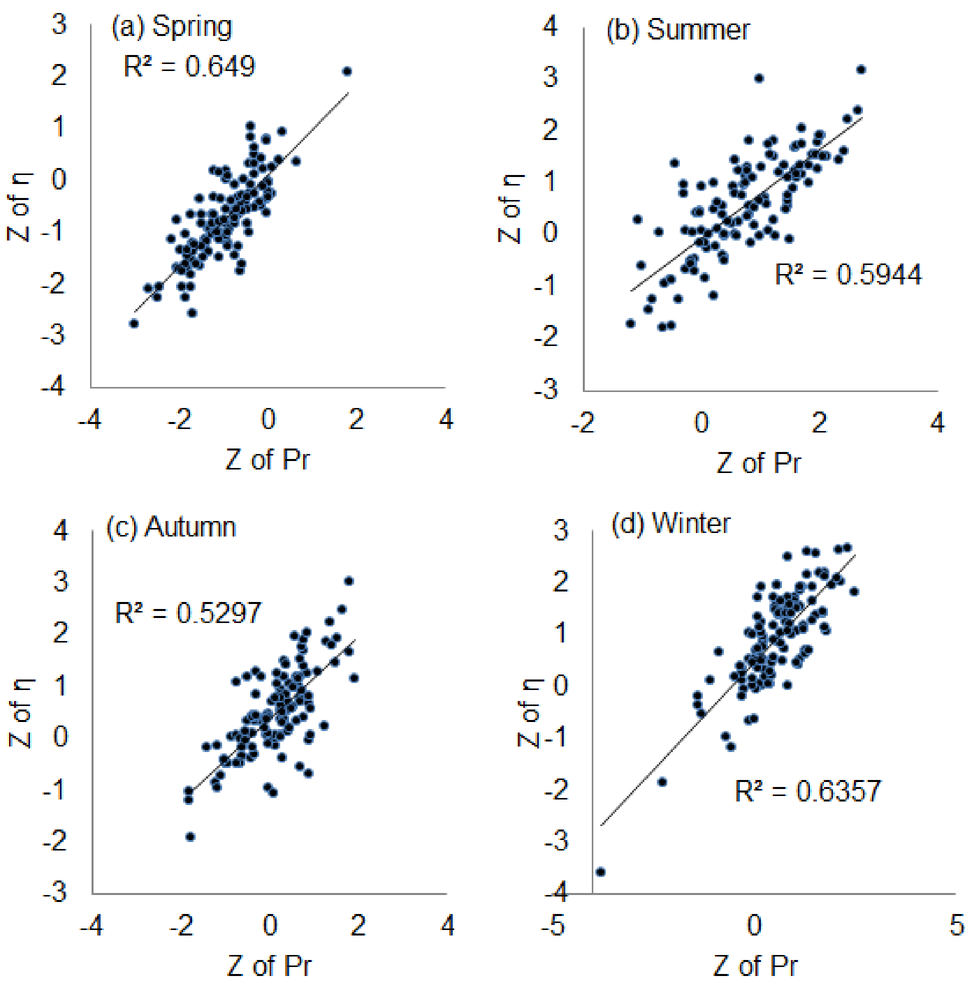

Figure 16. Comparison of seasonal trends statistics (Z) between Pr and η

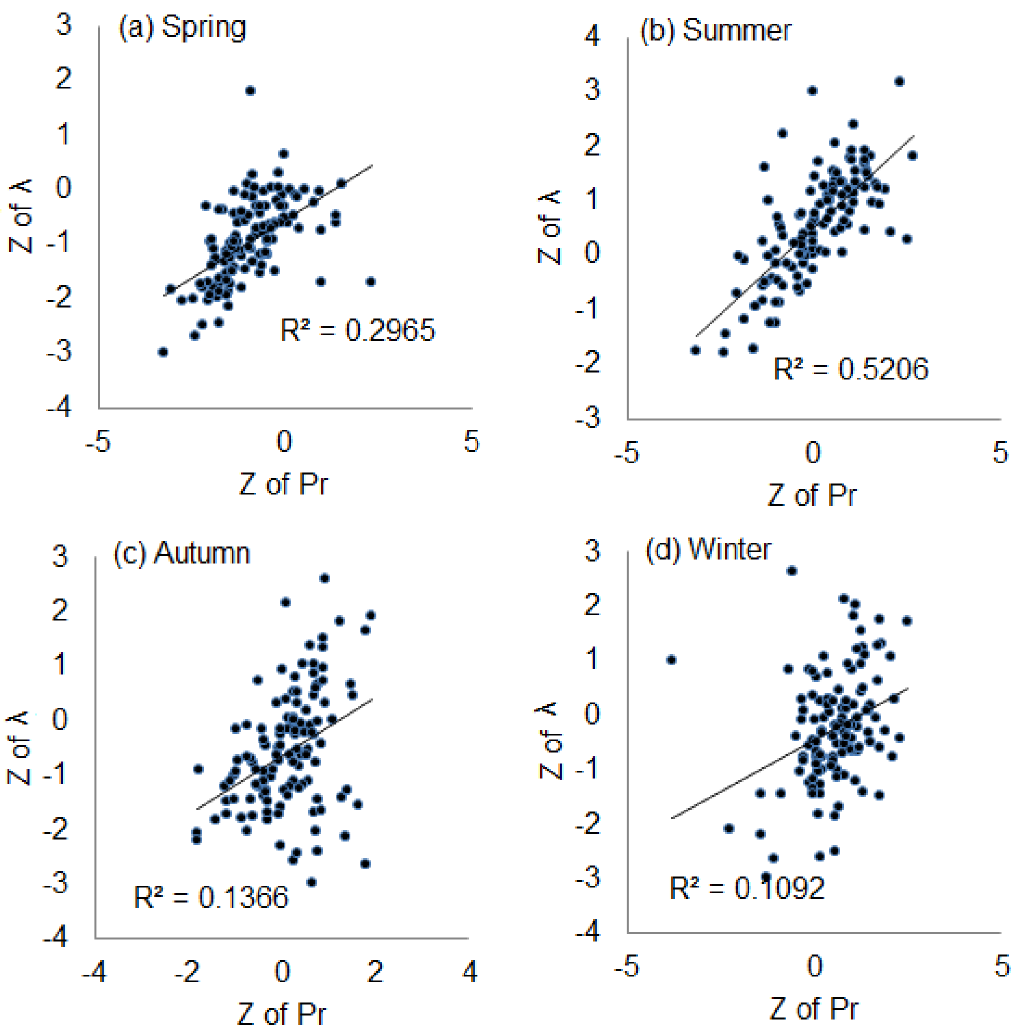

Figure 17. Comparison of seasonal trends statistics (Z) between Pr and λ

4.4 Qualitative categories of changes in annual and seasonal rainfall characteristics

Despite the change in rainfall characteristics was not a general phenomenon in statistics and the significant stations distributed unevenly in Taiwan, we could see that the spring Pr showed a negative tendency during the study period, while other seasons showed a positive trend in summer, autumn, and winter. In previous chapter, I mentioned the annual analysis, which showed Pr increased in 12 stations. As the 12 stations increased their annual Pr, I was curious about which season contributed the changes in annual Pr the most. To seek the fact, here I would like to categorize the relationships between annual trends and seasonal trends.

Applicability of slopes or statistics in categorizing

Before qualitatively categorizing the different groups in changing Pr, we needed to decide which of trend parameters would be used, i.e. the slope (b) or the trend statistics (Z). Theoretically, the larger the slope was, the more significant the equivalent statistic of trend would be, in terms of positive or negative. In order to verify whether the trend statistics (Z) could represent the trend slope (b), I checked the relationship between Z and b (Fig. 18). The results showed that Z and b were strong correlated, where their R^2 were 0.8583 in Pr, 0.8881 in η, and 0.8906 in λ, respectively. In addition, choosing either b or Z would not change the sign of trend. Thus, we might apply either to classify the qualitative categories of relationships in annual and seasonal Pr.

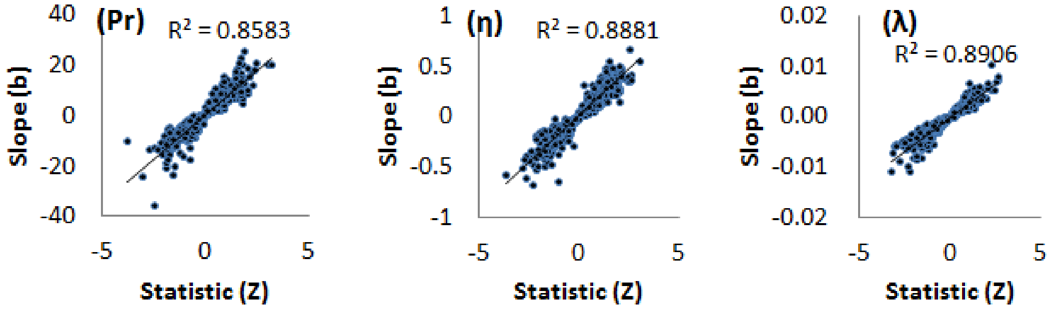

Figure 18 Relationships between trend slope (b) and trend statistics (Z) in seasonal rainfall characteristics.

Qualitative categories in changes of annual Pr with seasonal Pr

No matter using b or Z in accordance of classifying, the patterns of qualitative categories in annual and seasonal Pr showed as the same (Table 2). Most of the 120 stations were positive in annual Pr trend, in which, 38% of stations (44% of positive annual Pr stations) showed increasing potential in Pr in summer, autumn, and winter, while spring Pr tended to decrease (category no. 6). Here, 15% of stations (17% of 103 positive annual Pr stations) showed positive slopes in Pr in summer and winter, while spring and autumn Pr sloped down (category no. 2). However, there were over half (54%) of the 103 positive stations showed a tendency with positive summer and winter b or Z (category no.1, 2, 6 and 8). Consequently, this implied the increasing tendency in annual Pr might be contributed by those in summer and winter Pr in most of cases.

On the other hand, in annual trend, 17 of our 120 stations had negative b and Z; in which, they showed negative b and Z in spring (category no. 13 to 20 in Table 3) for 8 categories (94% of 17 negative stations). Therefore, the decreasing tendency in spring Pr was highly related to decreases in annual Pr.

Table 2. Major categories of changing rainfall amount (Pr)

Category No.	Long-term Pr slope (i) Annual	Spring	Summer	Autumn	Winter	Number of stations(ii)	Ratio of total stations
1	+	+	+	+	+	1	1%
2	+	+	+	-	+	1	1%
3	+	+	+	-	-	2	2%
4	+	+	-	+	+	3	3%
5	+	+	-	-	+	2	2%
6	+	-	+	+	+	45(5)	38%
7	+	-	+	+	-	10	8%
8	+	-	+	-	+	18(2)	15%
9	+	-	+	-	-	4(2)	3%
10	+	-	-	+	+	6(1)	5%
11	+	-	-	-	+	11(2)	9%
12	-	+	-	+	+	1	1%
13	-	-	+	+	+	3	3%
14	-	-	+	+	-	3	3%
15	-	-	+	-	+	3	3%
16	-	-	+	-	-	2	2%
17	-	-	-	+	+	1	1%
18	-	-	-	+	-	1	1%
19	-	-	-	-	+	1	1%
20	-	-	-	-	-	2(1)	2%

Note: (i) + or – sign in each category represented trends of Pr in annual, spring, summer, autumn, and winter, respectively; (ii) I quoted the significant stations in the parentheses, there were 12 stations significant increases in Pr and only one decreased, while 103 stations showed positive and 17 stations negative.

Qualitative categories in changes of annual η with seasonal η

Most of the 120 stations were positive in annual η trend, in which, 44% of stations (53 stations) showed increasing potential in η in summer, autumn, and winter, while spring η tended to decrease (category no. 5, 7, 9, 11, etc. in Table 3). Here, 54% of stations (65 stations) showed positive slopes in η in summer and winter (category no. 5 and 7). However, there were over half (54%) of the 103 positive stations showed a tendency with positive summer and winter b or Z (category no.6 and 8). Consequently, this implied that the increases in annual η might be contributed by summer and winter η in most of cases.

Qualitative categories in changes of annual λ with seasonal λ

To verify the combination in annual and seasonal trends in λ, I conducted the same work as former analysis. 23% (28 stations) of the 120 stations were negative in annual and all seasonal λ trends, in which, 6 stations showed significant decreases (category no. 22 in Table 4). Here, about 47% of stations showed negative slopes in λ in spring, autumn, and winter (category no. 18, 21, and 22). Further, we might notice that 75 stations decreased in both annual and spring trends, regardless of other seasons. Therefore, this implied the decreasing tendency in annual λ might be led by those in spring mainly.

Table 3. Major categories in trends of daily rainfall intensity (η)

Category of long-term slope (i)	Number of stations(ii)	Ratio of total stations
1. +++++	15	12%
2. +++-+	2	1%
3. +++--	2	2%
4. ++-++	3	3%
5. +-+++	53(16)	44%
6. +-++-	2	1 %
7. +-+-+	12(2)	10 %
8. +-+--	2	1%
9. +--++	12(4)	10%
10.+--+-	1	1%
11.+---+	7(4)	5%
12.+----	1(1)	1%
13.--+++	2	2%
14.--+-+	1	1%
15.--+--	1	1%
16.---++	1	1%
17.---+-	2	2%
18.-----	1	1%

Note: (i) + or – sign in each category represented trends of η in annual, spring, summer, autumn, and winter, respectively; (ii) I quoted the significant stations in the parentheses, there were 37 stations significant increases in η.

Table 4. Major categories in trends of number of rain days (λ).

Category of long-term slope [i]	Number of stations[ii]	Ratio of total stations
1. +++++	4	3%
2. +++-+	2	2%
3. ++--+	1	1%
4. +-+++	7	6%
5. +-++-	4	3%
6. +-+-+	5	4%
7. +-+--	5	4%
8. +--++	1	1%
9. +--+-	1	1%
10.+---+	2	2%
11.+----	2	2%
12.-++++	2	2%
13.-++--	6(1)	5%
14.-+---	3	3%
15.--+++	4	3%
16.--++-	5	4%
17.--+-+	5	4%
18.--+--	19(1)	16%
19.---++	1	1%
20.---+-	3	3%
21.----+	10	8%
22.-----	28(6)	23%

Note: (i) + or – sign in each category represented trends of λ in annual, spring, summer, autumn, and winter, respectively; (ii) I quoted the significant stations in the parentheses, there were 7 stations showed significant decreases in λ.

5

Rainfall time series forecasting

5.1. Rainfall time series forecasting

Herein this chapter, I would like to promote our results in previous chapter, making a simple application on predicting the future data in short-term. As well, aimed at conducting a general statistical model for Pr series, I applied the Box-Jenkins time series analysis (see section *2.4*) to conduct tentative diagnosis, find out the noise pattern part, build an intervention model with our previous works, and finally forecasting the future series. Here, I first analyzed the seasonal Pr series, and then monthly Pr series.

5.1.1 Seasonal Pr forecasting

I first observed time series among the 120 stations. The seasonality in Pr series was very strong, as well, I had obtained that trends existed probably in some seasons. Thus, I derived an intervention ARIMA model as Equation 18, combining our results with the time series analysis.

$$Z_t = \sum b_i x_i + \frac{(1-\theta_{22}B^{22})}{(1-\phi_4 B^4)} a_t \text{, where } a_t \overset{i.i.d}{\sim} (\mu, \sigma^2)$$

…Equation 18

In Equation 18, the former ($b_i x_i$)part was the trend part, assembled by trend slope (b) in each season, and x a dummy variable, i.e. spring as [1,0,0,0] (i=1), summer as [0,1,0,0] (i=2), autumn as [0,0,1,0] (i=3), and winter as [0,0,0,1] (i=4). The latter part is the time series noise, which controls the seasonality term. The AR parameter (ϕ_4) and MA parameter (θ_{22}) showed at lag 4 and lag 22, respectively. Thus, the model indicated the cycle occurring at one year (for lag-4 as one year) and 5-6 year (for lag-22 as 5.5 year), respectively.

Case: Station 01Q930

Take station 01Q930 (No. 110) as a sample, here I demonstrated the time series analysis. First, time series were examined through its plot (Fig. 19) and tentative model specification (ACF and PACF; Fig. 20a, 20b) The ACF showed strong in Lag-2,4,6,7,9,11… with no cut-off, and the PACF showed a cut-off at Lag-4, hence I fitted an AR(4) model and modified it. The parameters (Table 4) showed significances in their t value. As well, the ACF and the PACF in the residual were beneath the error limit (Fig. 21). Thus, the model was accepted.

Figure 22 contained the predicted series (red line) and its confident interval (blue line). Note that the model had not intervened in seasonal trend parameters. The forecasted Pr went beneath the zero (mm) horizon referred to negative Pr values. Therefore, this model was not reasonable. Consequently, I added the seasonal trends to forecast the series, shown as Fig. 23. In Figure 23, the forecasting seemed to be reasonable for there were no negative values.

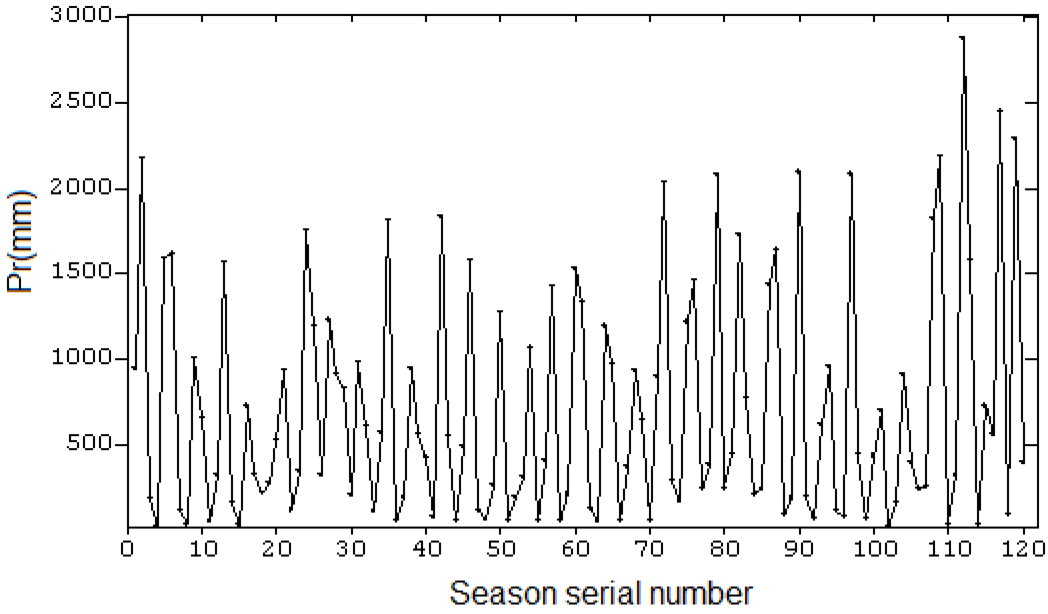

Figure 19. Time series plot of seasonal rainfall amount for a station

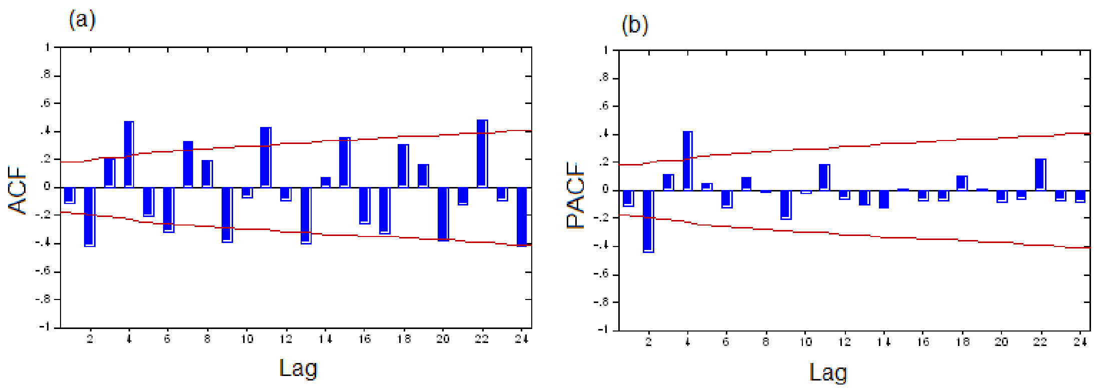

Figure 20. (a) ACF and (b)PACF plots of seasonal rainfall amount for a station.

Table 5. Summary of fitted seasonal model statistics for a station

Parameter	Value	t value
θ_{22}	-.6421	-8.72
ϕ_4	0.7294	12.11

Note: n=116 , r^2=0.446, residual standard error=507

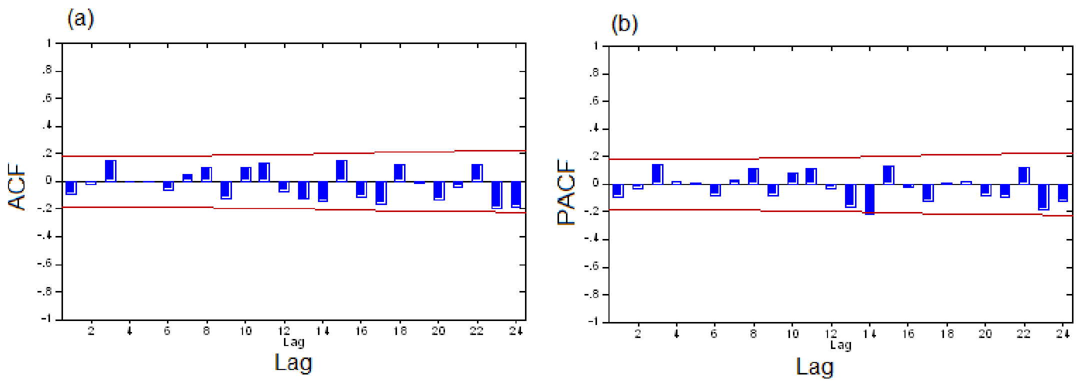

Figure 21. (a) ACF and (b) PACF plots of model residual for a station.

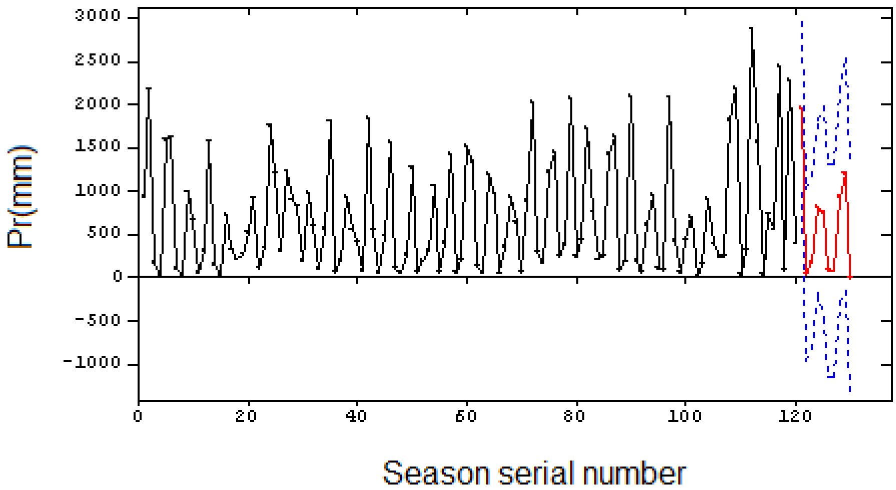

Figure 22. Forecasting before intervention for seasonal rainfall amount for a station.

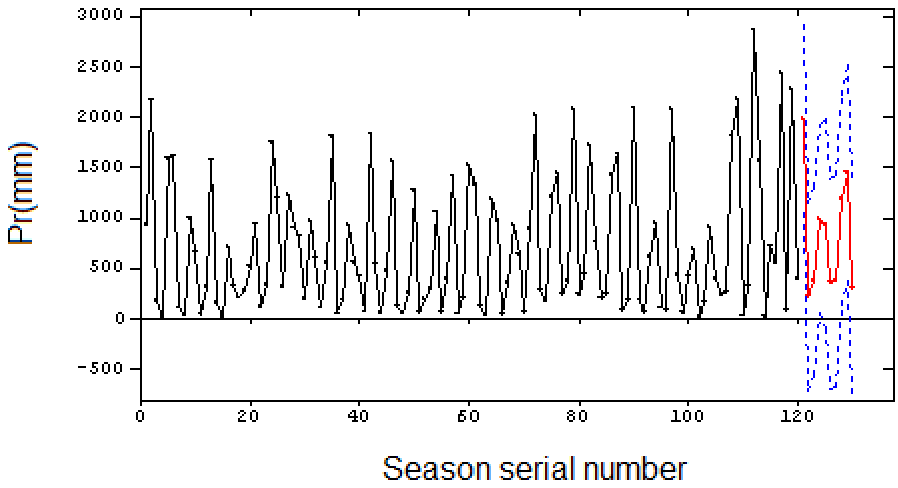

Figure 23. Forecasting after intervention for seasonal rainfall amount for a station.

5.1.2 Monthly Pr forecasting

I did not precede the monthly rainfall characteristics analysis in previous chapters; however, in this section, I would like to fit a model for monthly data. As the same as the former section, I built an ARIMA model based on intervention analysis to fit the monthly Pr data;

$$Z_t = \sum b_i x_i + \frac{(1-\theta_{11}B^{11})}{(1-\phi_{11}B^{11})} a_t \text{, where } a_t \overset{i.i.d}{\sim} (\mu, \sigma^2)$$

…Equation 19

The lag-11 terms at both AR and MA parameters indicated the cycle at one year. Here the dummy variable x_i was a 12 by 12 matrix and much complicated than seasonal ones,

$$x_i = \begin{bmatrix} 1 & 0 & \cdots & 0 & 0 \\ 0 & 1 & 0 & \vdots & 0 \\ 0 & 0 & \ddots & 0 & \vdots \\ 0 & \vdots & 0 & 1 & 0 \\ 0 & 0 & \cdots & 0 & 1 \end{bmatrix}$$

…Equation 20

Case: station 21C050

First, I examined time series through tentative model specification (ACF and PACF, see Fig. 24) The ACF showed a strong wave without any cut-off, and the PACF showed a cut-off at Lag-11, thus, I would fit an AR(11) model then modified it to Equation 19. The parameters (Table 5) in the model showed significances in their t value, and hence I entered a diagnostic check with residual analysis through the ACF and the PACF in the residual (Fig. 25).

Table 6. Summary of fitted monthly model statistics for a station

Parameter	Value	t value
θ_{11}	0.8812	22.24
ϕ_{11}	1.0000	164.70

Note: n=349 , r^2=0.280, residual standard error=161

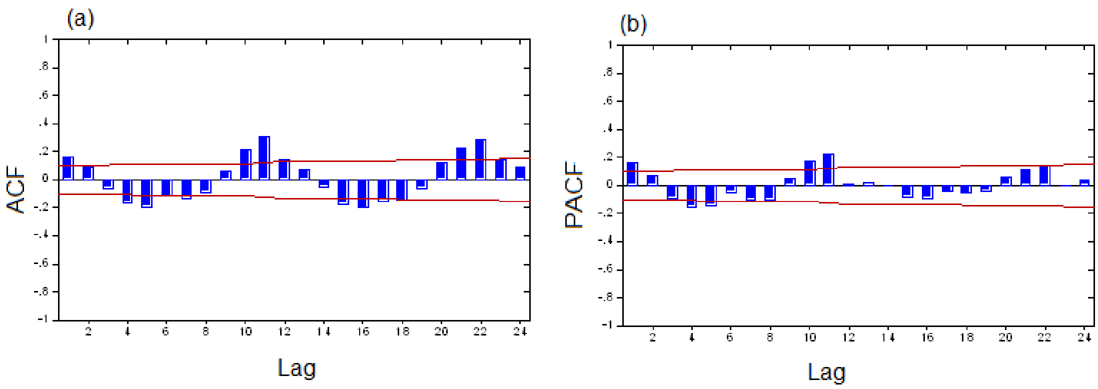

Figure 24. (a) ACF and (b) PACF plots of monthly rainfall amount in a station.

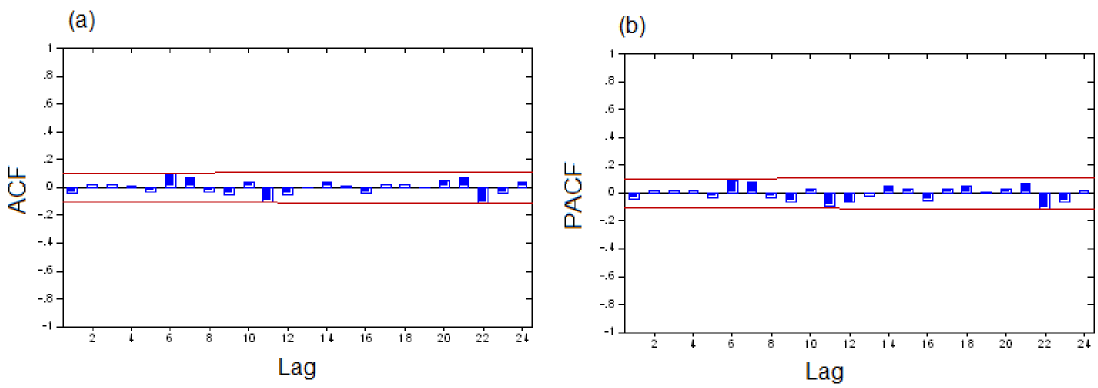

Figure 25. (a) ACF and (b) PACF plots of monthly model residual for a station.

Figure 26 contained the predicted series (red line) and its confident interval (blue line). Note that the intervention model (Fig. 26a) was similar to the model not intervened (Fig. 26b). Here we might observe estimated parameters of the intervention model, and we could see the monthly slopes, i.e., b in each month, were not significant (Table 6). Thus, I would suggest the monthly data would not need using the intervention analysis, just normally ARIMA would be fine; furthermore, this implied that the monthly trend might not be significant.

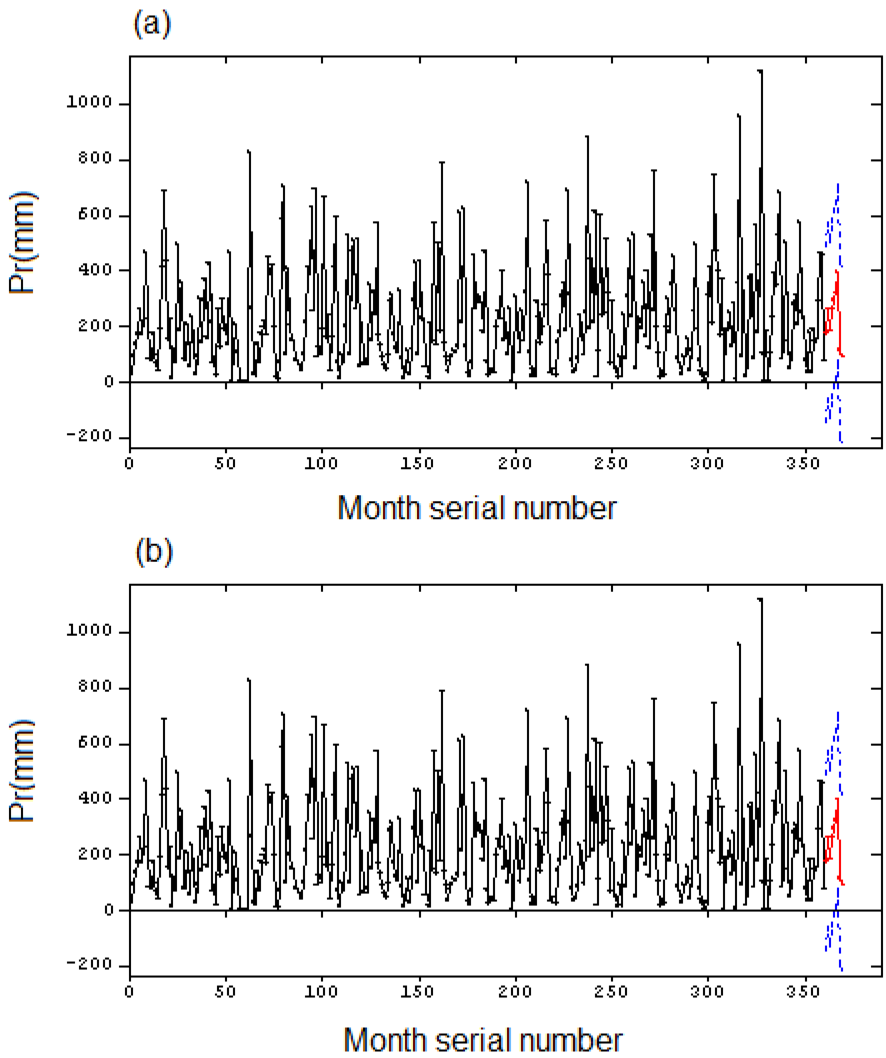

Figure 26. (a) Intervention analysis and (b) normal ARIMA model forecasts in monthly data of a station.

Table 7. Summary of monthly intervention model statistics

Parameter	Value	t-value
x_1	(n/a)	(n/a)
x_2	-20.1506	-0.59
x_3	-42.6622	-1.08
x_4	53.2118	1.35
x_5	-16.9619	-0.43
x_6	17.6016	0.45
x_7	-38.3804	-0.98
x_8	39.5157	1.01
x_9	0.5557	0.01
x_{10}	9.5343	0.24
x_{11}	-10.3206	-0.26
x_{12}	26.6857	0.78
θ_{11}	0.9661	38.02
ϕ_{11}	0.9998	125.74

Note: x_1 was not available in SCA report due to unknown error.

5.2 Potential impacts on hydrological cycles

In previous chapter, I did not suggest the change in Pr as a general phenomenon because significant stations allocated unevenly in Taiwan; on the other hand change in daily rainfall intensity was popular in the west of Taiwan. However, our study revealed that Pr could be more intense with heavy storms in some areas, especially, in the west and the southwest parts, where the Pr were large and trends simultaneously. These changes might have some impacts on hydrological cycles, thus we could discuss about some possible impacts of changes in rainfall regime on the hydrological cycles and further studies required.

The canopy rainfall interception is also one of the important hydrological components during and after rainfall in Taiwan (Chang et al. 2006). Note that forests spread broadly in mountainous Taiwan, which accounted for the 60% of the total land area (Su, 1984; Hsieh et al., 1994; Cheng et al., 2002). According to physical-based models for the rainfall interception such as Gash model (Gash et al., 1995; Murakami, 2007), numbers of rainfall events and rainfall duration could determine total amount of rainfall interception. While, heavy intensely storms might easily exceed water-holding capacity of forest canopies and trunks, and hence most of the rainwater could be discharged to the ground as the form of throughfall and stemflow (e.g., Manfroi et al., 2004; Manfroi et al., 2006; Kume et al. 2011). Therefore, total amount of rainfall interception could be conservative in response to the increased Pr and η without the increase of λ. Although some previous studies reported rainfall interception in various kind of ecosystems in Taiwan (e.g., Lin et al., 2000; Lai et al., 2007), there are few studies examined long-term rainfall interception there. Consequently, to understand the impacts of possible rainfall changes on rainfall interceptions, long-term monitoring of rainfall interception should be required.

Total amount of Pr and η are primary important factors determining runoff processes (Burns, 2001; McDonnell, 2003). Previous study suggested that a combination of increased Pr and reduction in D_{Pr} increased severity of floods (Singh et al., 2008; Cheng, 2010). Despite the change in annual Pr was not a general phenomenon in Taiwan, annual Pr and annual η could increase simultaneously in the west of CMR unevenly. This implied possible changes in η in finer time scale might happen, and it would probably result in higher frequency of flood, which is normally required finer temporal-scale analysis (< daily scale) (e.g., Norbiato et al., 2008; Cheng, 2010; McMillan et al., 2010).

In addition, decreases in λ might bring potential risks for water shortage in Taiwan. We could see λ had negative tendencies in trends at most stations while number of stations with significant decreases was relative few in both annual and seasonal analysis (Fig. 5c and 18). Notice that the spring Pr probably leaded to deceasing in annual Pr and it had negative tendencies at most (92%) of total stations. Less D_{Pr} would lead to more frequent in dry periods in a year. Considering the decreasing Pr, η, and λ in spring, the water resource management might face a challenge in future springtime.

Nevertheless, our studies used simple variables with a longer temporal resolution dataset to conduct the analysis. Further studies including analysis in finer temporal resolution and its long-term trend in Pr would contribute to the understanding of changes in the frequency of dry periods and hence the water resource management in Taiwan. As well, data with finer resolution in time would be required to facilitate flood controls in future, such as rain events analysis. In addition, the mountainous areas had no much rain stations for records; this study had discovered the rainfall characteristics were different between mountainous and lowland areas. For a general management of national land, we have to consider mountainous areas as a necessary part (CEPD, 2010). Thus, I sincerely suggested that it would be important to promote more stations in mountainous areas for observation.

In addition, since the number of stations was limited in mountainous areas, relative measurements would not be so easy to conduct. Recently, interdisciplinary applications combines other study fields have been promoted to investigate the water dynamics, such as time series analysis mentioned in this research, radar, and remote sensing. For example, radar could help to simulate extreme hydrological events even in areas of higher elevation (Biggs and Atkinson, 2011); to detect the evapotranspiration, specific indices in spectrum properties are feasible (e.g., Nishida et al., 2003; Glenn et al., 2007; Nagler et al., 2007; Anderson et al., 2008; Wu et al., 2010). Therefore, by advances in collaboration, there would be prospective tools for dedicating in hydrology in the future.

6

Conclusion and Future Prospects

Changes in rainfall have been received lots of attention in climate change, also, variations in rainfall characteristics were important for hydrological processes, while few studies examine these in Taiwan, especially in mountainous areas. This thesis were undertaken to study spatial and temporal variations in the rainfall amount (Pr), rainfall intensity (η), and the number of rain days (λ) based on rainfall data for 120 stations covering lowland and mountainous areas in Taiwan, from 1978 to 2008, in terms of annual and seasonal time-scale. We may look at the relationships between Pr, η, and λ for their spatial distribution, year-to-year variation, and marginal long-term trends. Based on these derived results, I fitted ARIMA models for time series forecasts, and then tentatively discussed on potential impacts on hydrological cycles.

In annual time-scale analysis, we could see the cue of the spatial variation in rainfall amount was different between the mountainous and the lowlands stations. The spatial variation in $\overline{\mathrm{Pr}}$ was primarily explained by both $\bar{\lambda}$ and $\bar{\eta}$ in the lowland stations, but only by $\bar{\eta}$ for in the mountainous stations. Thus, the rainfall characteristics seemed to be different between mountainous and lowland areas. Temporal analysis showed that η in most stations primarily explained the year-to-year variation in Pr rather than λ. We could also see that almost the same results in seasonal time-scale analysis.

In addition, long-term trend analysis clarified that, among the 120 stations, significant trends in Pr were found in less than 10% of total stations, regardless of annual or seasonal time scales, thus the long-term trends in Pr were not popular in Taiwan, while η increases in annual-time scale among 30% of the 120 stations. Besides, noticed that Pr decreases in springtime were different with other three seasons during the study period, the shortage in water resource could be expected and require more researches and relevant policies to face the risks.

The previous study (Hsu and Chen; 2002) examined spatial and temporal variations in rainfall characteristics in lowland areas in Taiwan. Although significant changes in rainfall characteristics were reported for some of the eight stations, implying such changes would be commonly observed in Taiwan. However, I did not show that such changes were common. Despite the nature of long-term trends in rainfall characteristics could be found in the west part rather than the east part, stations with significant long-term trends were located unevenly in Taiwan. Further, increases in Pr were simultaneous with number heavy rain days in their study; this research obtained a similar result in trends of Pr and η, which had high correlation.

To forecast rainfall time series, I had developed a stochastic ARIMA (4,0,22) and a ARIMA (11,0,11) models for seasonal and monthly intervention analysis, respectively, which combined our work in this thesis. As well, the intervention model implied that the monthly trend might be insignificant through the study period, while the seasonal slopes might be useful.

On the other hand, interdisciplinary applications combined other study fields, such as radar and remote sensing, have been promoted to investigate the water dynamics on terrestrial surface. By these collaborations, more tools could be expected for researching hydrological processes in future.

This thesis contributed a better understanding of spatial and temporal variations in rainfall characteristics based on numerous stations over the whole Taiwan including mountainous areas. Nevertheless, mountainous areas showed different tendency of rainfall amount, in which rainfall amount in the mountainous areas related to daily rainfall intensity but daily rainfall intensity and rain days in the lowland areas, while the number of stations was few and needed to promote. As changes in rainfall characteristics might influence the water resource management and the hydrological cycle, further studies were encouraged to combine interdisciplinary works, such as hydrological processes, water resources, and ecology, in terms of different spatial and temporal scales.

7

References

Adams RM, McCarl BA, Sergerson K, Rosenzweig C, Bryant KJ, Dixon BL, Conner R, Evenson RE, Ojima D. 2004. Chapter 2: Economic effects of climate change on US agriculture. In: R. Mendelsohn & J.E. Neumann (Eds). *The Impact of Climate Change on the United States Economy.* Cambridge University Press.

Akeda K, Reisner J, Parsons D. 1995. The role of mesoscale and topographically induced circulations initiating a flash flood observed during the TAMEX project. *Monthly Weather Review* **123**: 1720-1739.

Anderson MC, Norman JM, Kustas WP, Houborg R, Starks PJ, Agam N. 2008. A thermal-based remote sensing technique for routine mapping of land-surface carbon, water and energy fluxes from field to regional scales. *Remote Sensing of Environment* **112**: 4227-4241.

Anselin L, Syabri I, Kho Y. 2005. GeoDa: An Introduction to Spatial Data Analysis. Geographical Analysis 38(1), 5-22.

Bedient PB, Huber WC, Vieux BE. 2008. *Hydrology And Floodplain Analysis.* 4th ed. NJ: Prentice-Hall Inc.

Beven KJ. 2001. *Rainfall-Runoff Modelling: The Primer.* John Wiley & Sons: Chichester.

Biggs EM, Atkinson PM. 2011. A comparison of gauge and radar precipitation data for simulating an extreme hydrological event in the Severn Uplands, UK. *Hydrological Processes* **25**, 795-810.

Box GEP, Jenkins GM, Reisel GC. 2008. *Time Series Analysis, Forecasting and Control.* San Francisco, John Wily & Sons.

Box GEP, Tiao GC. 1975. Intervention analysis with applications to economic and environmental problems. *Journal of American Statistical Association* **70**: 70-79.

Brown MB, de la Roca I, Vallejo A, Ford G, Casey J, Aguilar B, Haacker R. 1996. *A Valuation analysis of the Role of cloud Forests in Watershged Protection. Sierra de las Minas Biosphere Reserve, Guatemala and Cusuco N.P., Honduras.* RARE Center for Tropical Conservation, Philadelpha, U.S.A.

Burns DA, McDonnell JJ, Hooper RP, Peters NE, Freer JE, Kendall C, Beven K. 2001. Quantifying contributions to storm runoff through end-member mixing analysis and hydrologic measurements at the Panola Mountain Research Watershed (Georgia, USA). *Hydrological Processes* **15**, 1903–1924. DOI: 10.1002/hyp.246.

Burton LDV. 2008. *Introduction to Forestry Science*, 2nd ed. NY: Delmar Thomson Learning.

Chang H, Kwon WT. 2007. Spatial variations of summer rainfall trends in South Korea, 1973-2005. *Environmental Research Letters* **2**: 045012. DOI: 10.1088/1748-9326/2/4/045012.

Chang LC, Chang FJ, Chiang YM. 2004. A two-step-ahead recurrent neural network for stream-flow forecasting. *Hydrological Processes* **18**, 81-92.

Chang MT. 2006. *Forest Hydrology: An Introduction to Water and Forests,* 2nd ed. FL: CRC Press.

Chen CS, Chen WS, Deng ZS. 1991. A study of a mountain-generated precipitation system in northern Taiwan during TAMEX IOP 8. *Monthly Weather Review* **119**: 2574-2606.

Chen CS, Chen YL. 2003. The Rainfall Characteristics of Taiwan. *Monthly Weather Review* **131**: 1323:1341. DOI: 10.1175/1520-0493 (2003)131 <1323:TRCOT> 2.0.CO;2.

Chen CS, Huang JM. 1999. A numerical study of precipitation characteristics over

Taiwan Island during the winter season. *Meteorology and Atmospheric Physics* **70**: 167-183. DOI: 10.1007/s007030050032.

Chen GTJ, Wang CC, Lin DTW. 2005. Characteristics of low-level jets over northern Taiwan in mei-yu season and their relationship to heavy rain events. *Monthly Weather Review* **131**: 20-43. DOI: 10.1175/MWR-2813.1.

Chen HH. 1990. *Forestry Hydrology*. Chien-Hwa Publish Ltd., Taipei, Taiwan (in Chinese).

Cheng JD, Lin LL, Lu HS. 2002. Influences of forests on water flows from headwater watersheds in Taiwan. *Forest Ecology and Management* **165** (3):11-28. DOI: 10.1016/S0378-1127(01)00626-0.

Cheng SJ. 2010. Hydrograph characteristics of quick and slow runoffs of a watershed outlet, Taiwan. *Hydrological Processes*, **24**: 2851-2870. DOI: 10.1002/hyp.7699.

Chin G, Yeston J. 2006. Ecology/Evolution: Wet Forests in Dry Lands. *Science* **313** (21): 275.

Council for Economic Planing and Development (CEPD). 2010. *Strategic Plan for National Spatial Development (Summary)*. Taipei: Executive Yuan of Taiwan (R.O.C.).

Crockford RH, Richardson DP. 2000. Partitioning of rainfall into throughfall, stemflow and interception: effect of forest type, ground cover and climate. *Hydrological Processes* **14**: 2903–2920.

D'Odorico P, Ridolfi L, Porporato A, Rodriguez-Iturbe I. 2000. Preferential states of seasonal soil moisture: The impact of climate fluctuations. *Water Resources Research* **36**: 2209-2219. DOI: 10.1029/2000WR900103.

Executive Yuan. 2003. *Soil and water Conservation Act*. Taipei: Executive Yuan. (In Chinese)

FAO. 2000. *Global forest resource assessment 2000* (main report). Forestry Paper 140.

FAO, Rome.

FAO. 2009. *States of the Worlds' Forests.* FAO, Rome.

Fisher G, Shah M, Tubiello FN, and van Velhuizen H. 2005. Socio-economic and climate change impacts on agriculture: an integrated assessment, 1990–2080. *Phil. Trans. R. Soc. B* (2005) 360, 2067–2083. doi:10.1098/rstb.2005.1744.

Fleischbein K, Wilcke W, Valarezo C, Zech W, Knoblich K. 2006. Water budgets of three small catchments under montane forest in Ecuador: experimental and modelling approach. *Hydrological Processes* **20**, 2491–2507

Furrer EM, Katz RW. 2008. Improving the simulation of extreme precipitation events by stochastic weather generators. *Water Resources Research*, **44**, W12439, doi:10.1029/2008WR007316

Gash JHC, Lloyd CR, Lachaud G. 1995. Estimating sparse forest rainfall interception with an analytical model. *Journal of Hydrology* **170**: 79–86. DOI:10.1016/0022-1694(95)02697-N

Geiger R, Aron AH, Todhunter P. 2003. *Climate near the Ground*. Lanham, MD: Rowman and Littlefield, Pp317-319.

Glenn EP, Huete AR, Nagler PL, Hirschboeck, KK, Brown P. Intergrating remote sensing and ground methods to estimate evaportranspiration. *Critical Reviews in Plant Sciences* **26**: 139-168.

Guan H, Hsu HH, Makhnin O, Xie H, Wilson JL. 2009. Examination of selected atmospheric and orographic effects on monthly rainfall of Taiwan using the ASOADeK model. *International Journal of Climatology* **29**: 1171-1181. DOI: 10.1002/joc.1762.

Harrison RM, and van Grieken RE, ed. 1998. *Atmospheric Particles*. UK: IUPAC.

Hewlett JD. 1981. *Principles of Forest Hydrology*. Georgia: University of Georgia Press.

Holliday D, Resnick R, Walker J. 2008. *Fundamentals of Physics Extended.* 8^{th} ed. NY: Wiley.

Hornberger GM, Raffensperger JP, Wiberg PL, Eshleman KN. 1998. *Elements of physical hydrology*. JHU press, Baltimore, Maryland. Pp 29-31.

Hsieh CF, Chen CF, Yang KC. 1994. Introduction to the flora of Taiwan, 3: floristics, phytogeography, and vegetation. In: *Flora of Taiwan*, 2^{nd} Edition, Vol. 1. Taipei: National Taiwan Univeristy.

Hsu HH, Chen CT. 2002. Observed and projected climate change in Taiwan. *Meteorology and Atmospheric Physics* **79**: 87-104. DOI: 10.1007 /s 703-002-8230-x.

Huang NE, Wu Z. 2008. A review on Hilbert-Huang transform: Method and its applications to geophysical studies. Reviews of Geophysics **46**, RG2006, 23 PP. DOI:10.1029/2007RG000228.

Intergovernmental Panel on Climate Change (IPCC). 2007. Summary for policymakers, in *Climate Change 2007: Working Group 1: The Physical Science Basis, Summary for Policymakers.* Contribution of Working Group I to the Fourth Assessment Report of the Intergovernmental Panel on Climate Change, edited by S. Solomon et al., pp. 1– 18, Cambridge Univ. Press, Cambridge, U. K.

IPCC. 2007. *AR4 Synthesis Report, Summary for Policymakers.* NY: IPCC Fourth Assessment Report, Cambridge University Press, New York.

Johnson GB. 2003. *The Living World*, 3^{rd} ed. NY: McGrawHill Inc. 50.

Johnson RH, Bresch JF. 1991. Diagnosed characteristics of precipitation systems over Taiwan during the May-June 1987 TAMEX. *Monthly Weather Review* **119**: 2540-2557. DOI: 10.1175/1520-0493(1991)119<2540:DCOPSO>2.0.CO;2.

Katz RW, Parlange MB. 1998. Overdispersion Phenomenon in Stochastic Modeling of Precipitation. *Journal of Climate*, **11**, 591–601. DOI: 10.1175 / 1520-0442

(1998) 011<0591:OPISMO>2.0.CO;2

Kendall MG. 1975. *Rank Correlation Methods*. Griffin: London.

Kerns J, Wesley B, Chen YL, Chang MY. 2010. The Diurnal Cycle of Winds, Rain, and Clouds over Taiwan during the Mei-Yu, Summer, and Autumn Rainfall Regimes. *Monthly Weather Review* **138**: 497–516. DOI: 10.1175 / 2009 MWR3031.1.

Komatsu H, Kume T, Otsuki K. 2010. A simple model to estimate monthly forest evapotranspiration in Japan from monthly temperature. *Hydrological Processes* **24**: 1896-1911.

Kumagai T, Katul GG, Saitoh TM, Sato Y, Manfroi OJ, Morooka T, Ichie T, Kuraji K, Suzuki M, Porporato A. 2004. Water cycling in a Bornean tropical rain forest under current and projected rainfall scenarios. *Water Resources Research*, **40**, W01104. DOI: 10.1029/2003WR002226.

Kumagai T, Yoshifuji N, Tanaka N, Suzuki M, Kume T. 2009. Comparison of soil moisture dynamics between a tropical rain forest and a tropical seasonal forest in Southeast Asia: Impact of seasonal and year-to-year variations in rainfall. *Water Resources Research* **45**, W04413. DOI: 10.1029/2008WR007307.

Kume T, Tanaka N, Kuraji K, Komatsu, H, Yoshifuji N, Saitoh TM, Suzuki M, Kumagai T. 2011. Ten-year evapotranspiration estimates in a Bornean tropical rainforest. *Agricultural and Forest Meteorology*, DOI: 10.1016/ j.agrformet. 2011.04.005.

Lai YJ, Wey TH, Chen HH, Lai HK. 2007. A Study on Canopy Interception and Rainfall within a Natural Stand of *Picea morrisonicola* Hay. in Tatachia Alpine Ecosystem, Central Taiwan. *Journal of Chinese Soil and Water Conservation* **38**:135-146. (In Chinese with English abstract)

Lee CS, Huang LR, Shen HS, Wang ST. 2006. A Climatology Model for Forecasting

Typhoon Rainfall in Taiwan. *Natural Hazards* **37**: 87-105.

Lee R. 1980. *Forest Hydrology*. New York: Columbia University Press.

Li JY, Chen YL, Lee WC. 1997. Analysis of a heavy rainfall event during TAMEX. *Monthly Weather Review* **125**: 1060-1081. DOI: 10.1175/1520-0493 (1997) 125<1060:AOAHRE>2.0.CO;2.

Li MH, Yang MJ, Soong R, Huang HL. 2005. Simulating Typhoon Floods with Gauge Data and Mesoscale-Modeled Rainfall in a Mountainous Watershed. *Journal of Hydrometeorology* **6**: 306-323.

Lin CT, Chen HH, Kume T, Chiou CR. 2010. Comparison of potential water supply and demand in Taiwan. *Water International* **35**(2):165-176. DOI: 10.1080/02508061003663452.

Lin TC, Hamburg SP, King HB, Hsia YJ. 2000. Throughfall patterns in a subtropical rain forest of northeastern Taiwan. *Journal of Environmental Quality* **29**, 1186-1193.

Liu LM, Box GEP, Tiao GC. 2002. Forecasting and time series analysis using the SCA statistical system. Chicago, Illinois: Scientific Computing Associates Corporation.

Liu SC, Fu C, Shiu CJ, Chen JP, Wu F. 2009. Temperature dependence of global precipitation extremes. *Geophysical Research Letters* **36**, L17702. DOI:10.1029/2009GL040218.

Manfroi OJ, Kuraji K, Suzuki M, Tanaka N, Kume T, Nakagawa M, Kumagai T, Nakashizuka T. 2006. Comparison of conventionally observed interception evaporation in a 100-m^2 subplot with that estimated in a 4-ha area of the same Bornean lowland tropical forest. *Journal of Hydrology* **329**: 329-349. DOI:10.1016/j.jhydrol.2006.02.020.

Manfroi OJ, Kuraji K, Tanaka N, Suzuki M, Nakagawa M, Nakashizuka T, Chong L.

2004. The stemflow of trees in a Bornean lowland tropical forest. *Hydrological Processes* **18**: 2455–2474. DOI: 10.1002/hyp.1474.

Mann HB. 1945. Nonparametric tests against trend. *Econometrica* **13**: 245-259.

Mays LW. 2011. *Water Resources Engineering*. 2nd ed. NJ: John Wiley & Sons, Inc.

McDonnell JJ. 2003. Where does water go when it rains? Moving beyond the variable source area concept of rainfall-runoff response. *Hydrological Processes* **17**, 1869-1875.

McMillan H, Freer J, Pappenberger F, Krueger T, Clark M. 2010. Impacts of uncertain river flow data on rainfall-runoff model calibration and discharge predictions. *Hydrological Processes* **24**,1270–1284. DOI: 10.1002/hyp.7587.

Mendelsohn R ,Neumann JE (Eds). 2004. *The Impact of Climate Change on the United States Economy.* Cambridge University Press.

Mills TC, Tsay RS, Young PC. 2011. Introduction to special issue commemorating the 50th anniversary of the Kalman Filter and 40th anniversary of Box and Jenkins. *Journal of Forecasting* **30**: 1-5. DOI: 10.1002/for.1202.

Mu Q, Heinsch FA, Zhao M, Running SW. 2007. Development of a global evapotranspiration algorithm based on MODIS and global meteorology data. *Remote Sensing of Environment* **111**: 519-536. DOI:10.1016/j.rse.2007.04.015.

Murakami S. 2007. Application of three canopy interception models to a young stand of Japanese cypress and interpretation in terms of interception mechanism. *Journal of Hydrology* **342**, 305-319. DOI:10.1016/j.jhydrol.2007.05.032.

Nabors MW. 2004. *Introduction to Botany*. CA: Pearson Education Inc.

Nagler P, Jetton A., Fleming J, Didan K, Glenn E, Erker J, Morino K, Milliken J, Gloss S. 2007. Evapotranspiration in a cottonwood (Populus fremontii) restoration plantation estimated by sap flow and remote sensing methods. *Agricultural and Forest Meteorology* **144**: 95-110.

Nishida K, Nemani RR, Running SW, Glassy JM. 2003. An operational remote sensing algorithm of land surface evaporation. *Journal of Geophysical Research* **108**(D9), 4270, doi:10.1029/2002JD002062, 2003.

Norbiato D, Borga M, Esposti SD, Gaume E, Anquetin S. 2008. Flash flood warning based on rainfall thresholds and soil moisture conditions: An assessment for gauged and ungauged basins. *Journal of Hydrology* **362**:274-290. DOI: 10.1016/j.jhydrol.2008.08.023.

Oki T, Kanae S. 2006. Global hydrological cycles and world water resources. Science **313**: 1068-1072.

Peña D, Tiao GC, Tsay RS. 2000. *A Course in Time Series Analysis*. San Francisco, John Wily & Sons.

Piao S, Ciais P, Huang Y, Shen Z, Peng S, Li J, Zhou L, Liu H, Ma Y, Ding Y, Friedlingstein P, Liu C, Tan K, Yu Y, Zhang T, Fang J. 2009. The impacts of climate change on water resources and agriculture in China. *Nature* **467**(2): 43-51.

Porporato A, Daly E, Rodriguez-Iturbe I. 2004 Soil Water Balance and Ecosystem Response to Climate Change. *The American Naturalist* **164**: 625-632. DOI:10.1086/424970

Qin N, Chen X, Fu G, Zhai J, Xue X. 2010. Rainfall and temperature trends for the Southwest China: 1960-2007. *Hydrological Processes* **24**: 3733-3744. DOI: 10.1002/hyp.7792.

Rivard C, Vigneault H. 2009. Trend detection in hydrological series: when series are negatively correlated. *Hydrological Processes* **23**: 2737-2743. DOI: 10.1002/hyp.7370.

Shinohara Y, Kume T, Komatsu K, Otsuki K. 2010. Spatial and temporal variations in summer rainfall in Japanese mountain areas. *Hydrological Processes* **24**:

1844-1855. DOI: 10.1002/hyp.7620.

Singh P, Kumar V, Thomas T, Arora M. 2008. Changes in rainfall and relative humidity in river basins in northwest and central India. *Hydrological Processes* **22**: 2982-2992. DOI: 10.1002/hyp.6871.

Staelens J, De Schrijver A, Verheyen K, Verhoest NEC. 2008. Rainfall partitioning into throughfall, stemflow, and interception within a single beech (Fagus sylvatica L.) canopy: influence of foliation, rain event characteristics, and meteorology. *Hydrological Processes* **22**, 33–45.

Su HJ. 1984. Studies on the climate and vegetation types of the natural forests in Taiwan (II): altitudinal vegetation zones in relation to temperature gradient. *Quarterly Journal of Chinese Forestry* **17**(4): 53-73.

Tabari H, Marifi S, Aeini A, Talaee PH, Mohammadi K. 2011. Trend analysis of reference evapotranspiration in the western half of Iran. *Agricultural and Forest Meteorology* **151**: 128-136.

Teng JH, Chen CS, Chen Wang TC, Chen YL. 2000. Orographic Effects on a Squall Line System over Taiwan. *Monthly Weather Review* **128**: 1123–1138. DOI: 10.1175/1520-0493(2000)128<1123:OEOASL>2.0.CO;2.

Tesemma ZK, Mohamed YA, Steenhuis TS. 2010. Trends in rainfall and runoff in the Blue Nile Basin: 1964–2003. *Hydrological Processes* **24**, 3747–3758. DOI: 10.1002/hyp.7893.

Tiao GC, Box GEP, Hamming WJ. 1975. Analysis of Los Angeles photochemical smog data: a statistical overview . *Journal of the Air Pollution Control Association* **25**: 260-268.

Tsukamoto Y. (Ed.). 1992. *Forest Hydrology*. Bunneido Shuppan Ltd., Tokyo, Japan (in Japanese).

U.S. Geological Survey (USGS). 2011. *Global 30 Arc-Second Elevation (GTOPO30)*.

Retrieved from: http://eros.usgs.gov/

USGS. 2010. The Water Cycle: Water Science for Schools. Retrieved from http://ga.water.usgs.gov/edu/watercycle.html (Jun. 10. 2010)

Wada N, Kawada K, Kawamura R, Aoki K, Kume A. 2004. Increased winter runoff in a middle-latitude mountain area of central Japan. *Journal of the Meteorological Society of Japan* **82**: 1589-1597. DOI: 10.2151/jmsj.82.1589.

Water Resource Agency (WRA). 2009. *Hydrological Year Book of Taiwan Republic of China 2009: Part 1 -Rainfall*. Water Resource Agency, Ministry of Economic Affairs; Taipei.

Wilby RL, Harris I. 2006. A framework for assessing uncertainties in climate change impacts: Low-flow scenarios for the River Thames, UK. *Water Resources Research*, **42**, W02419. DOI:10.1029/2005WR004065.

Wu CC, Yen TH, Kuo YH, Wang W. 2002. Rainfall Simulation Associated with Typhoon Herb (1996) near Taiwan. Part I: The Topographic Effect. *Weather Forecasting* **17**: 1001–1015.

Wu CD, Cheng CC, Lo HC, Chen YK. 2010. Application of SEBAL and Markov Models for future stream flow simulation through remote sensing. *Water resources management* **24**: 3773-3797, DOI: 10.1007/s11269-010-9633-9.

Wu Z, Huang NE, Long SR, Peng CK. 2007. On the trend, detrending, and variability of nonlinear and nonstationary time series. *PNAS* **104**: 14889-14894. DOI: 10.1073/pnas.0701020104

Xu CY, Singh VP. 1998. A Review on Monthly Water Balance Models for Water Resources Investigations. *Water Resources Management* **12**: 31–50. DOI: 10.1023 A:1007916816469

Yanger PM, Freer JE, Beven KJ. 2009. Detecting the effects of spatial variability of rainfall on hydrological modelling within an uncertainty analysis framework.

Hydrological Processes **23**, 1988-2003.

Yeh HC, Chen GTJ. 2004. Case study of an unusually heavy rain event over eastern taiwan during the mei-yu season. *Monthly Weather Review* **132**, 320–337. DOI: 10.1175/1520-0493(2004)132<0320:CSOAUH>2.0.CO;2.

Yeh HC, Chen YL. 1998. Characteristics of rainfall distribution over Taiwan during the Taiwan Area Mesoscale Experiment (TAMEX). *Journal of Applied Meteorology* **37**: 1457-1469. DOI: 10.1175 / 1520-0450 (1998) 037 <1457:CORDOT> 2.0.CO;2.

Yeh HC, Chen YL. 2002. The role of offshore convergence on coastal rainfall during TAMEX IOP 3. *Monthly Weather Review* **130**: 2709-2730. DOI: 10.1175/1520-0493(2002)130 <2709:TROOCO>2.0.CO;2.

Yen MC, Chen TC. 2000. Seasonal variation of the rainfall over Taiwan. *International Journal of Climatology* **20**: 803-809. DOI: 10.1002/1097-0088(20000615)20:7 <803::AID-JOC525>3.0.CO;2-4.

Yu PS, Yang TC, Chou CC. 2002. Effects of climate change on evapotranspiration from paddy fields in southern Taiwan. *Climatic Change* **54**, 165–179. DOI: 10.1023/A:1015764831165.

Yue S, Pilon P, Phinney B, Cavadias G. 2002. The influence of autocorrelation on the ability to detect trend in hydrological series. *Hydrological Processes* **16**: 1807-1829. DOI: 10.1002/hyp.1095.

Zhang X, Zwiers FW, Hegerl GC, Lambert FH, Gillett NP, Solomon S, Stott PA, Nozawa T. 2007. Detection of human influence on twentieth-century precipitation trends. *Nature* **448**, 461-466.

Zumdahl SS. 2005. *Chemical Principles*, 5th ed. NY: Houghton Mifflin Co. Ltd. 804-805.

8

Supplementary information

In main contents of this research, some information or tools were not stated for the coherence of the thesis; these included the geographical data, tentative diagnosis on correlations, software used in this research, and station information with their trend statistics. Herein this part, these were presented as much as possible for further researches or being as a reference. In addition, color figures are available in this part as well.

Appendix 1: Additional material and tools

Digital Elevation Model Data

The altitudinal data, Global 30 Arc-Second Elevation (GTOPO30), is a public digital elevation model (DEM) data. I acquired the data from the website of the Earth Resources Observation and Science (EROS) Center of the U.S. Geological Survey, U.S. Department of the Interior (http://eros.usgs.gov). This database offers a global DEM data with a horizontal grid spacing of approximately 1 km (USGS, 2011). In which, Taiwan is classified under the category, e100n40.

Correlation matrix

Despite the linear regression is classical to examine the relationship between two variables, when the number of variables are large, it is not easy to describe the relationships between each variable at once clearly. In the annual analysis case, I might approach the three variables (Pr, η, and λ) for 120 stations at a glance. When it came to seasonal analysis, I had the three variables in four seasons, respectively; here the number of variables was 12. If I considered the annual data simultaneously, the number of variables rises to 15, and the number of relationships between each two variables would gain to 98, i.e., 98 relationship assembles, which is hard to put in a one-page table.

To analyze such complicated correlations required a clean way, here the correlation matrix was applied on. The correlation matrix consists of *r* between variables, offering a clean table and its significance to examine degree to which the relationship was strong or not.

AnalystSoft ™ StatPlus®: Mac LE 2009 (StatPlus) is a free commercial application built for Microsoft ™ Excel ®: Mac (Excel) to compensate lack of the Analysis Toolpak in Excel in Macintosh. In this study, StatPlus was combined with Excel to examine the correlation among different variables via Pearson's correlation matrix and probability of *r* and its significance in probability (based on Eq. 13), which is not available in its counterpart, Analysis ToolPak of Excel in the Windows version.

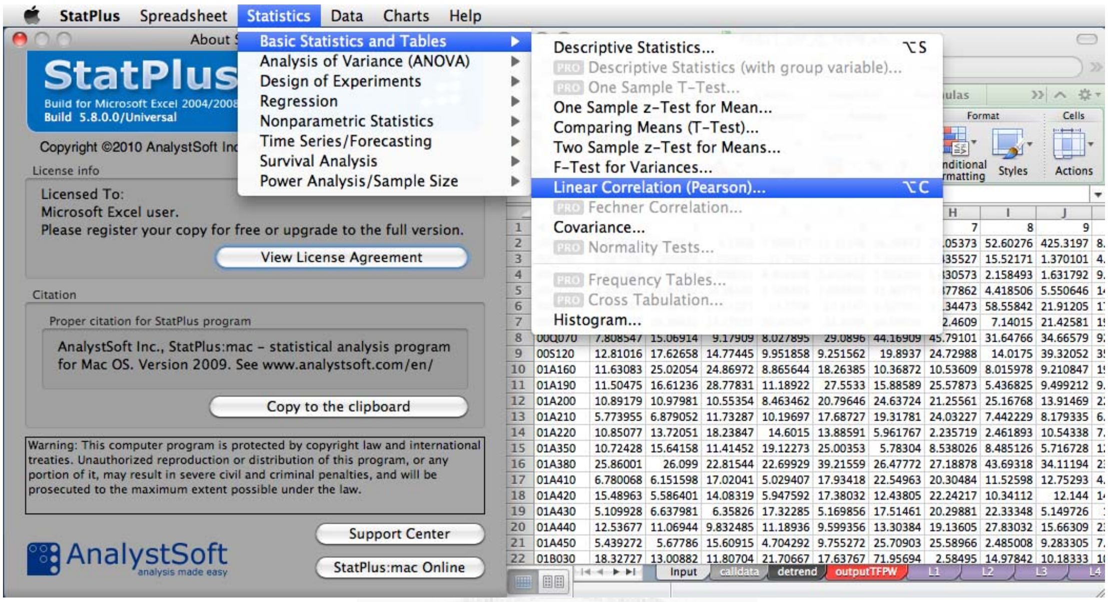

Figure 27. StatPlus and Excel screeshot.

Geographic information system in computer

Programs used for mapping in this study included a commercial mapping application, Golden Software ™ Surfer 10® (Surfer), and two open spatial information system, Quantum GIS 1.6.0 (QGIS) and OpenGeoDa (Aeslin et al., 2005).

In order to draw the spatial distribution of the 120 stations in this study, a series of data processes was conducted to create the maps. At first, the geographic information of all stations was summarized in Excel, including latitude, longitude, and altitude of each station. Then the rainfall data was attached to each station, involving period mean parameters and its trend statistics of the station. Finally, the work sheet would be transcribed into .DBF file and inputted into geographic information systems; here, Surfer, QGIS, and OpenGeoDa were used for interpolating data, showing sings, and transcribing data, respectively.

Despite Excel has removed the function of saving files in the database (.DBF) format, I may save the .DBF files through Microsoft ™ Access ® 2010 (Access). Note that it needs to save files as ASCII format in Excel and then export to the geographical information systems. In addition, it was strongly recommended to use simple ASCII characters in data title, i.e., complex characters were not recommended to record the data, such as traditional Chinese (BIG-5 coding) or other language (e.g. UTF-8, UTF-16) except for the Western codes.

SCA statistical system

The SCA statistical system (SCA) is a professional application for time series analysis and general statistics (Liu et al., 2002). In Windows ® 7, the SCA would meet some issues such as bad commands and floating error, this is owing to 16-bit scripts in the package, hence I strongly recommended to install the SCA in a Windows® XP or earlier versions of Microsoft ™ Windows ®. Here I specially thank to Professor George C. Tiao for his great helps in the Academia Sinica, conferences, and the software consults.

Note that SCA can directly fit ARIMA models and other models like ARCH, GARCH, etc., and SCA need no optional suites for advanced time series analysis, which was not available in the R Project or other statistical systems. In graphing and plotting, the traditional "graph" command would fail in recent Windows® environment, hence the Scientific Computing Association™ corporation recommends the "hgraph" command in terms of illustrating time series plots or other statistical plots. SCA is available in Department of Economy and Department of Finance of National Taiwan University, also you may buy it on the official website.

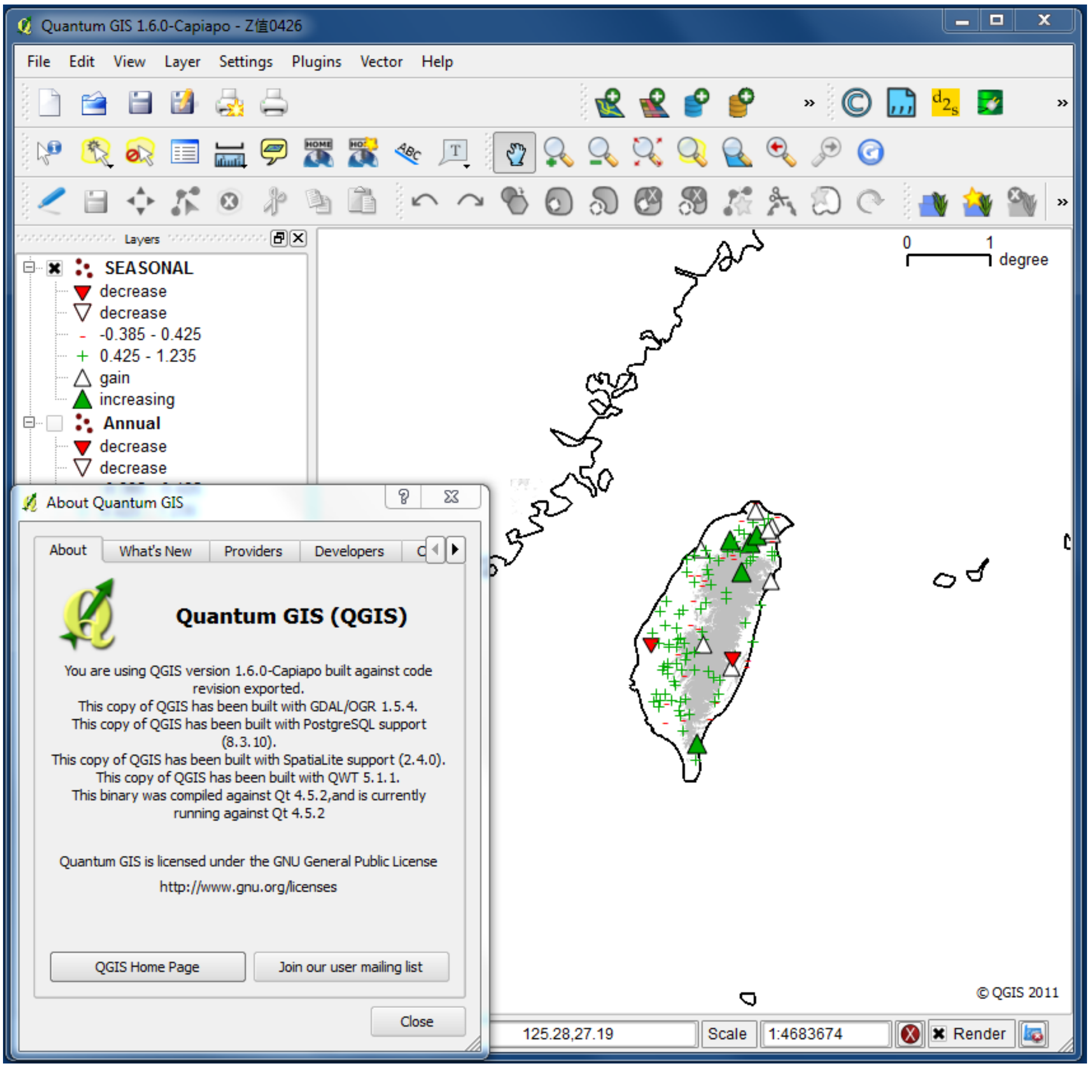

Figure 28. Quantum GIS screenshot.

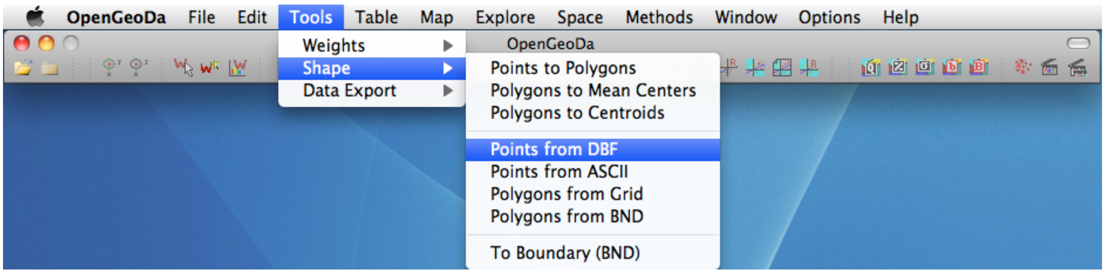

Figure 29. Using OpenGeoDa to create shapefiles.

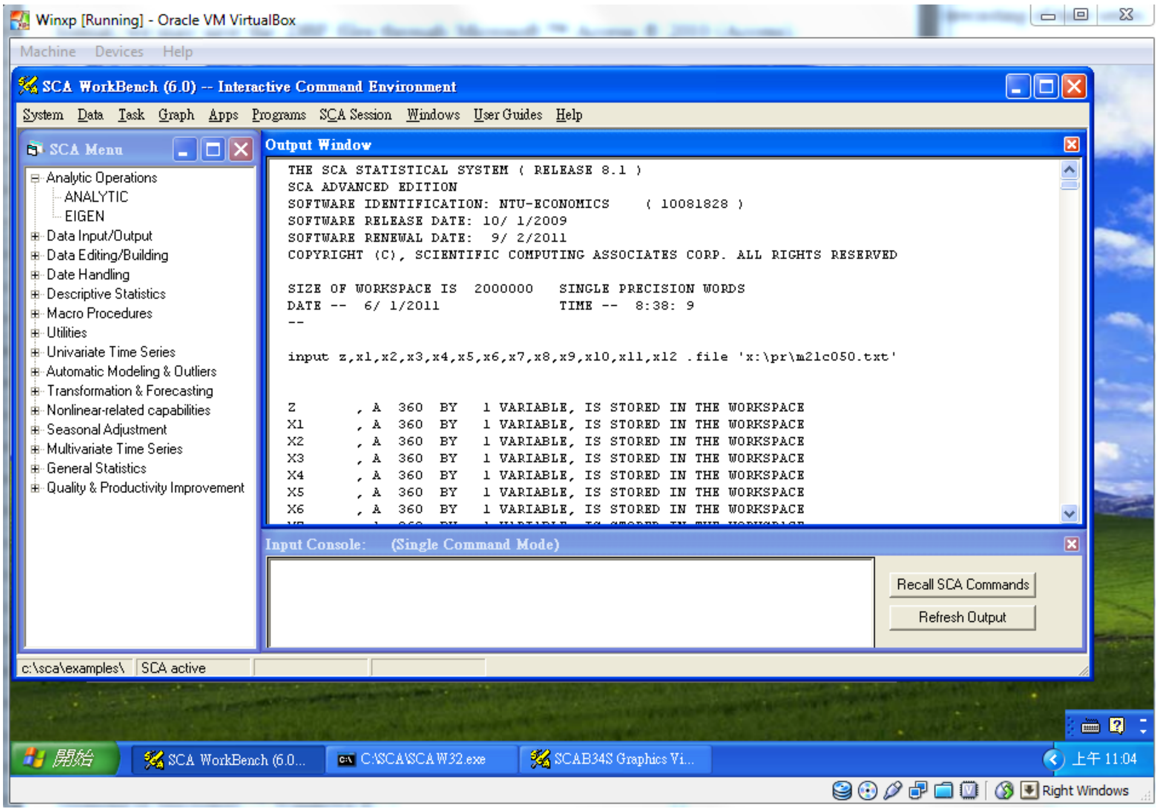

Figure 30. SCA ® under Windows® XP in Virtual Box ® environment in Windows ® 7

Appendix 2: The 120 WRA stations and their 31-year period mean rainfall amount, 31-year period mean daily rainfall intensity, and 31-year period mean numbers of rain days D_{Pr}.

Number	**Station**	**Longitude (E)**	**Latitude (N)**	**Altitude (m)**	**Data years**	$\overline{\mathrm{Pr}}$	$\bar{\eta}$	$\overline{D_{\mathrm{Pr}}}$
1	00A130	121.66	24.99	250	31	3340	18.5	183
2	00F390	120.91	24.29	553	29	2660	20.8	143
3	00H540	120.87	23.78	322	30	2111	17.3	129
4	00H710	120.77	23.83	215	31	2352	18.7	129
5	00J810	120.30	23.58	9	31	1330	17.8	73
6	00P470	120.48	22.88	64	31	2269	24.3	91
7	00Q070	120.47	22.65	25	31	2042	22.8	86
8	00S120	121.09	22.90	190	30	1799	16.6	113
9	01A160	121.38	25.08	250	30	2079	15.9	134
10	01A190	121.75	24.89	360	30	3824	18.3	210
11	01A200	121.75	24.98	380	31	4749	22.8	213
12	01A210	121.42	24.89	600	31	3423	20.1	184
13	01A220	121.36	24.94	33	31	2371	17.3	137
14	01A350	121.54	25.29	15	31	2173	15.1	139
15	01A380	121.80	25.11	101	31	4544	24.8	179
16	01A410	121.52	25.02	5	31	2283	17.5	126
17	01A420	121.54	25.16	605	31	4142	24.2	185
18	01A430	121.50	24.78	500	30	3377	19.2	186
19	01A440	121.56	24.88	916	30	4348	21.5	224
20	01A450	121.71	24.94	200	31	3596	20.3	178
21	01B030	121.70	25.08	16	31	3774	21.5	170
22	01C400	121.25	24.82	142	31	2363	18.4	129
23	01D100	121.15	24.63	940	30	2498	17.8	167
24	01D110	121.10	24.57	560	31	2447	19.2	141
25	01D180	121.21	24.68	560	31	2710	19.6	152
26	01D190	121.28	24.72	770	29	2915	20.2	162
27	01E030	120.97	24.47	550	31	2653	22.2	133
28	01E060	120.95	24.36	760	30	2594	21.9	140
29	01E080	120.99	24.40	1400	30	2679	21.3	169
30	01E120	120.90	24.71	42	31	1632	18.0	88
31	01E170	121.00	24.60	229	31	2628	20.7	130
32	01E230	120.81	24.31	337	31	1915	19.3	107

Number	Station	Longitude (E)	Latitude (N)	Altitude (m)	Data years	$\overline{\mathrm{Pr}}$	$\overline{\eta}$	$\overline{D_{\mathrm{Pr}}}$
33	01E240	120.96	24.69	45	31	1906	18.8	99
34	01E270	120.87	24.42	275	30	2173	20.6	112
35	01E290	120.77	24.41	269	31	1876	20.0	99
36	01E310	120.74	24.59	95	31	1555	17.9	86
37	01E330	120.73	24.43	190	29	1591	19.1	89
38	01E390	120.82	24.64	30	31	1579	17.4	88
39	01F350	121.03	24.28	2520	29	3770	25.4	221
40	01F680	120.81	24.12	480	30	2269	20.9	122
41	01G090	120.48	24.09	7	31	1254	16.4	75
42	01G240	120.42	23.96	11	30	1214	16.2	74
43	01H110	120.66	23.64	231	31	2744	21.7	129
44	01H210	121.20	24.18	1585	29	2800	20.9	181
45	01H310	121.20	24.11	2303	30	3286	22.2	217
46	01H390	120.93	23.62	2200	30	2601	17.8	212
47	01H400	120.93	23.56	1135	31	1996	15.9	157
48	01H470	120.92	23.71	1666	31	2500	16.5	198
49	01H590	120.64	23.93	420	31	1802	18.7	108
50	01H630	120.68	23.97	97	30	1616	18.0	91
51	01H680	120.89	23.99	330	31	2145	18.4	123
52	01H720	120.95	24.07	410	29	2159	19.8	121
53	01J100	120.46	23.80	30	31	1411	17.4	80
54	01J930	120.61	23.76	82	31	1882	18.5	101
55	01J960	120.62	23.63	205	31	2521	20.9	123
56	01J970	120.70	23.58	724	31	2623	20.8	144
57	01K060	120.31	23.70	13	30	1221	17.5	68
58	01L390	120.62	23.48	725	31	3359	26.4	145
59	01L480	120.60	23.53	545	30	3202	24.9	142
60	01L490	120.52	23.53	78	31	2096	21.0	97
61	01L910	120.52	23.57	95	31	2039	20.4	99
62	01M010	120.40	23.59	17	30	1391	17.1	81
63	01N840	120.58	23.12	480	28	3017	26.7	126
64	01N860	120.36	22.96	100	30	1985	23.3	86
65	01O070	120.51	23.33	350	31	2939	25.5	120
66	01O080	120.46	23.31	86	30	2338	23.1	101
67	01O190	120.45	23.27	80	30	2182	22.1	99
68	01O200	120.50	23.29	360	31	2865	25.9	117

Number	Station	Longitude (E)	Latitude (N)	Altitude (m)	Data years	$\overline{\mathrm{Pr}}$	$\bar{\eta}$	$\overline{D_{\mathrm{Pr}}}$
69	01P190	120.47	22.98	78	31	2406	24.5	96
70	01P260	120.72	22.91	458	31	3073	27.3	123
71	01P280	120.40	22.89	80	31	2143	24.5	86
72	01P390	120.40	22.81	90	31	2095	20.7	82
73	01P500	120.33	22.88	21	31	1915	23.7	78
74	01P660	120.59	23.08	355	31	2788	24.6	119
75	01P770	120.54	22.89	61	31	2745	25.0	107
76	01Q160	120.65	22.88	166	30	2949	25.6	117
77	01Q350	120.68	22.53	250	31	3543	31.8	114
78	01Q610	120.64	22.77	144	31	3038	26.4	116
79	01Q860	120.84	2 2.18	320	30	3043	20.7	153
80	01Q870	121.24	24.81	255	31	2468	24.6	106
81	01Q910	120.76	22.73	1320	31	3955	33.0	157
82	01Q920	120.69	22.68	750	29	4216	34.5	146
83	01Q930	120.65	22.71	150	31	2952	26.9	110
84	01S130	121.12	22.97	280	30	1912	16.4	124
85	01S210	121.00	22.69	100	30	2089	17.2	122
86	01S260	121.44	23.33	120	30	2138	16.8	131
87	01S270	121.46	23.40	120	30	2656	16.5	159
88	01S360	120.86	22.38	520	31	2398	18.6	142
89	01S430	121.04	23.17	910	30	1717	14.3	147
90	01S440	121.13	23.13	420	31	1670	16.6	111
91	01S470	120.98	23.25	2400	31	3419	18.8	252
92	01S570	121.06	22.88	220	31	2003	17.7	117
93	01T220	121.27	23.30	210	31	1917	16.5	119
94	01T230	121.31	23.43	180	31	2108	14.7	143
95	01T240	121.28	23.42	940	30	3346	16.4	228
96	01T500	121.60	24.04	20	28	2107	15.5	128
97	01T560	121.43	23.82	200	31	2631	16.5	159
98	01T730	121.52	23.60	30	30	2573	15.9	156
99	01U050	121.50	24.57	400	31	2562	15.2	174
100	01U060	121.53	24.61	295	31	2973	17.1	177
101	01U070	121.45	24.53	585	28	2651	14.8	191
102	01U080	121.38	24.44	1050	30	2428	12.1	227
103	01U120	121.75	24.62	60	29	4390	23.4	180
104	01U130	121.78	24.64	5	31	3499	20.6	163

Number	Station	Longitude (E)	Latitude (N)	Altitude (m)	Data years	$\overline{\mathrm{Pr}}$	$\overline{\eta}$	$\overline{D_{\mathrm{Pr}}}$
105	01U190	121.75	24.68	16	29	2907	17.9	157
106	01U230	121.74	24.33	48	31	2539	19.5	127
107	01U460	121.75	24.83	83	30	3027	16.7	175
108	01V060	120.82	23.27	850	30	2612	22.3	140
109	01V080	120.70	23.22	530	31	2955	24.4	133
110	21C050	121.24	24.81	255	31	2784	20.6	141
111	21C110	121.31	24.80	350	29	2956	20.9	147
112	21C150	121.37	24.67	630	29	2260	17.6	144
113	21D120	121.28	24.67	1450	30	2523	18.5	181
114	21D140	121.29	24.62	840	29	2081	18.0	140
115	H0O660	120.50	23.22	147	30	2715	24.9	111
116	H1M220	120.72	23.39	1550	30	2992	21.1	187
117	H1M230	120.82	23.47	2450	30	2483	17.6	216
118	H1M240	120.72	23.46	1850	30	2788	21.3	187
119	H1M250	120.60	23.34	1020	30	2707	22.7	148
120	H1P970	120.66	23.26	1100	30	2493	19.7	157

Appendix 3: Trends in annual rainfall amount (Pr), daily rainfall intensity (η), and ratio of rain days (λ) at 120 stations.

Note: + states for $p<0.1$, * for $p<0.05$, ** for $p<0.01$, *** for $p<0.001$.

	Pr		**η**			**λ**		
Station	**Z**	**Slope**	**Z**		**Slope**	**Z**		**Slope**
00A130	0.27	5.22	2.24	*	0.27	-1.29		-0.53
00F390	0.10	2.48	0.88		0.08	-1.50		-0.56
00H540	1.02	9.62	1.67	+	0.11	-1.05		-0.38
00H710	0.68	6.51	3.47	***	0.25	-1.46		-0.66
00J810	0.68	6.95	3.13	**	0.26	-1.53		-0.52
00P470	0.82	10.58	1.33		0.17	-0.37		-0.08
00Q070	1.05	13.34	2.38	*	0.31	-0.99		-0.37
00S120	0.58	7.51	1.53		0.15	-0.24		-0.07
01A160	-0.24	-3.36	1.12		0.07	-1.55		-0.58
01A190	0.27	9.01	1.73	+	0.18	-0.08		-0.02
01A200	0.75	19.88	1.77	+	0.17	-1.84	+	-0.50
01A210	1.56	27.15	1.05		0.09	-0.12		-0.04

Station	Pr			η			λ		
	Z		Slope	Z		Slope	Z		Slope
01A220	0.48		4.40	3.13	**	0.19	-1.73	+	-0.69
01A350	-0.44		-6.05	0.61		0.04	-1.09		-0.54
01A380	-2.01	*	-31.11	0.14		0.00	-1.70	+	-0.54
01A410	1.63		16.44	0.95		0.07	0.44		0.13
01A420	0.10		1.33	-0.07		-0.01	-0.10		-0.05
01A430	0.99		23.86	1.78	+	0.18	0.21		0.12
01A440	0.79		20.72	1.28		0.10	-0.25		-0.14
01A450	1.36		28.44	1.12		0.10	-0.24		-0.08
01B030	0.00		0.26	0.48		0.06	-0.34		-0.07
01C400	0.51		8.75	1.02		0.08	-1.29		-0.34
01D100	0.71		8.71	1.77	+	0.14	-1.73	+	-0.76
01D110	0.88		9.85	1.56		0.14	-2.04	*	-0.57
01D180	1.26		18.46	2.55	*	0.21	-1.09		-0.38
01D190	-0.86		-17.97	0.95		0.11	-0.78		-0.24
01E030	1.50		27.33	1.26		0.14	-1.10		-0.32
01E060	0.34		3.65	1.22		0.15	-1.33		-0.48
01E080	0.07		0.74	0.20		0.02	-1.46		-0.49
01E120	0.75		10.89	1.80	+	0.18	-1.70	+	-0.31
01E170	2.04	*	29.23	2.11	*	0.21	-1.60		-0.59
01E230	1.46		16.47	1.80	+	0.17	-0.14		-0.08
01E240	1.09		8.71	1.90	+	0.18	-1.33		-0.22
01E270	0.65		9.50	1.50		0.17	-2.04	*	-0.64
01E290	0.27		2.48	1.67	+	0.16	-1.50		-0.43
01E310	0.75		5.80	1.46		0.11	-0.85		-0.23
01E330	-0.32		-4.52	0.00		0.00	-0.90		-0.17
01E390	1.19		10.54	1.90	+	0.18	-1.29		-0.30
01F350	-0.18		-6.90	0.85		0.10	0.00		-0.02
01F680	-1.22		-16.67	0.10		0.01	-0.65		-0.25
01G090	1.19		10.36	2.31	*	0.21	-0.71		-0.26
01G240	1.36		10.85	2.01	*	0.20	-1.44		-0.47
01H110	1.29		20.89	2.31	*	0.18	-0.88		-0.33
01H210	1.16		24.79	1.26		0.11	-0.37		-0.10
01H310	0.00		-1.63	0.24		0.01	0.41		0.19
01H390	1.87	+	29.84	2.38	*	0.20	-0.20		-0.11
01H400	2.14	*	26.59	1.73	+	0.15	0.82		0.28
01H470	0.65		11.04	1.63		0.10	-0.99		-0.32

Station	Pr Z		Pr Slope	η Z		η Slope	λ Z		λ Slope
01H590	1.97	*	21.51	2.79	**	0.27	-1.34		-0.53
01H630	-0.03		-0.28	2.45	*	0.20	-2.01	*	-0.59
01H680	1.90	+	24.98	2.38	*	0.22	-1.33		-0.40
01H720	0.14		1.13	-0.61		-0.09	0.68		0.28
01J100	1.80	+	15.99	3.30	***	0.31	-1.87	+	-0.56
01J930	0.14		1.46	2.41	*	0.15	-1.87	+	-0.66
01J960	2.01	*	26.54	3.13	**	0.22	-0.82		-0.41
01J970	1.80	+	28.44	2.04	*	0.25	-0.20		-0.08
01K060	1.94	+	16.61	1.84	+	0.16	-0.85		-0.24
01L390	1.16		26.20	1.36		0.18	0.51		0.24
01L480	1.67	+	33.71	2.31	*	0.25	-0.37		-0.15
01L490	2.07	*	27.62	2.92	**	0.26	-0.20		-0.05
01L910	1.94	+	20.50	2.48	*	0.19	0.27		0.10
01M010	0.78		6.98	2.14	*	0.17	-1.99	*	-0.63
01N840	0.75		19.80	1.36		0.22	-0.61		-0.17
01N860	1.67	+	22.10	1.87	+	0.20	-0.88		-0.26
01O070	0.71		16.26	2.11	*	0.20	0.31		0.10
01O080	0.78		9.60	1.50		0.14	-0.78		-0.28
01O190	1.36		20.14	2.45	*	0.26	-0.95		-0.31
01O200	0.75		18.15	2.07	*	0.23	-0.27		-0.18
01P190	1.60		24.97	2.92	**	0.37	-0.82		-0.37
01P260	1.97	*	41.01	1.67	+	0.27	1.09		0.31
01P280	1.50		23.47	2.55	*	0.35	-0.68		-0.25
01P390	1.67	+	24.70	2.11	*	0.21	-0.31		-0.15
01P500	1.46		26.08	2.55	*	0.37	-0.51		-0.22
01P660	1.16		24.38	2.52	*	0.30	-1.14		-0.28
01P770	-0.07		-1.14	0.99		0.14	-0.95		-0.31
01Q160	2.18	*	45.78	2.14	*	0.32	-0.82		-0.27
01Q350	1.63		32.45	1.80	+	0.28	0.17		0.06
01Q610	2.07	*	33.42	0.68		0.10	1.16		0.36
01Q860	1.33		26.32	0.00		0.00	0.68		0.28
01Q870	0.75		10.22	0.07		0.02	0.65		0.25
01Q910	1.43		33.16	1.16		0.20	0.63		0.26
01Q920	1.97	*	66.13	1.56		0.50	0.03		0.02
01Q930	2.86	**	48.83	2.99	**	0.44	-0.85		-0.27
01S130	0.41		3.88	0.78		0.06	-0.10		-0.02

	Pr			η			λ		
Station	**Z**		**Slope**	**Z**		**Slope**	**Z**		**Slope**
01S210	0.17		1.42	-0.34		-0.02	0.07		0.02
01S260	-1.05		-12.79	-0.82		-0.06	0.73		0.31
01S270	-0.51		-6.28	-1.19		-0.07	0.68		0.39
01S360	1.67	+	20.50	1.80	+	0.18	0.17		0.05
01S430	0.82		6.77	1.56		0.12	-0.61		-0.19
01S440	0.37		2.80	1.05		0.09	0.17		0.07
01S470	0.58		9.37	1.50		0.10	-0.54		-0.22
01S570	-0.10		-1.48	0.85		0.07	-0.10		-0.10
01T220	0.03		0.11	0.07		0.01	0.05		0.00
01T230	0.20		2.98	0.00		0.00	0.39		0.22
01T240	-1.60		-23.39	-1.73	+	-0.12	-0.27		-0.06
01T500	0.43		8.87	1.56		0.11	0.48		0.17
01T560	0.00		1.09	-0.14		-0.01	1.16		0.40
01T730	0.07		1.85	-0.07		-0.01	0.88		0.25
01U050	0.27		5.52	0.75		0.07	-0.48		-0.16
01U060	0.14		2.73	1.09		0.08	-1.43		-0.63
01U070	1.18		19.69	1.26		0.09	-0.25		-0.17
01U080	1.33		19.14	1.46		0.09	0.14		0.04
01U120	-0.04		-2.78	1.60		0.19	-0.41		-0.12
01U130	0.00		0.06	1.70	+	0.12	-0.93		-0.36
01U190	-1.02		-14.64	0.41		0.02	-2.41	*	-0.78
01U230	1.50		32.99	1.16		0.10	1.43		0.53
01U460	0.82		10.72	2.52	*	0.18	-2.96	**	-1.14
01V060	0.79		18.82	0.21		0.04	0.86		0.37
01V080	1.43		31.31	1.29		0.18	0.61		0.30
21C050	2.11	*	25.64	2.18	*	0.19	-2.04	*	-0.85
21C110	1.53		25.31	2.38	*	0.20	0.24		0.11
21C150	1.77	+	27.20	2.35	*	0.30	-0.71		-0.25
21D120	2.07	*	28.83	1.87	+	0.19	-0.17		-0.05
21D140	-0.44		-6.85	1.60		0.16	-0.65		-0.25
H0O660	1.33		32.86	2.69	**	0.34	-1.84	+	-0.68
H1M220	1.29		30.91	1.39		0.19	-0.14		-0.04
H1M230	1.56		33.85	1.87	+	0.22	-0.46		-0.18
H1M240	1.12		27.90	0.92		0.13	0.31		0.18
H1M250	1.36		31.24	1.05		0.17	1.05		0.38
H1P970	1.36		34.86	1.12		0.16	1.09		0.29

Appendix 4: Seasonal rainfall amount (Pr) trend statistics

	Spring			Summer			Fall			Winter		
Time series	**Z**		**b**	**Z**		**b**	**Z**		**b**	**Z**		**b**
00A130	-0.81		-4.37	-0.36		-2.59	0.43		7.17	-0.24		-1.35
00F390	-1.59		-8.25	0.66		3.90	0.73		3.43	-0.69		-1.38
00H540	-0.96		-5.04	1.44		8.34	1.59		5.66	0.09		0.26
00H710	-1.97	*	-10.55	1.74	+	9.80	1.44		5.84	-0.32		-0.36
00J810	1.63		3.59	3.40	***	20.49	0.02		0.09	-3.55	***	-9.10
00P470	-2.01	*	-7.75	1.11		16.58	0.66		3.70	-0.24		-0.27
00Q070	-1.82	+	-6.22	1.44		21.82	0.28		1.31	0.32		0.34
00S120	0.47		1.83	0.66		5.82	0.84		5.65	0.32		0.44
01A160	-0.51		-2.93	0.88		6.92	-0.21		-1.24	-0.99		-6.00
01A190	0.51		4.80	2.27	*	13.99	0.51		7.09	1.52		19.33
01A200	0.00		-0.01	1.22		13.34	1.52		19.97	2.04	*	24.22
01A210	-0.21		-0.93	2.61	**	22.05	0.54		4.86	0.84		8.07
01A220	0.47		2.33	2.98	**	19.26	0.28		2.90	1.89	+	8.45
01A350	-0.21		-1.05	-0.39		-3.48	-0.47		-3.38	-1.29		-7.45
01A380	-1.33		-19.53	-1.48		-12.46	0.02		0.35	-0.62		-4.94
01A410	0.17		1.05	2.61	**	20.69	0.58		3.08	1.07		5.38
01A420	0.00		0.06	-0.02		-0.46	-0.02		-1.15	1.37		20.21
01A430	0.84		9.08	0.43		4.55	1.56		9.79	2.01	*	17.58
01A440	-0.51		-6.31	1.14		6.42	-0.06		-0.74	1.63		14.04
01A450	-0.32		-2.21	1.48		8.52	0.62		6.51	1.56		12.95
01B030	0.09		0.52	-1.59		-9.54	0.77		7.51	-0.02		-0.13
01C400	-0.32		-2.19	1.44		9.96	-0.81		-4.91	0.84		5.88
01D100	-0.96		-6.93	0.92		7.47	0.09		0.34	0.36		1.90
01D110	-0.43		-4.10	0.84		8.50	-1.97	*	-16.04	0.62		6.12
01D180	0.09		0.95	1.44		13.50	0.21		2.57	0.62		7.76
01D190	-0.58		-5.37	0.17		1.85	0.43		4.44	-0.02		-0.40
01E030	-1.37		-12.56	0.69		7.50	0.47		4.75	1.26		8.55
01E060	-0.66		-4.60	0.09		0.90	-0.84		-13.01	0.06		1.12
01E080	-1.93	+	-11.74	0.69		6.53	-1.07		-8.93	0.88		8.45
01E120	-0.24		-0.61	0.00		-0.04	-1.03		-4.56	1.86	+	7.80
01E170	-1.07		-7.04	0.77		7.39	-0.06		-0.68	1.48		11.03
01E230	0.21		1.52	1.67	+	14.85	-1.93	+	-15.48	0.92		6.08

	Spring			Summer			Fall			Winter		
Time series	Z		b	Z		b	Z		b	Z		b
01E240	-0.69		-4.45	0.73		4.89	-0.43		-3.34	0.69		4.33
01E270	0.96		4.59	1.22		8.98	-2.16	*	-16.18	-0.06		-2.22
01E290	0.32		1.81	-0.54		-4.29	-1.18		-9.89	0.06		0.70
01E310	-1.07		-7.45	1.82	+	12.27	-0.09		-0.36	1.41		4.91
01E330	-1.22		-7.91	-0.24		-1.44	-0.96		-4.64	0.54		3.20
01E390	-0.21		-0.41	1.07		6.37	-1.03		-5.65	0.81		2.88
01F350	-0.58		-5.42	1.29		18.64	-0.28		-6.62	0.36		4.54
01F680	-0.81		-6.22	0.54		5.21	0.06		1.21	-0.81		-8.17
01G090	-0.39		-1.63	2.23	*	12.30	-0.62		-4.26	0.24		1.66
01G240	0.21		0.60	1.67	+	8.66	0.28		0.95	0.54		3.93
01H110	-0.36		-4.19	-1.33		-11.83	-0.09		-1.11	1.07		11.50
01H210	-0.73		-6.95	0.39		4.19	0.69		4.75	0.73		7.57
01H310	-0.96		-5.68	0.84		12.41	0.32		5.13	0.21		2.13
01H390	-0.77		-8.64	1.48		12.37	-0.32		-3.08	1.07		10.63
01H400	-1.14		-9.12	-1.71	+	-12.72	0.36		1.70	2.12	*	10.01
01H470	-0.58		-5.17	-0.21		-2.77	-1.03		-12.83	2.23	*	12.30
01H590	-0.32		-1.24	2.61	**	19.62	0.09		0.71	-0.32		-2.49
01H630	-0.96		-6.18	1.67	+	7.49	0.36		2.48	-0.13		-1.16
01H680	-1.26		-10.23	2.34	*	17.70	0.92		7.26	0.96		7.65
01H720	-0.32		-2.84	0.17		1.37	-0.28		-1.20	0.69		3.09
01J100	-3.21	**	-17.86	1.44		9.57	0.77		5.12	0.88		3.35
01J930	-3.21	**	-21.16	0.51		4.70	-0.88		-6.24	0.47		2.88
01J960	-1.03		-6.29	0.06		0.38	-1.48		-17.83	1.37		15.20
01J970	-2.31	*	-19.62	1.44		14.19	-0.62		-4.62	0.62		5.60
01K060	-1.18		-6.16	-0.09		-0.54	-0.17		-1.46	1.37		7.41
01L390	-1.82	+	-26.17	0.43		6.44	-0.21		-1.47	-0.24		-3.10
01L480	-1.26		-10.32	-0.06		-1.30	-0.02		-1.14	0.99		13.54
01L490	-2.72	**	-13.08	1.44		11.42	0.69		5.84	0.47		4.96
01L910	-1.86	+	-9.52	0.54		5.97	-0.88		-6.90	0.58		5.94
01M010	-1.71	+	-8.56	-1.44		-9.32	1.11		5.83	1.11		4.12
01N840	-2.57	*	-32.99	0.77		7.93	1.37		14.50	1.33		16.12
01N860	-1.63		-15.87	-0.81		-6.74	-0.58		-3.93	0.17		2.67
01O070	-1.11		-13.44	-1.78	+	-18.56	-0.73		-5.19	1.07		11.28
01O080	-1.71	+	-18.40	-0.66		-6.24	0.43		5.01	0.66		8.07
01O190	-1.82	+	-15.74	-0.54		-6.04	-0.62		-6.84	0.92		11.51
01O200	-1.07		-7.29	-1.29		-11.69	-0.43		-3.89	1.03		10.77

	Spring			Summer			Fall			Winter		
Time series	Z		b	Z		b	Z		b	Z		b
01P190	-0.88		-6.69	-0.28		-3.13	-0.84		-8.57	0.58		7.04
01P260	-1.26		-14.21	-0.02		-0.82	-0.28		-4.41	0.96		10.95
01P280	-1.03		-6.58	-0.62		-5.93	-0.69		-4.44	1.07		10.77
01P390	-0.54		-3.55	-0.51		-4.61	0.36		2.94	1.22		9.46
01P500	-0.73		-2.34	0.69		6.34	-0.62		-3.69	1.18		8.76
01P660	-1.11		-7.29	0.81		8.97	0.81		6.93	1.22		13.93
01P770	-1.33		-8.54	1.37		12.81	-0.32		-2.78	0.92		7.69
01Q160	-0.73		-6.11	0.39		4.91	-0.54		-3.34	0.24		3.05
01Q350	-0.62		-7.75	1.33		10.15	0.39		7.60	1.18		20.36
01Q610	-1.14		-9.05	1.44		11.33	0.54		5.99	0.21		3.48
01Q860	-0.54		-3.95	1.41		10.67	0.92		10.44	1.78	+	23.56
01Q870	-1.63		-10.92	0.62		5.38	0.58		5.01	1.26		10.40
01Q910	-0.99		-11.68	1.48		16.39	0.06		1.75	0.73		11.87
01Q920	-0.39		-2.43	1.71	+	11.75	-0.96		-7.70	0.81		16.80
01Q930	-1.11		-8.31	1.63		12.42	0.92		10.47	0.58		7.61
01S130	-1.18		-5.72	1.18		6.20	0.00		-0.04	0.66		5.51
01S210	-0.58		-3.39	0.02		0.22	2.42	*	16.89	-0.77		-6.34
01S260	-0.54		-3.51	0.43		3.83	-0.28		-1.89	-0.62		-3.86
01S270	-0.51		-3.12	0.88		6.78	0.84		6.08	-0.24		-0.92
01S360	-1.37		-11.08	0.96		7.81	0.58		2.38	2.49	*	21.32
01S430	-0.81		-3.84	1.26		5.63	-0.13		-1.21	0.54		3.61
01S440	-1.29		-6.00	1.26		6.02	0.24		1.52	1.03		8.81
01S470	-1.11		-11.22	1.07		7.30	-0.62		-7.15	0.62		6.64
01S570	-0.96		-6.71	1.07		4.98	0.09		0.82	1.14		8.04
01T220	-1.56		-7.39	1.86	+	8.64	0.32		1.67	1.52		9.88
01T230	-1.71	+	-8.39	1.59		9.79	-0.21		-0.70	1.37		12.17
01T240	-1.44		-11.43	-0.51		-3.09	0.58		5.10	-2.12	*	-14.52
01T500	-0.17		-0.91	0.28		0.97	0.54		2.79	1.63		10.86
01T560	-0.24		-2.91	1.41		7.96	-0.06		-0.41	1.33		7.99
01T730	-0.24		-2.47	1.56		7.32	0.21		1.56	2.01	*	14.48
01U050	-0.96		-5.01	1.26		9.43	-0.21		-0.76	0.13		0.63
01U060	-0.88		-6.11	0.00		-0.06	0.02		0.27	-0.02		-0.06
01U070	-2.57	*	-9.13	1.56		9.94	-0.09		-0.58	0.92		7.61
01U080	-1.41		-4.95	1.78	+	8.01	-0.73		-2.96	2.16	*	9.96
01U120	0.24		1.34	-0.21		-2.57	0.54		8.54	1.07		10.46
01U130	-0.43		-2.93	-0.21		-0.90	0.51		3.91	0.96		11.68

	Spring			Summer			Fall			Winter		
Time series	Z		b	Z		b	Z		b	Z		b
01U190	-0.69		-4.93	-0.73		-4.66	1.26		6.85	0.88		3.46
01U230	-0.54		-3.28	1.59		7.46	0.32		2.50	1.67	+	14.29
01U460	-1.33		-8.18	0.73		4.40	-0.84		-6.63	-0.02		-0.41
01V060	-0.99		-8.42	1.11		10.17	0.02		0.23	0.88		9.08
01V080	-0.99		-9.94	1.56		16.18	0.88		8.38	0.39		5.42
21C050	-0.73		-2.87	1.97	*	18.25	-0.06		-1.94	2.23	*	13.44
21C110	-1.18		-8.79	2.42	*	20.44	-0.17		-2.52	0.36		3.01
21C150	-0.88		-7.41	1.56		13.85	-0.24		-2.29	0.43		4.54
21D120	-1.11		-8.02	1.78	+	12.75	-0.77		-4.86	0.62		5.60
21D140	-1.67	+	-7.64	0.96		9.81	-1.37		-8.35	-1.26		-7.59
H0O660	0.28		2.94	1.74	+	11.17	0.62		4.84	0.51		4.70
H1M220	0.02		0.03	1.78	+	22.11	0.66		4.87	0.51		6.81
H1M230	0.17		2.05	1.93	+	14.99	0.36		6.20	0.92		6.46
H1M240	0.17		1.48	1.41		11.33	0.66		8.07	0.51		5.38
H1M250	0.32		2.86	1.63		14.25	0.58		4.52	0.36		5.19
H1P970	0.17		1.29	1.44		11.80	0.54		3.46	0.51		8.22

Appendix 5: Seasonal daily rainfall intensity (η) trend statistics

Time series	Spring			Summer			Fall			Winter		
	Z		b	Z		b	Z		b	Z		b
00A130	-1.74	+	-0.35	0.47		0.11	1.22		0.42	-0.39		-0.05
00F390	-0.09		-0.01	0.28		0.23	-0.21		-0.05	-0.24		-0.08
00H540	-0.13		-0.05	-0.47		-0.25	0.66		0.10	-0.02		0.00
00H710	-0.62		-0.18	-0.69		-0.30	-0.02		-0.01	0.00		0.00
00J810	1.97	*	0.33	1.41		0.64	-0.39		-0.10	-3.55	***	-0.61
00P470	-1.26		-0.33	0.13		0.13	-0.88		-0.35	-0.99		-0.05
00Q070	-2.57	*	-0.81	-0.39		-0.50	-0.51		-0.13	-0.96		-0.03
00S120	0.99		0.05	0.88		0.19	1.03		0.16	1.33		0.08
01A160	-0.02		0.00	1.37		0.26	0.36		0.06	0.13		0.03
01A190	0.99		0.22	2.31	*	0.36	0.69		0.11	1.41		0.34
01A200	0.17		0.04	2.19	*	0.36	2.68	**	0.49	2.53	*	0.57
01A210	-0.39		-0.06	2.64	**	0.47	1.26		0.23	1.52		0.29
01A220	0.88		0.16	2.46	*	0.40	1.74	+	0.31	2.76	**	0.39
01A350	0.09		0.01	-0.39		-0.09	0.96		0.12	-0.24		-0.03

Time series	Spring			Summer			Fall			Winter		
	Z		b	Z		b	Z		b	Z		b
01A380	-1.33		-0.22	-0.02		0.00	1.37		0.23	0.51		0.06
01A410	0.13		0.03	2.01	*	0.37	1.48		0.26	1.41		0.21
01A420	-0.43		-0.11	0.58		0.10	0.58		0.10	1.78	+	0.52
01A430	0.24		0.07	0.13		0.01	2.34	*	0.30	1.56		0.30
01A440	-0.47		-0.09	1.14		0.15	0.77		0.11	2.19	*	0.32
01A450	-0.28		-0.05	1.03		0.16	1.74	+	0.44	2.01	*	0.44
01B030	0.43		0.07	-0.32		-0.05	0.32		0.05	0.66		0.14
01C400	0.58		0.10	0.77		0.11	0.21		0.02	1.22		0.18
01D100	0.13		0.03	1.52		0.19	0.66		0.11	1.33		0.19
01D110	0.17		0.05	1.03		0.19	-2.01	*	-0.44	0.58		0.11
01D180	0.54		0.15	1.56		0.30	1.29		0.27	1.56		0.32
01D190	-0.32		-0.09	0.09		0.02	0.84		0.18	0.36		0.04
01E030	-0.58		-0.06	0.88		0.23	0.17		0.04	0.62		0.16
01E060	-0.88		-0.24	0.36		0.05	-0.51		-0.14	0.13		0.06
01E080	-1.11		-0.21	1.14		0.23	-0.69		-0.09	1.26		0.29
01E120	-0.21		-0.05	0.73		0.14	-0.73		-0.14	1.41		0.22
01E170	-0.39		-0.04	1.11		0.23	0.54		0.13	1.41		0.27
01E230	-0.21		-0.05	0.36		0.13	-1.48		-0.32	0.99		0.33
01E240	-0.69		-0.14	0.84		0.19	-0.17		-0.07	0.02		0.02
01E270	0.09		0.03	0.43		0.16	-1.22		-0.29	0.32		0.10
01E290	-0.13		-0.02	0.36		0.05	-0.62		-0.14	0.58		0.16
01E310	-1.71	+	-0.38	0.96		0.21	0.73		0.17	1.07		0.24
01E330	-0.99		-0.23	-0.02		-0.01	-0.62		-0.10	1.97	*	0.39
01E390	-0.32		-0.05	1.59		0.20	-0.43		-0.17	0.28		0.03
01F350	-0.51		-0.17	1.33		0.32	-0.81		-0.17	0.51		0.17
01F680	-1.22		-0.24	0.36		0.06	-0.21		-0.08	-1.11		-0.15
01G090	-0.28		-0.06	2.23	*	0.38	0.77		0.16	1.26		0.23
01G240	0.73		0.17	1.26		0.24	1.59		0.27	0.92		0.19
01H110	-0.13		-0.03	-0.43		-0.07	0.47		0.08	0.96		0.22
01H210	-1.14		-0.22	0.51		0.11	0.66		0.14	0.51		0.07
01H310	-1.41		-0.25	0.24		0.04	1.11		0.26	-0.06		-0.01
01H390	-1.22		-0.17	0.77		0.17	0.43		0.07	1.59		0.32
01H400	-1.14		-0.17	-1.07		-0.13	0.81		0.13	1.59		0.22
01H470	-1.33		-0.21	0.21		0.03	-0.06		-0.01	1.82	+	0.24
01H590	0.17		0.01	2.72	**	0.53	1.29		0.30	-0.32		-0.08
01H630	-0.32		-0.04	1.67	+	0.30	0.99		0.16	1.11		0.19

Time series	Spring			Summer			Fall			Winter		
	Z		b	Z		b	Z		b	Z		b
01H680	-1.44		-0.26	1.78	+	0.36	1.71	+	0.35	0.96		0.23
01H720	-0.17		-0.07	0.13		0.04	-1.33		-0.27	0.13		0.03
01J100	-3.10	**	-0.50	1.82	+	0.33	1.44		0.35	1.74	+	0.38
01J930	-3.25	**	-0.55	1.26		0.21	-0.32		-0.06	1.33		0.18
01J960	-0.02		0.00	1.18		0.20	-0.69		-0.15	3.28	**	0.46
01J970	-2.23	*	-0.40	1.86	+	0.31	0.02		0.01	1.33		0.22
01K060	-0.66		-0.14	0.17		0.05	1.29		0.27	2.23	*	0.48
01L390	-1.63		-0.47	0.66		0.14	0.00		-0.01	0.47		0.25
01L480	-0.02		-0.01	-0.43		-0.09	0.66		0.15	1.29		0.44
01L490	-2.76	**	-0.43	0.88		0.19	1.71	+	0.40	1.56		0.31
01L910	-2.83	**	-0.40	0.62		0.11	0.36		0.05	1.74	+	0.32
01M010	-1.82	+	-0.27	-0.58		-0.13	1.59		0.35	1.44		0.27
01N840	-2.12	*	-0.56	1.44		0.27	1.56		0.59	2.38	*	0.55
01N860	-1.18		-0.31	-0.39		-0.08	-0.99		-0.16	1.48		0.37
01O070	-1.33		-0.35	-0.73		-0.20	0.73		0.11	2.27	*	0.53
01O080	-1.52		-0.32	0.17		0.02	0.84		0.22	1.93	+	0.48
01O190	-1.48		-0.30	-0.13		-0.03	0.28		0.07	2.04	*	0.63
01O200	-1.03		-0.22	-0.96		-0.29	-0.39		-0.10	1.33		0.44
01P190	-0.66		-0.12	-0.69		-0.14	-0.54		-0.15	1.86	+	0.56
01P260	-0.92		-0.21	-0.69		-0.14	-0.06		-0.03	0.96		0.27
01P280	-0.96		-0.28	-0.92		-0.22	-0.32		-0.10	1.37		0.42
01P390	-0.66		-0.16	-0.39		-0.09	0.73		0.19	1.67	+	0.46
01P500	-1.03		-0.23	0.47		0.16	0.06		0.01	2.01	*	0.65
01P660	-0.99		-0.30	0.84		0.28	1.22		0.31	2.12	*	0.69
01P770	-0.88		-0.21	1.03		0.32	-0.02		0.00	1.48		0.33
01Q160	-0.36		-0.06	0.62		0.15	-0.06		-0.01	1.56		0.60
01Q350	-1.56		-0.38	1.37		0.43	0.58		0.24	1.78	+	0.71
01Q610	-2.87	**	-0.59	0.92		0.18	0.88		0.27	0.84		0.30
01Q860	-1.59		-0.29	0.84		0.19	0.54		0.14	0.69		0.15
01Q870	-1.78	+	-0.44	0.99		0.34	0.54		0.18	0.73		0.26
01Q910	-1.03		-0.26	0.84		0.33	0.24		0.06	0.58		0.25
01Q920	-0.77		-0.32	1.37		0.52	-0.69		-0.29	1.52		0.83
01Q930	-1.63		-0.33	1.63		0.35	1.07		0.30	1.78	+	0.49
01S130	-0.99		-0.18	0.84		0.11	0.13		0.05	0.66		0.15
01S210	-1.07		-0.21	-0.62		-0.04	1.26		0.24	-0.24		-0.07
01S260	-1.14		-0.16	-0.47		-0.09	-1.48		-0.22	-1.07		-0.21

Time series	Spring			Summer			Fall			Winter		
	Z		b	Z		b	Z		b	Z		b
01S270	-0.47		-0.08	0.24		0.03	0.17		0.03	-0.84		-0.11
01S360	-0.84		-0.17	1.22		0.28	0.58		0.16	2.27	*	0.59
01S430	-0.32		-0.05	1.56		0.13	-0.24		-0.05	0.17		0.03
01S440	-1.41		-0.19	1.74	+	0.25	-0.17		-0.04	0.69		0.16
01S470	-1.11		-0.23	0.73		0.12	-1.18		-0.17	0.39		0.11
01S570	-1.26		-0.23	0.47		0.12	0.02		0.03	0.73		0.25
01T220	-0.99		-0.11	1.97	*	0.29	0.24		0.03	1.03		0.26
01T230	-1.59		-0.19	1.78	+	0.20	0.32		0.04	1.52		0.30
01T240	-1.29		-0.15	0.09		0.02	0.21		0.03	-1.82	+	-0.20
01T500	-0.43		-0.05	0.09		0.04	0.58		0.10	1.03		0.14
01T560	-0.39		-0.06	1.14		0.20	0.28		0.02	0.96		0.18
01T730	-0.32		-0.07	0.73		0.10	-0.17		-0.05	1.33		0.20
01U050	-0.88		-0.11	1.37		0.18	0.73		0.07	0.51		0.08
01U060	-0.69		-0.11	0.73		0.11	0.58		0.07	0.39		0.04
01U070	-1.78	+	-0.16	1.78	+	0.18	0.17		0.02	1.03		0.12
01U080	-0.81		-0.06	1.44		0.14	-0.66		-0.03	1.89	+	0.15
01U120	0.13		0.01	0.51		0.11	1.78	+	0.43	2.87	**	0.33
01U130	0.47		0.04	0.17		0.03	1.11		0.25	1.44		0.28
01U190	-0.77		-0.08	0.00		0.00	2.19	*	0.28	2.57	*	0.25
01U230	-0.58		-0.13	0.84		0.17	0.17		0.03	1.03		0.21
01U460	-0.13		-0.02	1.07		0.14	0.24		0.03	1.03		0.13
01V060	-1.11		-0.19	0.00		-0.01	-0.09		-0.01	0.96		0.16
01V080	-1.07		-0.27	0.99		0.28	1.18		0.38	0.81		0.15
21C050	0.39		0.06	1.93	+	0.30	0.62		0.11	2.38	*	0.37
21C110	-0.58		-0.10	2.01	*	0.36	0.54		0.09	1.29		0.25
21C150	-0.51		-0.07	1.82	+	0.35	0.36		0.06	1.82	+	0.27
21D120	-1.03		-0.13	1.74	+	0.18	0.17		0.03	0.02		0.03
21D140	-0.73		-0.07	0.96		0.16	-0.69		-0.13	-0.09		-0.03
H0O660	-0.02		-0.01	2.04	*	0.48	1.48		0.29	1.29		0.42
H1M220	0.02		0.02	2.08	*	0.42	0.39		0.11	0.77		0.31
H1M230	0.09		0.01	1.86	+	0.22	0.81		0.18	1.48		0.26
H1M240	-0.66		-0.14	1.11		0.25	0.51		0.15	0.81		0.28
H1M250	-0.24		-0.09	2.12	*	0.45	1.03		0.24	0.92		0.21
H1P970	-0.17		-0.04	1.14		0.23	0.88		0.12	1.11		0.33

Appendix 6: Seasonal ratio of rain days (λ) trend statistics

Time series	Spring			Summer			Fall			Winter		
	Z		b	Z		b	Z		b	Z		b
00A130	0.69		0.00	-1.29		0.00	-2.72	**	-0.01	-0.51		0.00
00F390	-0.88		0.00	-0.32		0.00	1.33		0.00	0.98		0.00
00H540	-0.51		0.00	1.18		0.00	1.63		0.01	0.17		0.00
00H710	-1.14		0.00	1.89	+	0.00	1.26		0.00	0.36		0.00
00J810	-1.41		0.00	0.02		0.00	-0.32		0.00	1.48		0.00
00P470	0.51		0.00	0.69		0.00	0.99		0.00	3.17	**	0.01
00Q070	2.53	*	0.01	1.97	*	0.01	1.63		0.00	2.12	*	0.01
00S120	-0.47		0.00	-0.36		0.00	0.00		0.00	-0.58		0.00
01A160	-0.54		0.00	-0.99		0.00	-0.86		0.00	-2.34	*	0.00
01A190	-2.14	*	-0.01	-0.24		0.00	-0.73		0.00	0.02		0.00
01A200	-0.17		0.00	-1.67	+	0.00	-2.27	*	0.00	-0.99		0.00
01A210	-0.09		0.00	0.81		0.00	-2.83	**	-0.01	-0.66		0.00
01A220	0.09		0.00	2.42	*	0.01	-2.01	*	0.00	-0.81		0.00
01A350	-0.54		0.00	-0.13		0.00	-1.82	+	0.00	-1.74	+	0.00
01A380	-0.99		0.00	-2.79	**	-0.01	-1.82	+	0.00	-0.99		0.00
01A410	-0.77		0.00	1.48		0.00	-1.89	+	0.00	-0.84		0.00
01A420	1.44		0.00	-0.58		0.00	-2.61	**	-0.01	0.41		0.00
01A430	0.64		0.00	1.07		0.00	-1.56		0.00	1.01		0.00
01A440	0.96		0.00	0.81		0.00	-2.31	*	0.00	-1.11		0.00
01A450	0.39		0.00	2.19	*	0.00	-2.31	*	0.00	-0.54		0.00
01B030	-0.13		0.00	-2.79	**	-0.01	-0.54		0.00	-1.33		0.00
01C400	-1.67	+	0.00	1.22		0.00	-2.57	*	-0.01	0.02		0.00
01D100	-0.96		0.00	-0.36		0.00	-0.51		0.00	-0.69		0.00
01D110	-1.69	+	0.00	-0.32		0.00	-0.51		0.00	0.56		0.00
01D180	-0.99		0.00	0.51		0.00	-2.16	*	0.00	-0.58		0.00
01D190	-0.73		0.00	1.07		0.00	-0.06		0.00	-0.36		0.00
01E030	-2.42	*	-0.01	-0.13		0.00	0.00		0.00	0.92		0.00
01E060	-0.36		0.00	0.21		0.00	-0.32		0.00	-1.07		0.00
01E080	-1.71	+	0.00	0.24		0.00	-2.23	*	-0.01	-0.92		0.00
01E120	-0.73		0.00	-0.92		0.00	-0.69		0.00	1.18		0.00
01E170	-0.62		0.00	-0.69		0.00	-0.84		0.00	0.69		0.00
01E230	0.99		0.00	1.86	+	0.01	-2.08	*	-0.01	0.38		0.00
01E240	-0.58		0.00	-0.92		0.00	-1.56		0.00	1.14		0.00
01E270	1.67	+	0.00	0.88		0.00	-2.53	*	-0.01	0.06		0.00

Time series	Spring			Summer			Fall			Winter		
	Z		b	Z		b	Z		b	Z		b
01E290	0.62		0.00	-0.58		0.00	-1.29		0.00	-0.13		0.00
01E310	-0.39		0.00	0.69		0.00	-1.67	+	0.00	-0.13		0.00
01E330	-0.24		0.00	0.09		0.00	-1.11		0.00	-1.44		0.00
01E390	-0.02		0.00	0.02		0.00	-1.89	+	0.00	1.22		0.00
01F350	-0.39		0.00	1.22		0.00	0.08		0.00	-0.54		0.00
01F680	-1.11		0.00	0.60		0.00	0.92		0.00	-1.18		0.00
01G090	-1.14		0.00	0.28		0.00	-1.61		0.00	-0.69		0.00
01G240	-0.88		0.00	1.26		0.00	-1.26		0.00	-0.32		0.00
01H110	-1.41		0.00	-1.33		0.00	-0.36		0.00	0.28		0.00
01H210	-0.36		0.00	-0.69		0.00	0.13		0.00	1.93	+	0.00
01H310	-0.28		0.00	1.03		0.00	-0.75		0.00	0.17		0.00
01H390	-1.52		0.00	1.71	+	0.01	-0.36		0.00	-0.45		0.00
01H400	-1.37		0.00	-1.71	+	0.00	0.73		0.00	1.13		0.00
01H470	-1.56		0.00	-0.62		0.00	0.32		0.00	0.36		0.00
01H590	-1.22		0.00	1.74	+	0.01	-1.82	+	-0.01	-0.81		0.00
01H630	-1.52		0.00	-0.06		0.00	-0.77		0.00	-1.97	*	0.00
01H680	-1.82	+	-0.01	1.67	+	0.01	-0.51		0.00	0.21		0.00
01H720	0.62		0.00	-0.36		0.00	0.24		0.00	1.22		0.00
01J100	-2.61	**	-0.01	1.11		0.00	-0.62		0.00	-0.88		0.00
01J930	-3.66	***	-0.01	0.09		0.00	-1.82	+	0.00	-0.96		0.00
01J960	-1.41		0.00	-2.72	**	-0.01	-1.37		0.00	-0.92		0.00
01J970	-1.93	+	-0.01	1.14		0.00	-2.42	*	-0.01	-0.84		0.00
01K060	-1.52		0.00	-0.13		0.00	-1.11		0.00	0.81		0.00
01L390	-1.93	+	-0.01	0.06		0.00	-1.03		0.00	-1.89	+	0.00
01L480	-1.97	*	-0.01	-0.99		0.00	-0.58		0.00	-0.36		0.00
01L490	-2.49	*	-0.01	1.78	+	0.01	-1.22		0.00	-0.43		0.00
01L910	-1.11		0.00	0.06		0.00	-0.62		0.00	-0.54		0.00
01M010	-2.33	*	0.00	-1.11		0.00	-0.66		0.00	0.08		0.00
01N840	-2.79	**	-0.01	0.51		0.00	1.07		0.00	0.00		0.00
01N860	-3.13	**	-0.01	-0.69		0.00	-0.21		0.00	-0.99		0.00
01O070	-1.33		-0.01	-2.76	**	-0.01	-0.23		0.00	-0.02		0.00
01O080	-1.63		-0.01	-1.14		0.00	-1.11		0.00	-0.28		0.00
01O190	-1.71	+	-0.01	-0.84		0.00	-1.56		0.00	-0.47		0.00
01O200	-1.37		-0.01	-1.14		0.00	-1.37		0.00	0.49		0.00
01P190	-2.16	*	-0.01	-0.99		0.00	-0.96		0.00	-0.28		0.00
01P260	-1.67	+	-0.01	0.06		0.00	-1.93	+	0.00	1.74	+	0.00

Time series	Spring			Summer			Fall			Winter		
	Z		b	Z		b	Z		b	Z		b
01P280	-1.18		0.00	-0.69		0.00	-0.58		0.00	1.52		0.00
01P390	-1.44		0.00	-0.24		0.00	0.06		0.00	0.56		0.00
01P500	-1.14		0.00	0.47		0.00	-0.58		0.00	-0.21		0.00
01P660	-1.07		0.00	0.39		0.00	-1.18		0.00	-0.54		0.00
01P770	-1.41		0.00	0.88		0.00	-0.99		0.00	-0.38		0.00
01Q160	-1.37		-0.01	-0.17		0.00	-0.54		0.00	-1.03		0.00
01Q350	-1.03		0.00	0.92		0.00	1.03		0.00	0.47		0.00
01Q610	-0.69		0.00	1.93	+	0.01	0.66		0.00	0.73		0.00
01Q860	1.44		0.00	2.79	**	0.01	3.06	**	0.01	2.72	**	0.01
01Q870	-1.48		0.00	0.58		0.00	0.43		0.00	1.41		0.00
01Q910	-0.88		0.00	1.26		0.01	0.21		0.00	0.02		0.00
01Q920	-0.54		0.00	1.29		0.00	0.17		0.00	-0.86		0.00
01Q930	-1.48		0.00	1.03		0.00	0.09		0.00	-0.32		0.00
01S130	-1.82	+	0.00	1.14		0.00	0.39		0.00	0.06		0.00
01S210	-0.24		0.00	1.93	+	0.00	1.59		0.00	-0.77		0.00
01S260	1.48		0.00	2.01	*	0.00	1.86	+	0.00	0.77		0.00
01S270	0.54		0.00	1.07		0.00	2.42	*	0.01	0.62		0.00
01S360	-2.61	**	0.00	0.23		0.00	0.17		0.00	0.79		0.00
01S430	-1.78	+	0.00	0.54		0.00	-0.43		0.00	-0.09		0.00
01S440	-1.82	+	0.00	0.39		0.00	1.35		0.00	1.11		0.00
01S470	-1.71	+	0.00	0.66		0.00	-0.28		0.00	0.47		0.00
01S570	-1.67	+	0.00	1.97	*	0.00	-1.59		0.00	0.17		0.00
01T220	-2.57	*	-0.01	0.84		0.00	0.51		0.00	1.59		0.00
01T230	-2.04	*	0.00	0.62		0.00	-0.38		0.00	0.54		0.00
01T240	-1.71	+	0.00	-0.81		0.00	0.58		0.00	-1.78	+	0.00
01T500	-1.48		0.00	0.06		0.00	-0.24		0.00	2.19	*	0.00
01T560	-0.39		0.00	0.88		0.00	-0.49		0.00	0.86		0.00
01T730	0.92		0.00	1.67	+	0.00	-0.58		0.00	1.63		0.00
01U050	-0.99		0.00	1.13		0.00	-1.56		0.00	-1.18		0.00
01U060	-1.59		0.00	-1.71	+	0.00	-1.37		0.00	-0.73		0.00
01U070	-2.91	**	-0.01	-0.06		0.00	-0.32		0.00	0.99		0.00
01U080	-1.67	+	0.00	1.52		0.00	-1.18		0.00	1.63		0.00
01U120	0.11		0.00	-1.18		0.00	-1.61		0.00	-1.52		0.00
01U130	-1.56		0.00	-2.27	*	0.00	-1.03		0.00	-0.92		0.00
01U190	-0.92		0.00	-2.34	*	-0.01	-1.11		0.00	-2.34	*	0.00
01U230	0.84		0.00	1.89	+	0.00	0.69		0.00	1.82	+	0.00

Time series	Spring			Summer			Fall			Winter		
	Z		b	Z		b	Z		b	Z		b
01U460	-2.68	**	-0.01	-1.01		0.00	-1.97	*	-0.01	-1.52		0.00
01V060	-0.28		0.00	2.08	*	0.01	0.32		0.00	0.43		0.00
01V080	-0.69		0.00	1.71	+	0.01	0.62		0.00	0.43		0.00
21C050	-2.08	*	-0.01	0.92		0.00	-1.29		0.00	-0.17		0.00
21C110	-1.48		0.00	2.23	*	0.01	-1.52		0.00	-1.37		0.00
21C150	-0.88		0.00	0.81		0.00	-1.20		0.00	-2.42	*	-0.01
21D120	-1.44		0.00	1.78	+	0.00	-1.71	+	0.00	-0.21		0.00
21D140	-1.41		0.00	1.29		0.00	-1.86	+	0.00	-2.72	**	-0.01
H0O660	-1.22		0.00	0.88		0.00	-0.21		0.00	-0.58		0.00
H1M220	-0.21		0.00	1.56		0.00	-0.66		0.00	0.06		0.00
H1M230	-0.96		0.00	1.88	+	0.01	-0.69		0.00	-0.54		0.00
H1M240	-0.17		0.00	2.12	*	0.01	0.09		0.00	-0.02		0.00
H1M250	0.73		0.00	2.12	*	0.01	0.00		0.00	0.32		0.00
H1P970	-0.47		0.00	1.86	+	0.00	-0.32		0.00	0.19		0.00

Appendix 7: SCA codes used in this thesis

A.7.1 Seasonal ARIMA in SCA

*/*Call seasonal data, here the time series is "z", "b1" was given slope of trend made by TFPW and MK test. "x1", "x2", "x3", and "x4" were dummy variable for each season. "x0" was a test variable which was included in data and hence I had to define it or the SCA would not recognize all variables; and then I build a ARIMA model, m1 as* $(1-B^4)z=(1-B^{22})a_t$*. The parameters were estimated through the exact likelihood function*/*

```
    input x0,z,x1,x2,x3,x4,b1.file 'x:\pr\01q930.txt'
     tsm m1.model (4)Z=(22)noise
     estim m1 .method exact .hold resi (r1)
```

*/*I added the dummy variable and their parameters, c1,c2,c3, and c4, to build the intervention model. These parameters would be estimated through exact likelihood. */*

```
     tsm m1.add (c1)x1+(c2)x2+(c3)x3+(c4)x4
    oestim m1 .method exact .hold resi (r1)
    oforecast m1 .method exact .origins 100 .nofs 10 .hold forecast(f1),std_errs(s1)
    oforecast m1 .hold forecast(f1),std_errs(s1)
    uforecast m1 .method exact .origins 100 .nofs 10 .hold forecast(f1),std_errs(s1)
```

```
hgraph z,f1,s1 .type fcst
```

/ Here I plotted the forecasting graph with prediction and error, as well, I examined the ACF and PACF in the residual. */*

```
hgraph r1.type acf
hgraph r1.type pacf
hgraph z.type acf
hgraph z.type pacf
```

A.7.2 Monthly ARIMA in SCA

*/*Call monthly data, here the variables, "x_i", are the dummy variable for each month, the model, m1, was built as Equation 19. */*

```
input z,x1,x2,x3,x4,x5,x6,x7,x8,x9,x10,x11,x12 .file 'x:\pr\m21c050.txt'
tsm m1.model (11)Z=(11)noise
oestim m1 .method exact .hold resi (r1)
  estim m1 .method exact .hold resi (r1)
```

*/*the SCA would not take many variables added in the model at once, hence I revised the model twice and then estimated the parameters*/*

```
  tsm m1.add
      @(c1)x1+(c2)x2+(c3)x3+(c4)x4+(c5)x5+(c6)x6+(c7)x7+(c8)x8+(c9)x9
tsm m1.add (c10)x10+(c11)x11+(c12)x12
uforecast m1 .method exact .origins 300 .nofs 100 .hold forecast(f1),std_errs(s1)
oestim m1 .method exact .hold resi (r3)
oforecast m1 .method exact .origins 300 .nofs 36 .hold forecast(f3),std_errs(s3)
hgraph z,f3,s3 .type fcst
```

Appendex 8: Color figures

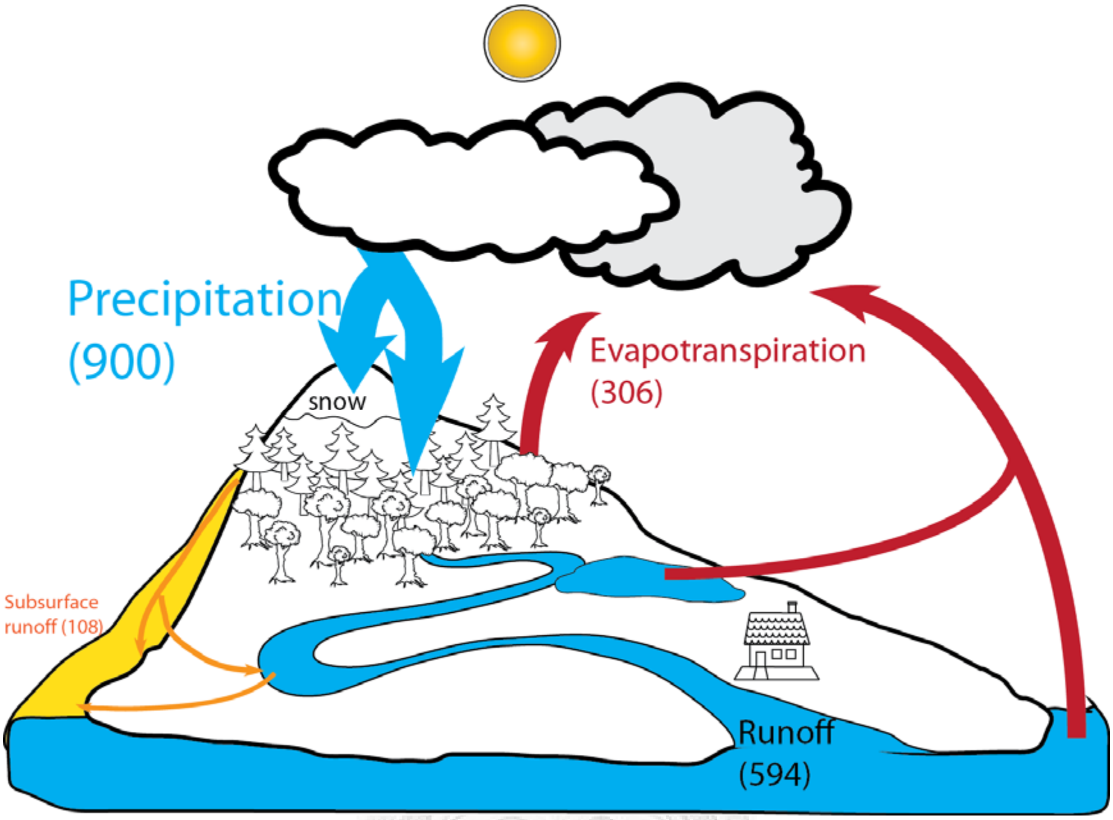

Figure 1. The terrestrial hydrological cycle with estimations in Taiwan.

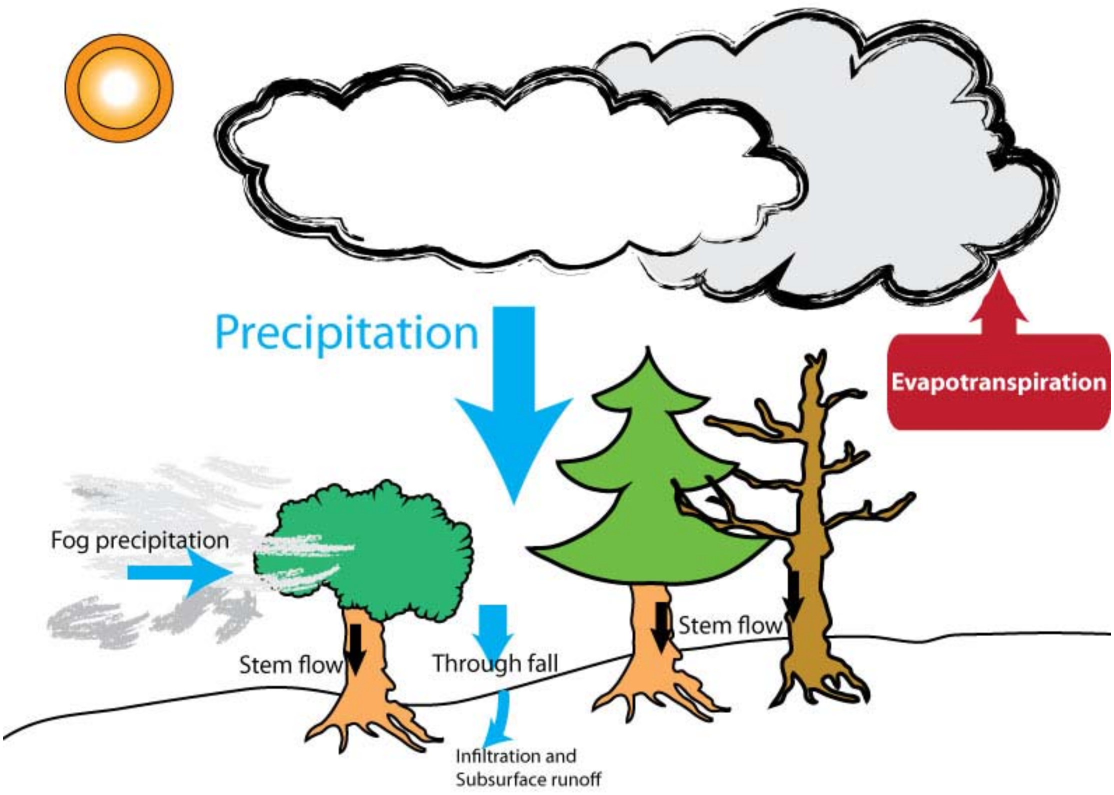

Figure 2. Rainfall partitioning in a forest

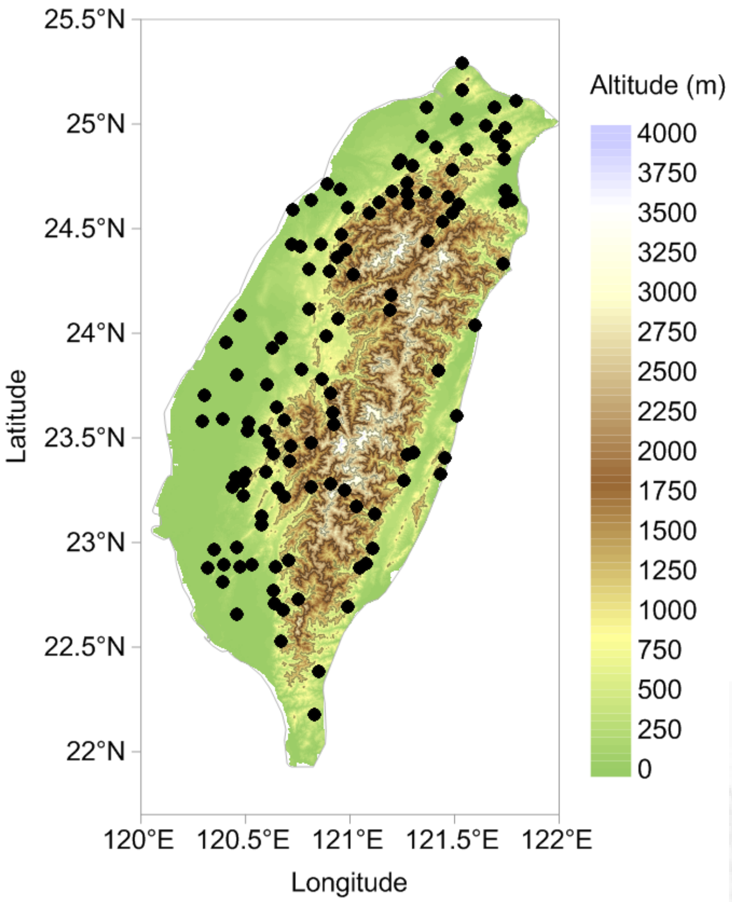

Figure 3. Spatial distribution of the 120 WRA stations

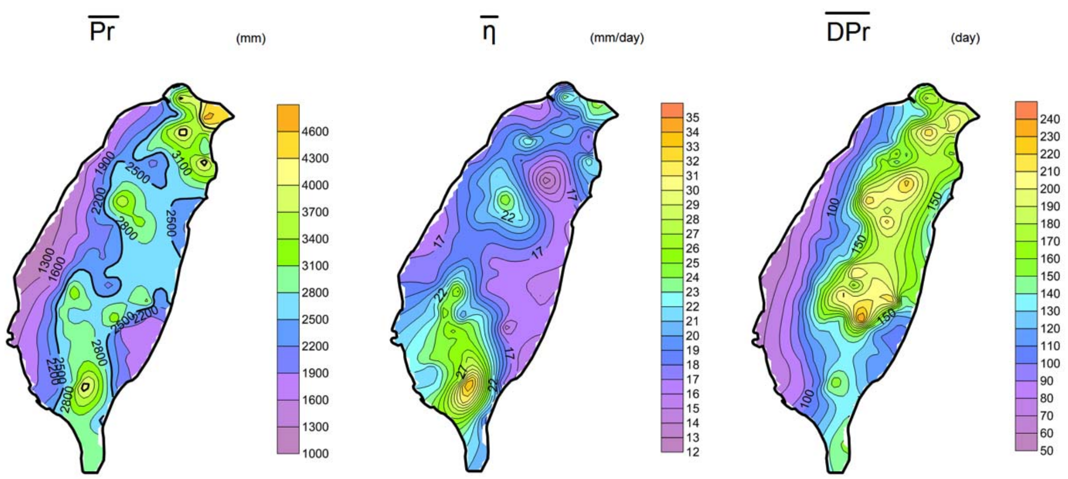

Figure 4. Contour map for annual rainfall characteristics of $\overline{\mathrm{Pr}}$ (mm), $\overline{\eta}$ (mm/day), and mean $\overline{D_{\mathrm{Pr}}}$ at 120 stations through 1978 to 2008.

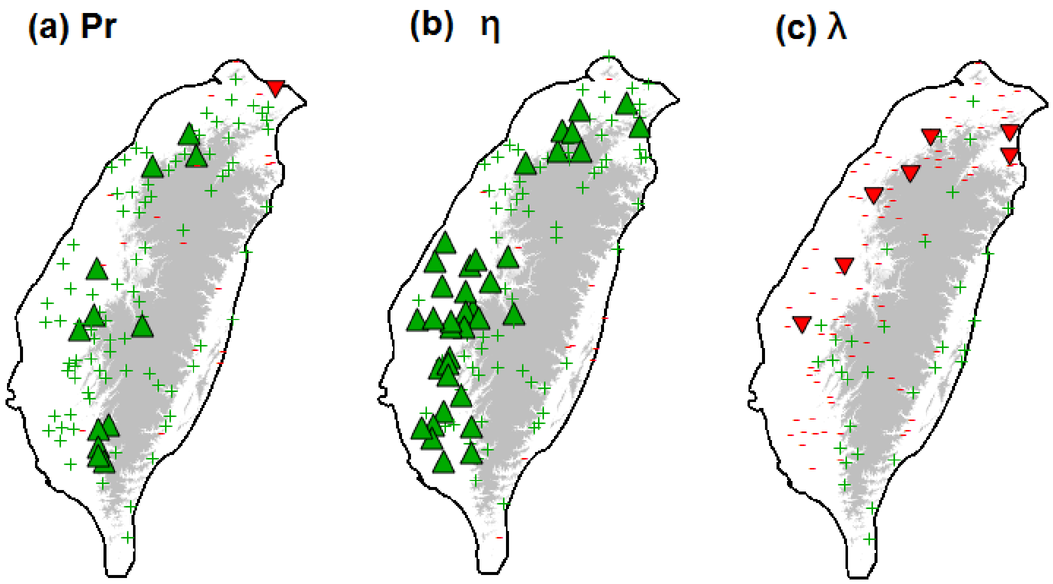

Figure 7. MK test of Pr, η, and λ trends' statistics of each station with TFPW process through 1978 to 2008. The plus (+) or minus (-) signs showed positive or negative trends without significant ($p>0.05$); at $p<0.05$ for solid triangles (▲, ▼); gray color indicated the mountainous areas.

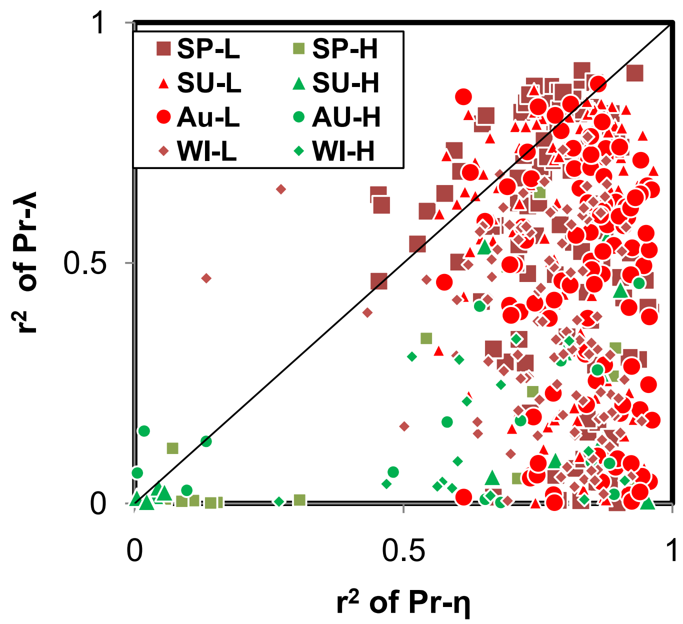

Figure 14. Comparison of correlation coefficient (r) between seasonal rainfall amount (Pr), seasonal ratio of rain days (λ) (r^2 of Pr-λ), and seasonal daily rainfall intensity (η) (r^2 of Pr-η) at 120 rain stations.

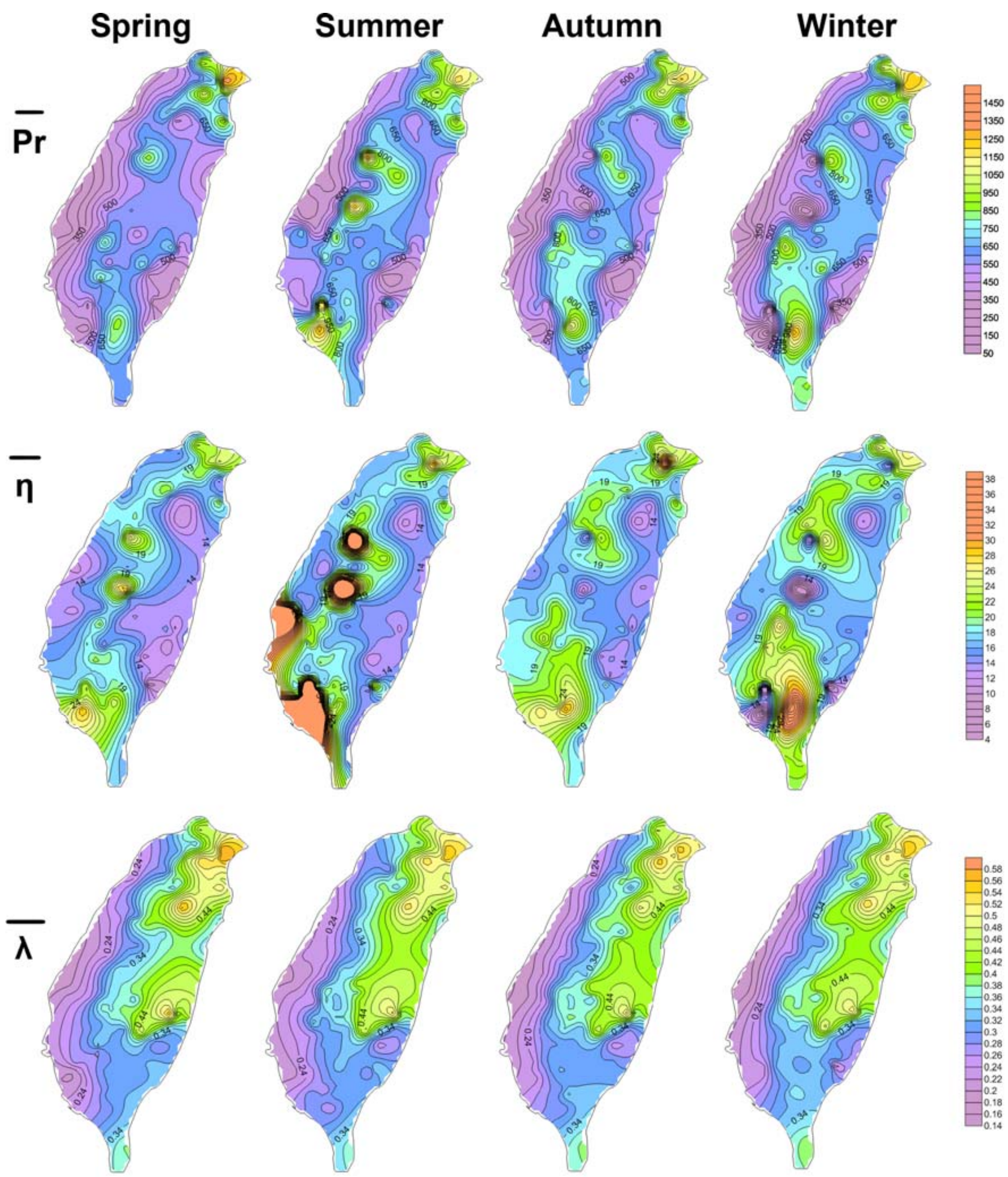

Figure 9. Seasonal period mean rainfall amount ($\overline{\mathrm{Pr}}$) (mm), period mean daily rainfall intensity ($\overline{\eta}$) (mm/day), and period mean ratio of rain days ($\overline{\lambda}$) at 120 stations through 1978 to 2008.

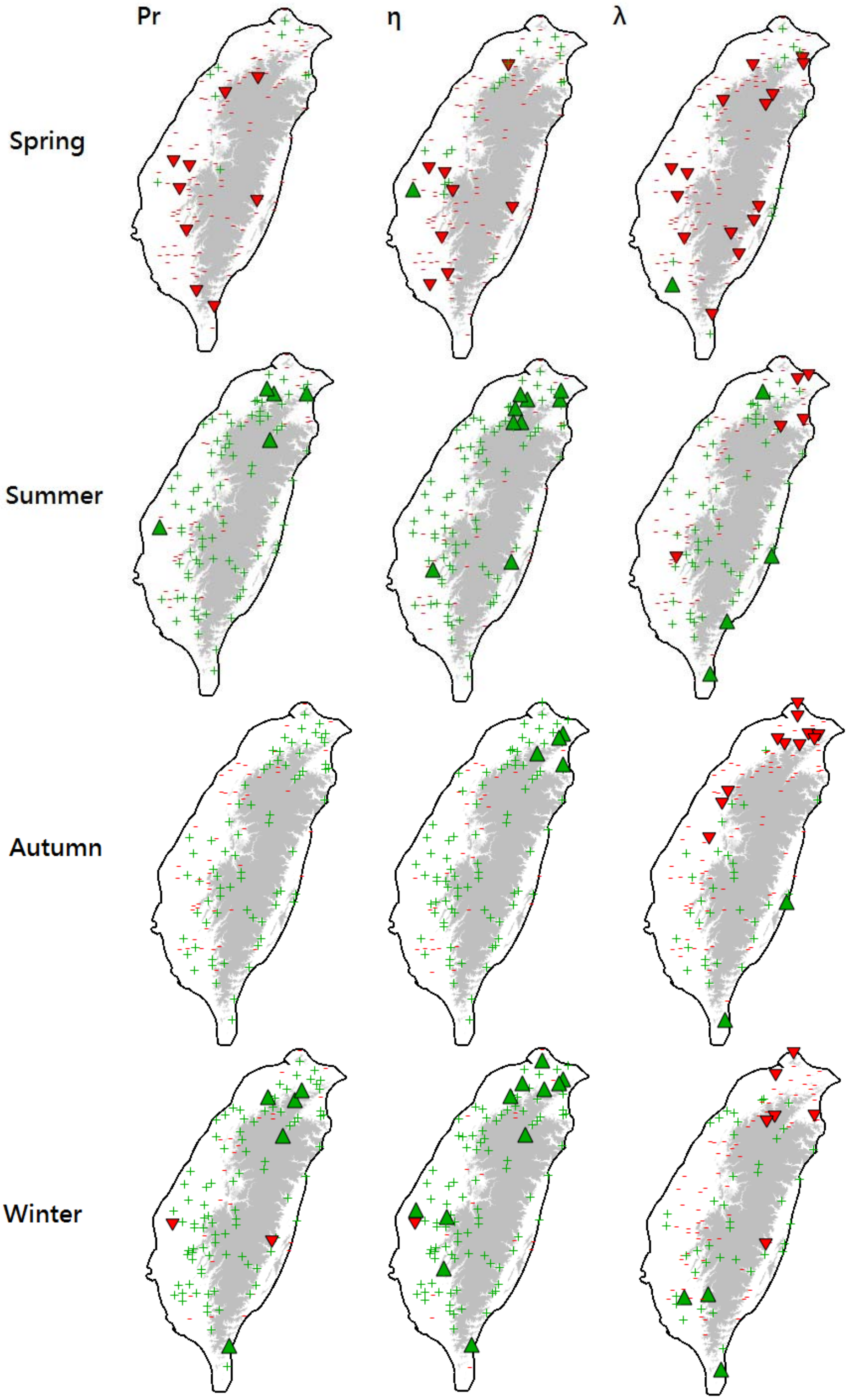

Figure 15. Seasonal trends in rainfall amount (Pr), daily rainfall intensity (η), and ratio of rain days (λ). "+", "-", "▲", and "▼"showed positive, negative, significant positive, and significant negative ($p<0.05$); gray indicated the mountainous areas.